Contract Report 2009-09

Hydrologic Modeling of the Fox River Watershed Using SWAT2000: Model Development, Calibration, and Validation

Elias G. Bekele and H. Vernon Knapp

August 2009

Illinois State Water Survey
Institute of Natural Resource Sustainability
University of Illinois at Urbana-Champaign

Champaign, Illinois

Hydrologic Modeling of the Fox River Watershed Using SWAT2000: Model Development, Calibration, and Validation

by
Elias G. Bekele and H. Vernon Knapp

Center for Watershed Science
Illinois State Water Survey
Champaign, IL 61820

August 2009

Hydrologic Modeling of the Fox River Watershed Using SWAT2000: Model Development, Calibration, and Validation

by
Elias G. Bekele and H. Vernon Knapp
Center for Watershed Science

Abstract

Regional water-supply planning efforts in Illinois are attempting to better understand potential impacts of climate change on low flow hydrology and surface water availability for meeting increasing water use. For this purpose, models are being developed for selected priority watersheds to analyze hydrologic sensitivity to a range of climate scenarios. One of these watersheds is the Fox River watershed, which is located in southeastern Wisconsin and northeastern Illinois with a total watershed area of 2658 square miles. A suite of hydrologic models was developed for streamflow simulations in the Fox River watershed. The FORTRAN version of the USDA's Soil and Water Assessment Tool (SWAT) and its ArcView interface (AVSWAT2000) were used in developing the hydrologic simulation models.The AVSWAT2000 was mainly used in preparing input data for watershed simulation. Hydrologic models were developed for three subwatersheds, designated as Subwatershed I, Subwatershed II, and Subwatershed III; a single model was also designed for the entire Fox River watershed. The development of subwatershed models serves two important purposes: (1) it ensures distributed parameter calibration, and (2) more observed data can be used during model parameter estimation. The hydrologic models developed in this study will be used to analyze potential impacts of various climate change scenarios on flows and surface water availability. In order to ensure the model's ability in simulating the response in streamflow to various climate conditions, the hydrologic model was calibrated under two calibration scenarios representing drought and average conditions.

This report presents the hydrologic model development for the Fox River watershed and calibration and validation of the model for streamflows. The report is divided into five sections. The first section is the introduction and the second section presents a brief description of the hydrologic model (SWAT) and the major hydrologic processes that the model is capable of simulating. The third section describes hydrologic modeling of the Fox River watershed, which includes the types of input data used and data processing involved. The fourth section describes calibration and validation of the hydrologic models developed, the automatic calibration method used, and the calibration procedure employed. This section also presents results of the model calibration and long-term model evaluations. Finally, the fifth section summarizes the hydrologic model development, calibration, and validation results.

Contents

Contents (concluded)

List of Tables

List of Figures

List of Figures (continued)

List of Figures (concluded)

Hydrologic Modeling of the Fox River Watershed Using SWAT2000: Model Development, Calibration, and Validation

by
Elias G. Bekele and H. Vernon Knapp
Center for Watershed Science

1. Introduction

The Fox River, one of the tributaries of the Illinois River, originates near Menomonee Falls in Wisconsin. The Fox River in northern Illinois and southeastern Wisconsin flows through the western suburbs of both the Chicago and Milwaukee metropolitan areas. In Wisconsin, it flows for about 62 miles, draining a total area of 938 square miles before it enters Illinois. The Illinois portion of the watershed has an area of 1720 square miles with a river length of approximately 115 miles before it joins the Illinois River at Ottawa, Illinois. The elevation of the watershed ranges from 459 to 1010 feet with an average slope of 2.7 percent. The Fox River flows through a series of interconnected lakes known as Fox Chain of Lakes, which include Fox Lake, Nippersink Lake, Pistakee Lake, Petite Lake, Grass Lake, Channel Lake, Bluff Lake, Lake Marie, and Lake Catherine. The Chain of Lakes and the Fox River have been used for recreational purposes providing unique aesthetic attractions. The main stem of Fox River is being used as a source of public water supply. Both the main stem and its tributaries receive storm water and effluents from a number of waste water treatment plants. Figure 1.1 shows the Fox River watershed with its major tributaries and United States Geological Survey (USGS) gauging stations selected for model calibration.

By 2050, the population in the Illinois portion of the watershed is expected to increase by over 1 million people, an increase of more than 130 percent. In addition to the pressure of increased water use on the low flows of the river, potentially, the river's hydrology may be further affected by climate changes over the next 50 years. Although the extent of potential climate change is far from certain, ongoing water supply planning efforts require an improved understanding of its potential modification on water supply availability in the region. Therefore, the objective of this study was to develop a hydrologic model for the Fox River watershed that will help analyze the sensitivity of water supply availability to climatic influences. The developed hydrologic model can perform continuous-time streamflow simulations, and it is capable of simulating the response in streamflows to various climate scenarios. The model is calibrated and validated using historical flow records at multiple gauging stations located within the watershed. The United States Department of Agriculture's (USDA) Soil and Water Assessment Tool, which is a physically based, semi-distributed watershed model, was selected for model development. Both the FORTRAN version and its ArcView interface (AVSWAT2000) have been used during the modeling exercise. To efficiently calibrate the hydrologic simulation model, the Fox River watershed was divided into three subwatersheds. For each of these subwatersheds, a stand-alone hydrologic model was developed and calibrated using an automatic calibration routine developed in this study. Based on the calibration results for the

three subwatersheds and additional adjustment of parameters, the hydrologic model for the entire Fox River watershed was developed and recalibrated. The hydrologic models developed in this study will ultimately be used to simulate various climate change scenarios that will help evaluate their potential impact on the water resources of the watershed. Such simulations render useful information for planning and management of future water supply capabilities.

Acknowledgments and Disclaimer

This material is based upon work supported by the Illinois Department of Natural Resources (IDNR), Office of Water Resources under Award No. OWRWS1. Additional project support was provided by the Illinois State Water Survey (ISWS), a Division of the Institute of Natural Resource Sustainability at the University of Illinois. Lisa Sheppard edited the report, Becky Howard formatted the report, and Momcilo Markus and Yanqing Lian provided technical review. Any opinions, findings, and conclusions or recommendations expressed in this publication are those of the authors and do not necessarily reflect the views of the ISWS or IDNR.

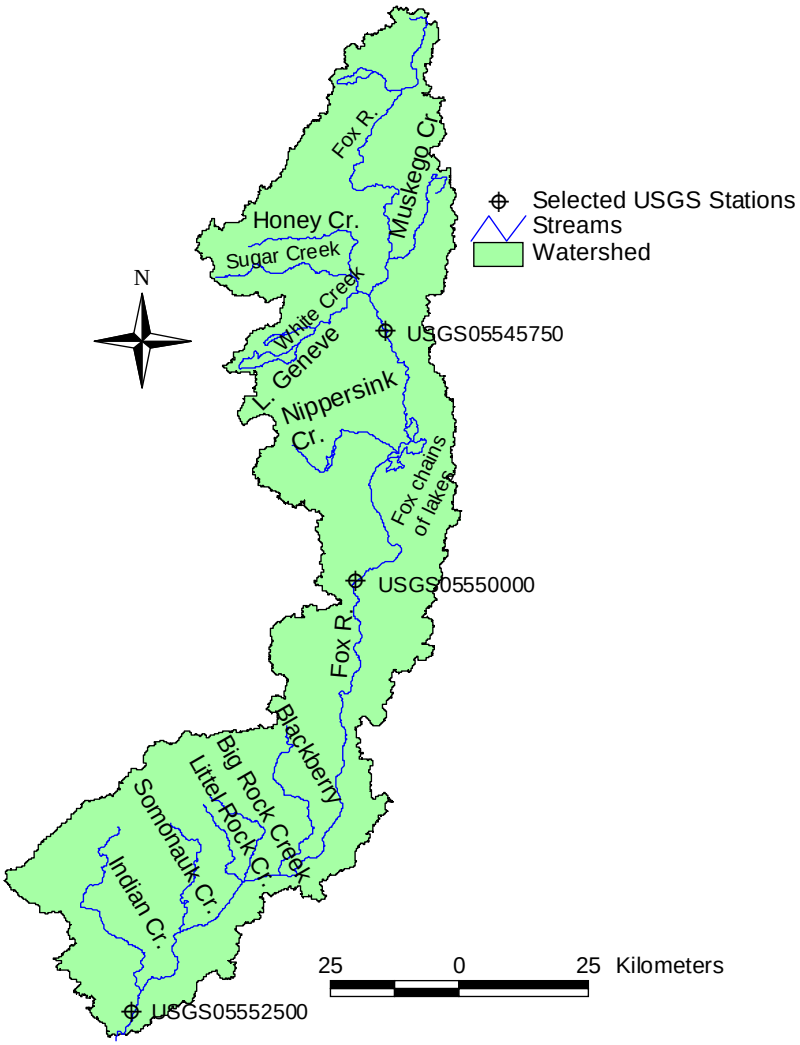

Figure 1.1. Fox River watershed and its major tributaries

2. The Hydrologic Model - Soil and Water Assessment Tool (SWAT)

The Soil and Water Assessment Tool (SWAT) is a basin-scale hydrologic model developed by the Agricultural Research Service of the USDA. SWAT is one of the most widely used, semi-distributed hydrologic models in the U.S. It is designed to predict the long-term impacts of land management practices on water, sediment, and agricultural chemical yields in agricultural watersheds with varying soils, land use, and management conditions (Arnold et al., 1999). Although SWAT operates on a daily time step, it is not designed to accurately simulate single-event flood routing; rather it is a long-term yield model (Neitsch et al., 2001). The model requires explicit information regarding weather, topography, soil properties, vegetation, and land management practices to simulate physical processes such as surface and subsurface flows, sediment transport, nutrient transport and cycling, and crop growth. It incorporates a weather generator developed for the contiguous U.S. that generates weather data using monthly average values summarized over a number of years. The weather generator can also be used to fill in gaps in measured records.

ArcView-SWAT Interface (AVSWAT2000)

To support visualization and processing of model inputs such as topography, land use, soils, and other digital data in SWAT input format, Di Luzio et al. (2002) developed the ArcView interface of SWAT (AVSWAT2000). AVSWAT2000 can also be used to execute SWAT simulations and display model results within the ArcView platform. SWAT is also integrated to the U.S. Environmental Protection Agency's (USEPA) BASINS 3.0, which is a multipurpose environmental analysis system software package. Data required to run SWAT for watersheds are available predominantly from government agencies (Neitsch et al., 2001).

In modeling with AVSWAT2000, the first step is to identify the watershed area of interest. AVSWAT2000 uses a digital elevation model (DEM) to delineate the watershed and further subdivide the watershed into a number of subbasins. The process of delineation involves preprocessing of the DEM to fill up sinks or depressions so as to determine the actual flow directions. Stream networks are then determined based on flow directions, amount of flow accumulations, and a user-defined critical source area, which sets the minimum drainage area required to form the origin of a stream. Selection of the watershed outlet completes the delineation process. In the stream network, the confluence of two tributaries defines an outlet, which results in subdivision of the watershed into subbasins. Geomorphic parameters that are required by the model are then computed for all subbasins. Note that routing of flow and its constituents are performed at the subbasin level. Being a semi-distributed model, AVSWAT2000 uses digital land use and soil maps to identify the land uses and soil types in each subbasin of the delineated watershed. Further subdivision of subbasins into a number of hydrologic response units (HRUs) can be done based on a unique intersection of land use and soil categories.

Major Hydrologic Processes Modeled in SWAT

SWAT incorporates a suite of algorithms to model various physical processes occurring in a watershed. The model components include weather, hydrology, soil properties, plant growth, nutrients, pesticides, pathogens, and land management. With respect to this application, the most important one is the hydrology component, and therefore, a brief description of the major hydrologic processes modeled by SWAT is provided hereafter. For a detailed description of all model components, refer to the SWAT user's documentation (Neitsch et al., 2001).

Irrespective of the type of problem being studied, the main driving force behind everything that occurs in a watershed is the water balance (Neitsch et al., 2001). The water balance equation can be expressed as

$$SW_t = SW_o + \sum_{i=1}^{t} \left(R_{day} - Q_{surf} - E_a - W_{seep} - Q_{gw} \right) \tag{2.1}$$

where SW_t is the final soil water content ($mm\ H_2O$), SW_o is the initial soil water content on day i ($mm\ H_2O$), t is the time ($days$), R_{day} is the amount of precipitation on day i ($mm\ H_2O$), Q_{surf} is the amount of surface runoff on day i ($mm\ H_2O$), E_a is the amount of evapotranspiration on day i ($mm\ H_2O$), W_{seep} is the amount of water entering the vadose zone from the soil profile on day i ($mm\ H_2O$), and Q_{gw} is the amount of baseflow or return flow on day i ($mm\ H_2O$).

Surface Runoff

Also known as overland flow, surface runoff is the flow that occurs along a sloping surface when the infiltration capacity of the soil is less than the intensity of precipitation. SWAT incorporates two procedures for simulating surface runoff. The first procedure is a modified version of USDA's Soil Conservation Service (SCS, 1972) Curve Number method. It is an empirical method developed to provide a consistent basis for estimating the amount of surface runoff from a watershed with varying land use and soil types. The second one is the Green-Ampt method (Green and Ampt, 1911), which requires sub-daily precipitation data to model infiltration by assuming a homogeneous soil profile and uniformly distributed antecedent moisture in the soil profile. The surface runoff is then computed as a remainder of the infiltration.

In this study, the SCS Curve Number method is used and is given as

$$Q_{surf} = \frac{\left(R_{day} - 0.2S \right)^2}{R_{day} + 0.8S} \tag{2.2}$$

where Q_{surf} is the accumulated runoff or rainfall excess ($mm\ H_2O$), R_{day} is the rainfall depth for the day (mm), and S is the retention parameter (mm), which is a function of the Curve Number, CN. It is calculated as

$$S = 25.4\left(\frac{1000}{CN} - 10\right) \tag{2.3}$$

where CN is the Curve Number for the day, which is a function of soil permeability, land use, and antecedent soil moisture conditions. Based on the infiltration capacity of soils, the U.S. National Resources Conservation Service (NRCS) classifies soils into four hydrologic groups. According to NRCS (1996), soils with similar runoff potential under similar storm and cover conditions belong to the same hydrologic soil group. These are: hydrologic soil group *A*, soil with high infiltration rate (i.e., low runoff potential); hydrologic soil group *B*, soil with moderate infiltration rate; hydrologic soil group *C*, soil with slow infiltration rate; and hydrologic soil group *D*, soils with very slow infiltration rate or high runoff potential. Antecedent moisture conditions are the soil moisture conditions of a watershed at the beginning of a storm. These conditions affect the volume of runoff generated by a particular storm event. SCS (1972) defined three antecedent moisture conditions: moisture condition I, which refers to dry soil condition that leads to a permanent wilting point; moisture condition II, soils with average moisture condition; and moisture condition III, wet soil condition, where the soil is at field capacity. Typical Curve Numbers for moisture condition II under varying land cover and soil types are provided by SCS (1986). These values are, however, appropriate only when slopes of the subbasins are 5 percent. For all other slopes, curve numbers must be adjusted using an equation developed by Williams (1969) and expressed as

$$CN_{2s} = \frac{\left(CN_3 - CN_2\right)}{3} \times \left[1 - 2 \times \exp\left(-13.86 \times slp\right)\right] + CN_2 \tag{2.4}$$

where CN_{2s} is the moisture condition II Curve Number adjusted for slope, CN_3 is the moisture condition III Curve Number for the default 5 percent slope, CN_2 is the moisture condition II Curve Number for the default 5 percent slope, and *slp* is the average percent slope of the subbasin. SWAT adjusts the daily Curve Number value for moisture condition II based on the soil moisture content, but not for slope. Therefore, the above equation is added to the SWAT source code in order to adjust the Curve Number for slope effects. In addition, SWAT incorporates a method for estimating runoff from frozen soils, which are usually higher due to their reduced infiltration capacity. The model has a surface runoff storage routine to lag a portion of the surface runoff release to the main channel. This routine is particularly essential in large watersheds whose time of concentration is greater than a day.

In order to estimate constituent loadings from a subbasin or watershed, it is necessary to determine the peak runoff rate, which is an indicator of the erosive power of the runoff. SWAT computes the peak runoff rate using the modified rational formula (Williams, 1975). The modified rational formula is based on the assumption that the rate of runoff increases until the basin's time of concentration is reached, whereby the entire subbasin area is contributing to the flow at the outlet. It is expressed as

$$q_{peak} = \frac{\alpha_{tc} \times Q_{surf} \times A}{3.6 \times t_{con}} \tag{2.5}$$

where q_{peak} is the peak runoff rate (m^3/s), α_{tc} is the fraction of daily rainfall that occurs during the time of concentration, Q_{surf} is the surface runoff ($mm\ H_2O$), A is area of the subbasin (km^2), t_{con} is the time of concentration for the subbasin (hr), and 3.6 is a unit conversion factor.

Potential Evapotranspiration

Evapotranspiration, which is an important component of the hydrologic cycle, accounts for evaporation from the ground, water bodies and canopy interception, and transpiration. The rate at which evapotranspiration would occur from a large area completely and uniformly covered with growing vegetation that has access to an unlimited supply of soil water is termed as potential evapotranspiration. SWAT incorporates three methods for estimating potential evapotranspiration, which include Hargreaves (Hargreaves et al., 1985), Priestley-Taylor (Priestley and Taylor, 1972), and Penman-Monteith (Allen, 1986; Allen et al., 1989). In addition, the model allows reading potential evapotranspiration data calculated using other methods.

Infiltration

In SWAT, the SCS Curve Number method, which is used for surface runoff computation in this application, operates at a daily time-step and thus, infiltration cannot be directly modeled as it requires sub-daily data. Consequently, the amount of water entering the soil profile is calculated as precipitation minus the surface runoff. The initial rate of infiltration depends on the antecedent moisture condition of the soil, and its final rate is the same as the saturated hydraulic conductivity of the soil. The difference in water content in the soil profiles results in the continuous movement of infiltrated water through the profile. Once the field capacity of a soil layer is exceeded, percolation occurs. The saturated conductivity of a soil layer governs the flow rate and the soil temperature in a particular layer determines if there is flow out of that layer. When the soil layer temperature is less than or equal to zero, no percolation is allowed. SWAT uses a storage routing method to simulate the downward flow through each soil layer, and it is given as

$$Q_{perc} = DV_{sly} \times \left[1 - \exp\left(\frac{-\Delta t}{TT_{perc}}\right)\right] \tag{2.6}$$

where Q_{perc} is the amount of water percolating to the underlying soil layer on a given day ($mm\ H_2O$), DV_{sly} is the drainable volume of water in the soil layer on a given day ($mm\ H_2O$), Δt is the time step (hrs), and TT_{perc} is the percolation travel time (hrs).

Interflow

Interflow is the lateral flow that originates below the surface but above the saturated zone. Its contribution to streamflow is significant in areas where the soil has higher hydraulic conductivity in the surface layers and lower or no permeability at a shallower depth. To predict interflow in a given soil layer, SWAT uses a kinematic storage model (Sloan et al., 1983; Sloan

and Moore, 1984) developed for subsurface flow. The storage model accounts for variations in hydraulic conductivity, slope, and soil water content, and it is expressed as

$$Q_{\text{int } f} = 0.024 \times \left[\frac{2 \times DV_{sly} \times K_{sat} \times S_{hl}}{\phi_d \times L_{hl}} \right] \tag{2.7}$$

where DV_{sly} is as defined earlier in equation (2.6), K_{sat} is the saturated hydraulic conductivity (*mm/hr*), S is the slope of the hillslope segment, ϕ_d is the drainable porosity of the soil layer, and L_{hl} is the hillslope length (*m*).

Baseflow

Baseflow, which is also known as return flow, is the groundwater contribution to the streamflow. In SWAT, two groundwater aquifer systems are simulated in each subbasin. The first one is a shallow, unconfined aquifer that contributes to flow in the main channel or reach of the subbasin. The second is a deep, confined aquifer, which is assumed to contribute to streamflow somewhere outside of the watershed (Arnold et al., 1993). Percolated water is partitioned into fractions of recharges to both aquifer systems. The recharge to the deep aquifer is considered to be lost in the system and hence, it is not used in future water budget calculations. The water balance for the shallow aquifer can be given as

$$W_{shaq,i} = W_{shaq,i-1} + W_{shrc,i} - Q_{gw,i} - W_{revap,i} - W_{shpp,i} \tag{2.8}$$

where $W_{shaq,i}$ is the amount of water stored in the shallow aquifer on day *i* (*mm*), $W_{shaq,i-1}$ is the amount of water stored in the shallow aquifer on day *i*-1 (*mm*), $W_{shrc,i}$ is the amount of recharge entering the shallow aquifer on day *i* (*mm*), $Q_{gw,i}$ is the ground return flow, or baseflow into the main channel on day *i* (*mm*), $W_{revap,i}$ is the amount of water moving into the soil zone in response to water deficiencies on day *i* (*mm*), and $W_{shpp,i}$ is the amount of water removed from the shallow aquifer by pumping on day *i* (*mm*).

SWAT incorporates an exponential decay function used in the groundwater response model by Sangrey et al. (1984) to compute recharges to both shallow and deep aquifers. The decay function is given as

$$W_{rchg,i} = \left[1 - \exp\left(-1/\delta_{gw}\right)\right] \times W_{perc,i} + \exp\left(-1/\delta_{gw}\right) \times W_{rchg,i-1} \tag{2.9}$$

where $W_{rchg,i}$ is the amount of recharge entering the aquifers on day *i* (*mm*), δ_{gw} is the delay time or drainage time of the overlying geologic formations (*days*), $W_{perc,i}$ is the total amount of water exiting the bottom of the soil profile on day *i* (*mm*), and $W_{rchg,i-1}$ is the amount of recharge entering the aquifers on day *i*-1 (*mm*). A portion of the recharge is routed to the deep aquifer and the remaining goes to the shallow aquifer, which eventually contributes to the baseflow. Integrating the steady-state response to the groundwater recharge (Hooghoudt, 1940) and the non-steady-state response of groundwater flow to periodic recharge (Smedema and Rycroft, 1983), the baseflow in SWAT is given as

$$Q_{gw,i} = \left[\exp\left(-\alpha_{gw} \times \Delta t\right)\right] \times Q_{gw,i-1} + \left[1 - \exp\left(-\alpha_{gw} \times \Delta t\right)\right] \times W_{shrc,i} \quad (2.10)$$

where $Q_{gw,i}$ is the baseflow on day i (*mm*), $Q_{gw,i-1}$ is the baseflow on day i-1 (*mm* H_2O), α_{gw} is the baseflow recession constant, Δt is the time step (*1 day*), and $W_{shrc,i}$ is the amount of recharge entering the shallow aquifer on day i (*mm*). The storage-outflow relationship depicted in equation (2.10) can be considered a representation of the baseflow with two linear reservoirs in a series. There will be baseflow contributions to the main channel only if the amount of water stored in the shallow aquifer exceeds a user-defined threshold water level.

Channel Routing

In SWAT, channel routing of water including constituents such as sediment, nutrients, and organic chemicals can be performed. For water routing, the model employs either the Muskingum River routing method (Brakensiek, 1967; Overton, 1966) or the variable storage routing method (Williams, 1969). Both methods are variations of the kinematic wave model. The Muskingum routing procedure, which is used in this study, can be expressed as

$$V_{stored} = K \times \left(X \times q_{in} + \left(1 - X\right) \times q_{out}\right) \quad (2.11)$$

where V_{stored} is storage volume (m^3), q_{in} is the inflow rate (m^3/s), q_{out} is the discharge rate (m^3/s), K is the storage time constant for the reach (*s*), which is calculated as the ratio of storage to discharge, and X is the weighting factor that controls the relative importance of inflow and outflow in determining the storage in a reach with a value varying between 0.0 and 0.3 for rivers. The storage time constant, *K*, is estimated as

$$K = C_1 \times K_{bkfl} + C_2 \times K_{0.1bkfl} \quad (2.12)$$

where C_1 and C_2 are weighting coefficients, K_{bkfl} is the storage time constant calculated for the reach segment with bankfull flows (*s*), and $K_{0.1bkfl}$ is the storage time constant calculated for the reach segment with one-tenth of the bankfull flows (*s*). Both K_{bkfl} and $K_{0.1bkfl}$ are calculated using an equation developed by Cunge (1969) and given as

$$K = \frac{1000 \times L_{ch}}{c_k} \quad (2.13)$$

where *K* is the storage time constant (*s*), L_{ch} is channel length (*km*), and c_k is the celerity corresponding to the flow for a specified depth (*m/s*). The weighting factors *X*, C_1, and C_2 can be determined through calibration and in this study, model default values were used during all simulations.

Reservoir Routing

An impoundment in the main channel that receives water from all upstream subbasins is considered as a reservoir in SWAT. The water balance for a reservoir is given as

$$R = R_{st} + R_{in} - R_{out} + R_{pcp} - R_{ep} - R_{sp} \tag{2.14}$$

where R is the reservoir volume at the end of the day (m^3), R_{st} is the reservoir volume at the beginning of the day (m^3), R_{in} is the inflow to the reservoir during the day (m^3), R_{out} is the reservoir outflow during the day (m^3), R_{pcp} is the volume of precipitation falling on the reservoir during the day (m^3), R_{ep} is the volume of evaporated water from the reservoir during the day (m^3), and R_{sp} is the volume of water lost from the reservoir by seepage (m^3). In order to determine the amount of precipitation falling on the reservoir as well as the amount of evaporation and seepage, the reservoir surface area needs to be known. This surface area varies with the change in the volume of water stored in the reservoir and is updated daily using the following equation

$$A_R = \beta \times V^{\alpha} \tag{2.15}$$

where A_R is the reservoir surface area (ha), V is the volume of water in the impoundment (m^3 H_2O), β and α are parameters to be determined through calibration process.

Three alternative ways of estimating reservoir outflow is incorporated in SWAT. The first option allows reading in measured outflows. The second option requires a water release rate and is designed for small, uncontrolled reservoirs. Using this option, water release is in effect when the reservoir volume exceeds the principal storage. If the reservoir volume exceeds the storage corresponding to the emergency spillway level, the extra water is released within one day. The third and last option is designed for larger, managed reservoirs, and it allows the user to specify monthly target volumes for the reservoir.

3. Modeling of the Fox River Watershed

The modeling of the Fox River watershed is conducted using both the FORTRAN version and the ArcView interface of SWAT (AVSWAT2000). The AVSWAT2000 is primarily used to generate model input files and default parameters of the model from a suite of digital data, including the digital elevation model (DEM), land use map, soil map, and climate data. A 30m DEM was derived for the entire Fox River watershed from the National Elevation Data (NED) set for the upper and lower Fox River watershed (downloaded from BASINS's Web site at http://www.epa.gov/waterscience /ftp/basins/gis_data/huc/. The DEM is used to delineate the watershed and subbasin boundaries and derive average slopes for the subbasins. The stream network is defined based on a reach file obtained from the aforementioned Web site and using AVSWAT's burn-in option. A total of 207 subbasins as shown in Figure 3.1 is used to represent the Fox River watershed. The figure shows the stream network, outlets for subbasins and effluent discharges, the location of Stratton Dam, and the three subwatersheds designated as Subwatershed I, Subwatershed II, and Subwatershed III. The Fox River watershed was divided into these large subwatersheds for calibration purposes, which are further subdivided into smaller subbasins. Subwatershed I is the watershed area upstream of the *USGS_05545750* gauging station at New Munster in Wisconsin and Subwatershed II is the drainage area between New Munster and the *USGS_05550000* gauging station at Algonquin, Illinois. The remaining portion of the watershed downstream of Algonquin is designated as Subwatershed III and the *USGS_05552500* gauging station at Dayton is close to the watershed outlet. A total number of 207 subbasins is obtained for the Fox River watershed by choosing a critical source area (CSA) of 1500 hectares, which defines the detail of the stream network. The CSA is fixed with the intention of incorporating sufficient variability of input factors such as weather, land use, and soils that will eventually help enable fairly accurate hydrologic simulation.

As indicated earlier, subbasins can be further subdivided into hydrologic response units (HRUs) based on the unique intersection of land use and soil category. AVSWAT2000 has two options of subdividing subbasins into HRUs. The first option is to represent the land use and soil types of a subbasin by their dominant types in that particular subbasin, in which case a subbasin is the same as an HRU. The second option is based on threshold values assigned for land use and soil categories resulting in multiple HRUs in a subbasin. The model identifies the land use and soil types of multiple HRUs, however, without locating their exact positions. Basically, partitioning the subbasins into a number of HRUs helps introduce sufficient variability of model inputs that could impact the hydrology of the watershed. This variability can also be achieved, however, through detailed subdivision of the watershed into subbasins. The advantage of the second option is that it guarantees hydrologic connectivity between HRUs and the exact location of the HRUs is known, increasing the practical utility of the model being developed for other applications. Because of these reasons, the first option has been used in this study, resulting in an equal number of subbasins and HRUs (i.e., 207 HRUs).

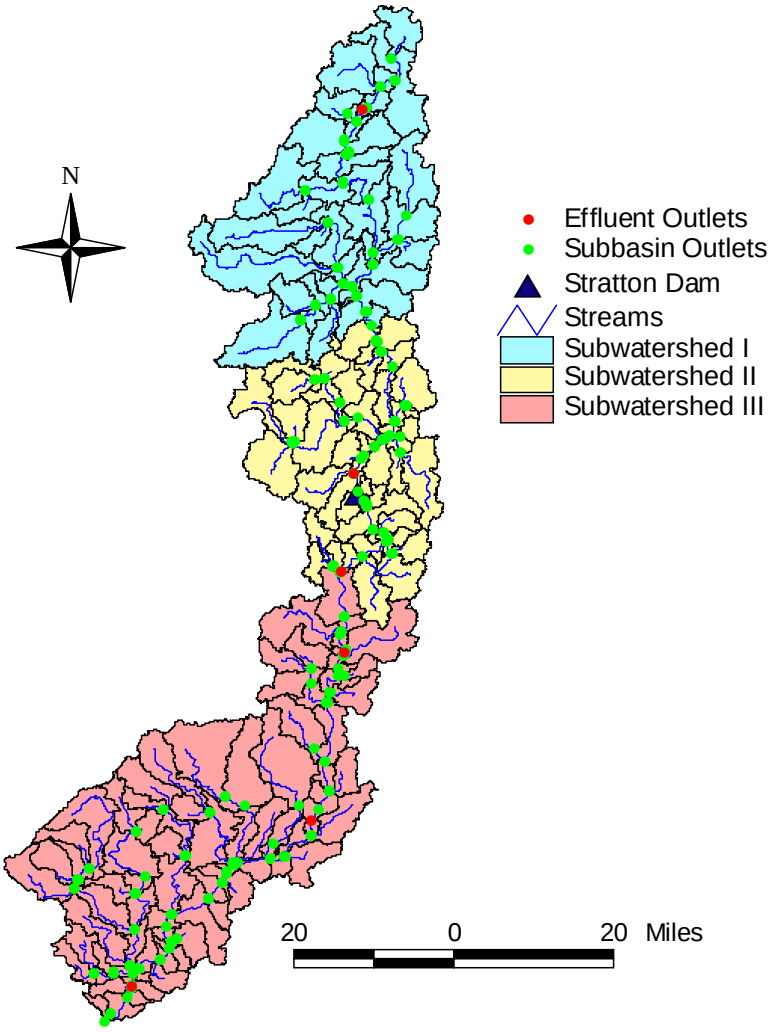

Figure 3.1. Fox River watershed after delineation into 207 subbasins

Land Uses

Land use data for the Illinois portion of the watershed were obtained from the Illinois Interagency Landscape Classification Project (IILCP), which is based on the 1999-2000 land cover inventory. The 2000 land use data for the Wisconsin portion of the watershed were obtained from the Southeastern Wisconsin Regional Planning Commission (SEWRPC). Since the land use classifications of these two data sources are different, the Illinois land use classification is adopted for the entire watershed. The distribution of land use types in the Fox River watershed after the reclassification is presented in Figure 3.2. Nearly 60 percent of the watershed is covered with agricultural land uses, which include corn (CORN), soybean (SOYB), and pasture (PAST). Urban areas (UINS, URML) account for 24 percent of the watershed. The remaining area of the watershed is covered by forest (FRST, 10 percent), wetlands (WETN, 5 percent) and water (WATR, 3 percent).

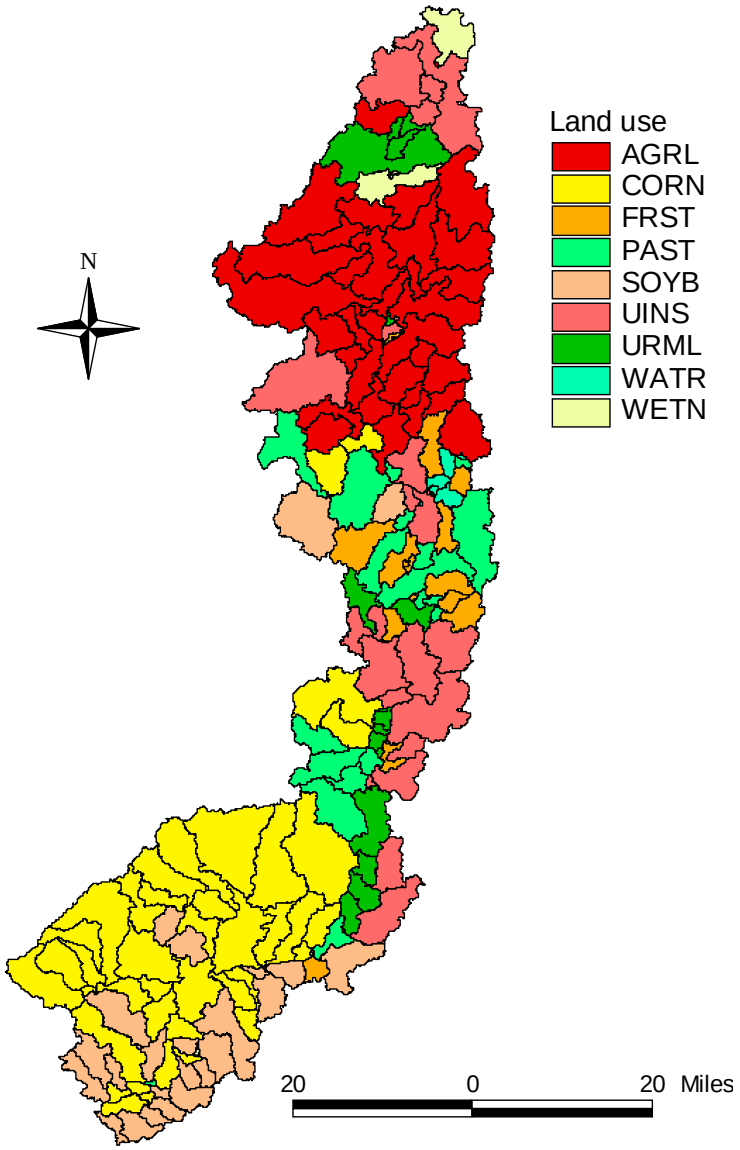

Figure 3.2. Land use types in the Fox River watershed

Soils

SWAT utilizes the State Soil Geographic (STATSGO) database to derive physical characteristics of soils in the watershed including soil permeability and available soil water capacity. The STATSGO soil map is created by generalizing more detailed soil survey maps, and is designed to support regional, multi-state, state, and river basin resource planning, management, and monitoring. The STATSGO soil data for Fox River watershed are obtained from the BASINS's Web site and are shown in Figure 3.3. SWAT assigns the STATSGO soil properties to the HRUs based on the dominant soil component within the STATSGO map unit.

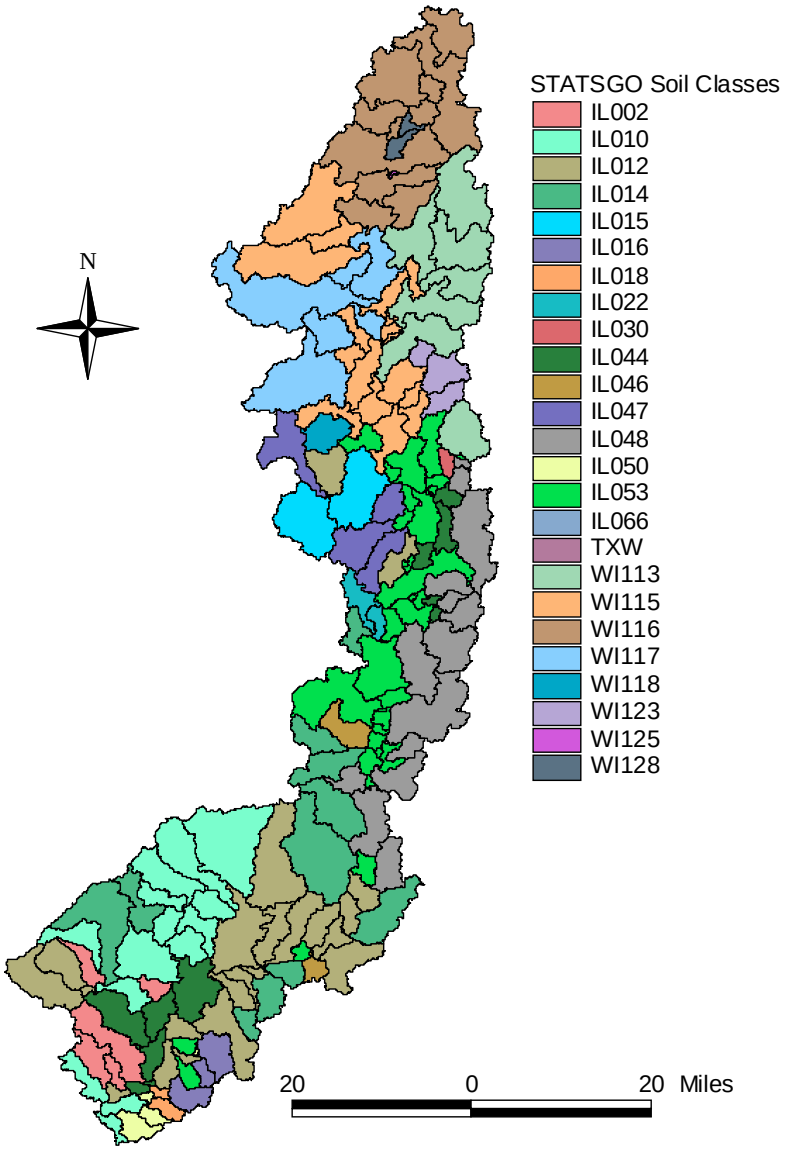

Figure 3.3. STATSGO soil classes in the Fox River watershed

One of the most important soil properties derived from the STATSGO maps is soil permeability, which influences the infiltration of precipitation and the generation of runoff. The soils of the Fox River watershed belong to various hydrologic groups, which classify soils according to their infiltration capacity or runoff potential. Figure 3.4 illustrates the spatial distribution of the soil hydrologic groups in the watershed. The figure shows that more than 70 percent of the watershed belongs to the hydrologic soil group B, indicating that most areas of the watershed have soils with a moderate infiltration rate. About 27 percent of the watershed has soils belonging to hydrologic group C with a slower infiltration rate. A small fraction of the watershed (i.e., less 0.5 percent) has soils of hydrologic group A or D.

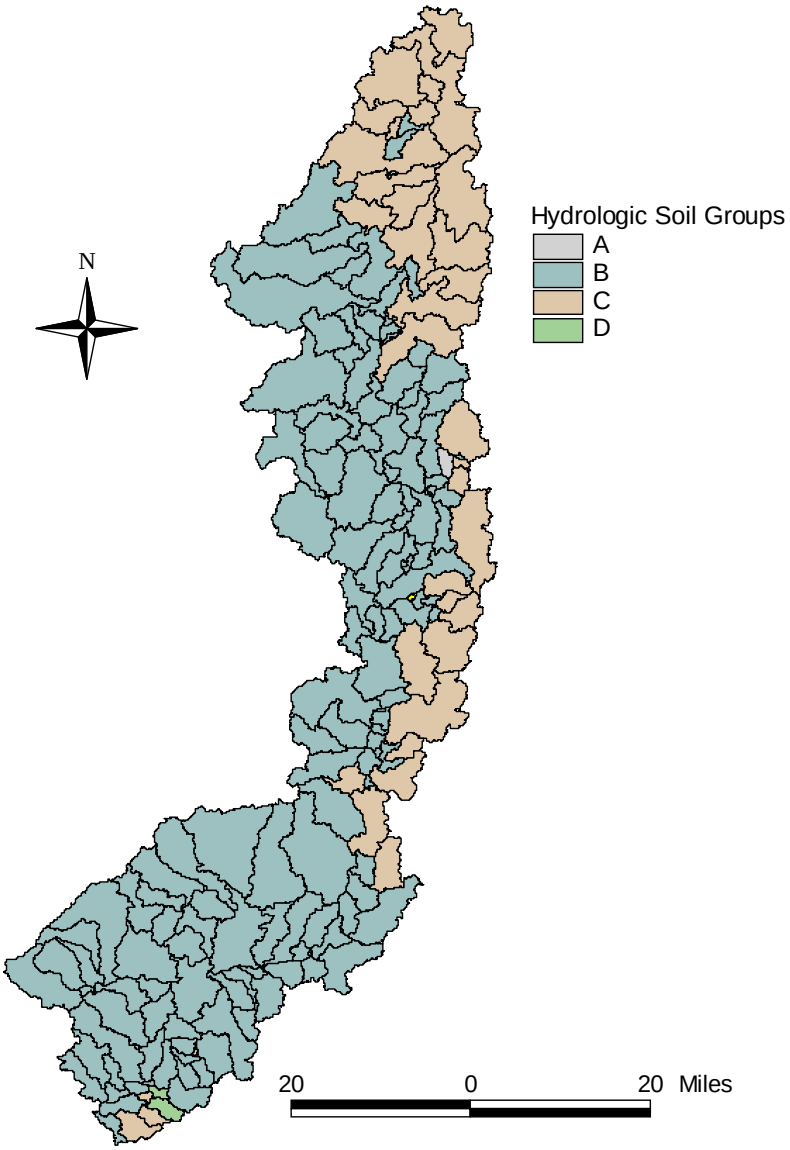

Figure 3.4. Spatial distribution of soil hydrologic groups in the Fox River watershed

Weather Inputs

Weather inputs are required by the SWAT model in order to simulate the various physical processes occurring in the watershed. SWAT utilizes weather inputs for a number of simulations including streamflow, potential evapotranspiration, snowmelt, and crop growth. Note that evapotranspiration can be either simulated or incorporated into the model whenever data are available. SWAT simulations require daily weather data, including precipitation depths, minimum and maximum temperatures, solar radiation, relative humidity, and wind speed. Weather data obtained from stations within or in close proximity to the watershed were used for the study. SWAT fills in missing weather data using its own weather-generator tool. However, in this application, an algorithm was developed to fill in missing data from nearby stations.

Table 3.1 lists the 11 weather stations used in simulating the Fox River watershed. These stations have precipitation and temperature data. Other climate inputs, such as relative humidity, solar radiation, and wind speed, are generated from long-term monthly average values included in SWAT's database using the model's weather-generator tool. Daily average relative humidity is calculated from a triangular distribution and monthly average values. Daily solar radiation is generated from a normal distribution, and daily wind speed is simulated using a modified exponential function and mean monthly values. Potential evapotranspiration is estimated using the Penman-Monteith method, which requires climate inputs such as relative humidity, solar radiation, and wind speed. While modeling the watershed, the weather stations were assigned to each subbasin based on their proximity to the centroids of the subbasins. Their spatial distribution in the watershed, including coverage percentage, is shown in Figure 3.5.

For modeling of the Fox River watershed, precipitation and temperature data spanning from 1925 to 2005 were prepared for each of the 11 weather stations. In cases where there were shorter periods of record, data from neighboring stations were used. Figure 3.6 shows the average annual precipitation for the weather stations based on the records from 1931 to 2005. The figure shows a general trend of increasing precipitation from north to south, and it also indicates that the Illinois portion of the watershed gets more precipitation than does the Wisconsin portion. The Elgin weather station (*112736*), which is assigned to more than 10 percent of the watershed area, has the maximum average annual precipitation of 37.2 inches. In comparison, the Germantown station (*473058*) has the lowest annual average precipitation of 32.4 inches, and is assigned to only 3 percent of the watershed area during the modeling process. The Aurora weather station (*110338*), which is assigned to one-fifth of the watershed area, has an average annual precipitation of 36.9 inches for the period considered.

Table 3.1 Weather Stations Used in the Watershed Simulation

Site code	*Station name*	*Latitude (N)*	*Longitude (W)*	*Precipitation data*	*Temperature data*
473058	Germantown	43.23	88.12	1944 to date	1944 to date
478937	Waukesha	43.00	88.25	1893 to date	1894 to date
479190	Whitewater	42.83	88.72	1941 to date	1949 to date
471205	Burlington	42.65	88.25	1948 to date	1951 to date
478723	Union Grove	42.68	88.02	1941 to date	1964 to date
474457	Lake Geneva	42.58	88.42	1945 to 2003	1945 to 2003
115493	McHenry Stratton	42.30	88.25	1948 to date	1992 to date
112736	Elgin	42.05	88.28	1898 to date	1897 to date
110338	Aurora	41.77	88.30	1887 to date	1887 to date
116661	Paw Paw	41.70	89.00	1912 to date	1962 to date
116526	Ottawa	41.32	88.90	1889 to date	1890 to date

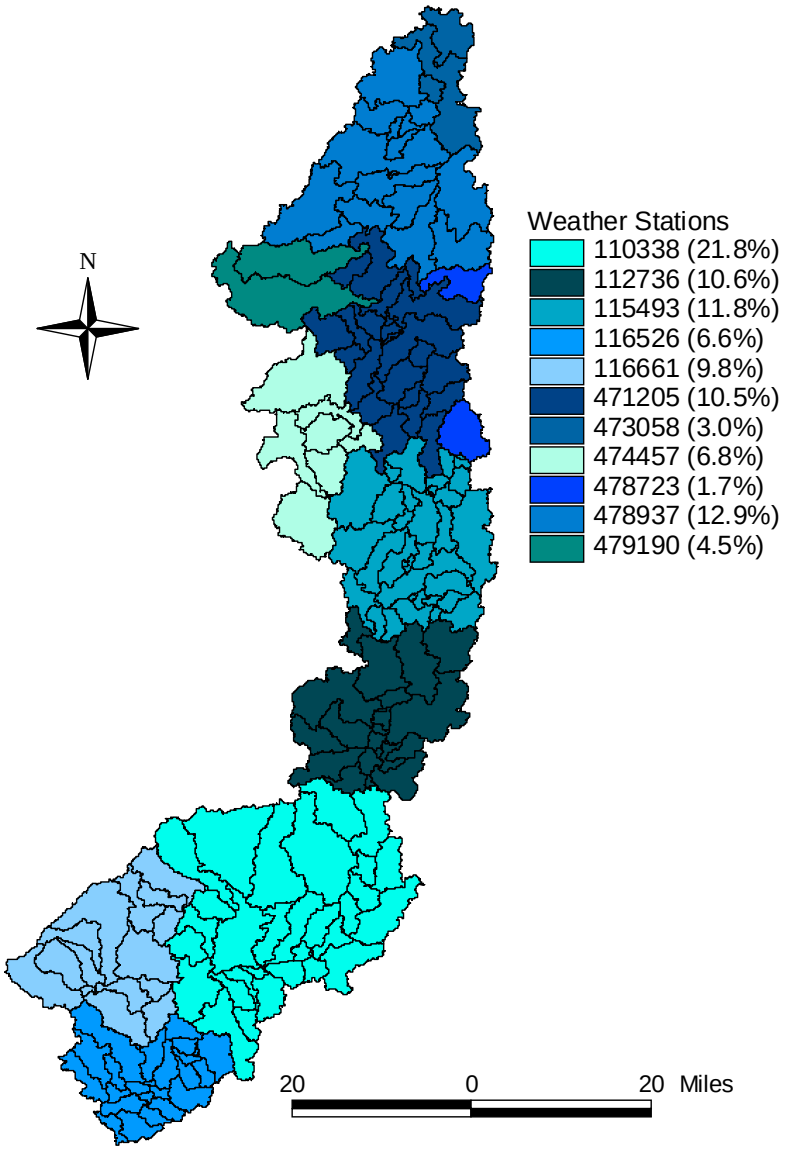

Figure 3.5. Assignment of weather stations to subbasins in the watershed

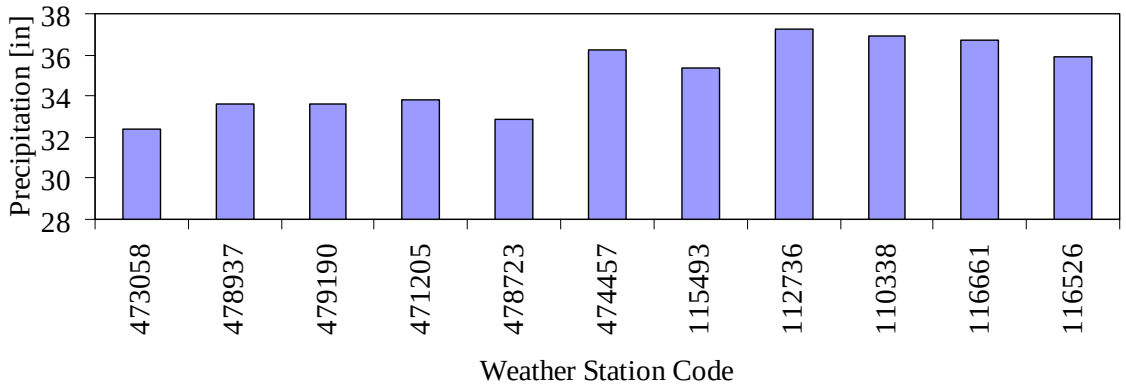

Figure 3.6. Average annual precipitation (1930-2005)

Streamflows

Streamflow data from three USGS gauging stations were obtained for use in model calibration and validation of the Fox River watershed. Two of the gauging stations are located in the Illinois portion of the watershed: Algonquin (*USGS_05550000*) and Dayton (*USGS_05552500*). The third gauging station is located at New Munster (*USGS_05545750*) in the Wisconsin portion of the watershed. The locations of these USGS gauging stations are shown in the watershed map presented in Figure 1.1. As can be seen in this figure, all three of the gauging stations are located at the main stem of the Fox River. For the purpose of calibrating and validating the hydrologic simulation model with various periods of records, 66 years of daily streamflow data spanning from 1940 to 2005 were obtained for the New Munster gauging station and 75 years of record spanning from 1931 to 2005 were obtained for Algonquin and Dayton gauging stations. The maximum and minimum daily flows recorded at New Munster from 1940 to 2005 were 7,100 and 35 cubic feet per second (cfs), respectively, and the mean daily flow during this period was 565 cfs. At Algonquin, the daily flow records range from a maximum of 6610 cfs to a minimum of 12 cfs during the period from 1931 to 2005, and the mean daily flow was 895 cfs. It must be noted that the amount of flow at Algonquin is affected by the operation of Stratton Dam. During the same period, the maximum and minimum daily flows at Dayton gauging station were 46,600 and 44 cfs, respectively, and the mean daily flow for this station was 1,846 cfs.

Base Flow Separation

In order to evaluate SWAT's prediction capability of surface and subsurface flows, the base flow is separated from the total stream flow using a base flow filter program developed by Arnold and Allen (1999). The base flow separation program reads in daily streamflow values and provides the fraction of the base flow for the entire period, daily base flow values, and the base flow recession constant (*ALPHA_BF*). Although the base flow program outputs the average recession constant, optimal values were determined through automatic calibration. Figures 3.7, 3.8, and 3.9 show the annual streamflow and base flow volumes per drainage area for *USGS_05545750* at New Munster, *USGS_05550000* at Algonquin, and *USGS_05552500* at

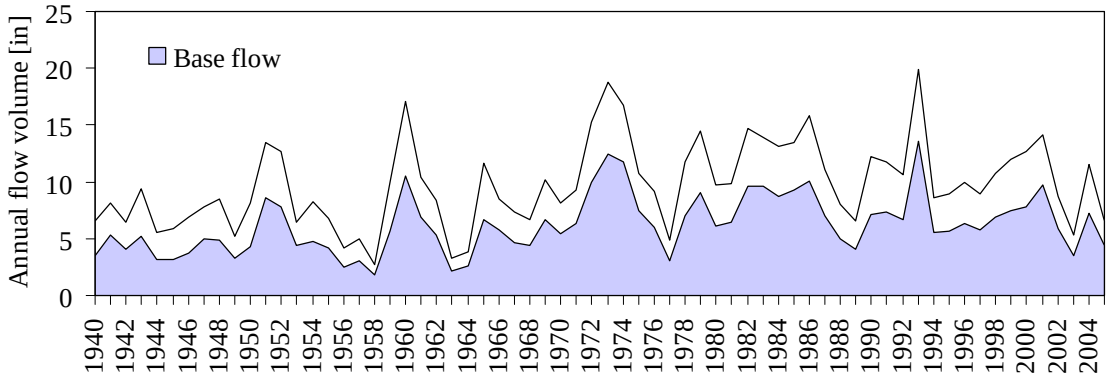

Figure 3.7. Annual total flow and base flow for *USGS_05545750* at New Munster

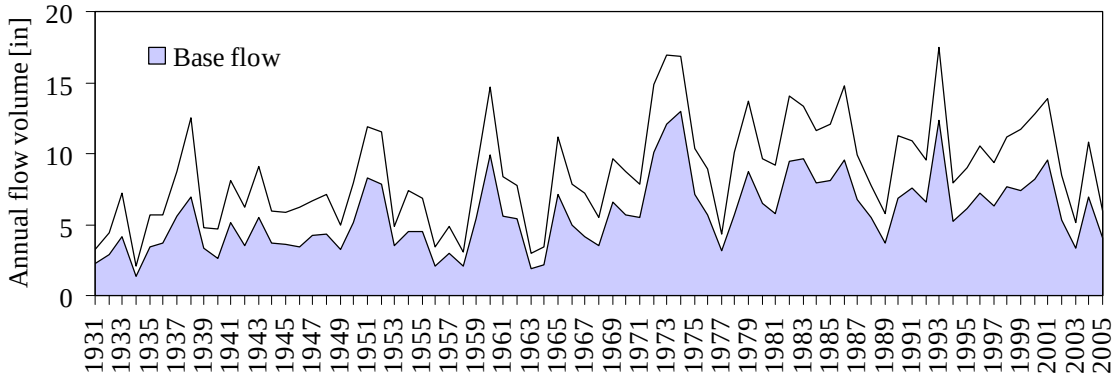

Figure 3.8. Annual total flow and base flow for *USGS_05550000* at Algonquin

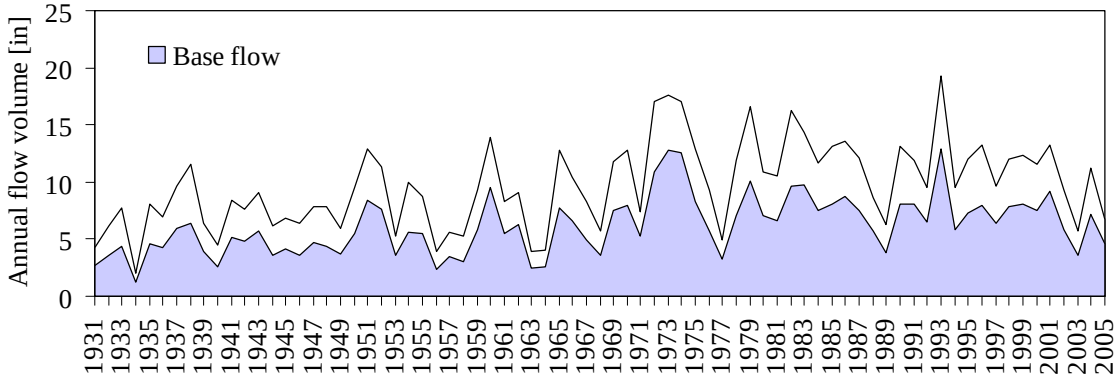

Figure 3.9. Annual total flow and base flow for *USGS_05552500* at Dayton

Dayton, respectively. The average base flow proportions for each of these stations are above 60 percent, indicating that the base flow is a major component of the streamflows in the Fox River watershed.

Fox River Effluent Discharges and Withdrawals

In the Fox River watershed, a number of municipal and industrial waste water treatment facilities discharge effluents to the tributaries and main stem of the Fox River. These effluent discharges constitute a significant portion of the streamflows during low flow periods and thus, they are incorporated in the hydrologic modeling of the Fox River watershed. The effluents from various sources are summed up and incorporated as point discharges to six locations on the main stem of the Fox River. It must be noted that these locations are selected to be downstream of the respective effluent sources. These locations are displayed in Figure 3.1 as effluent outlets. They are located on river reaches upstream of New Munster (NWMN), between New Munster and Stratton Dam (STRT), between Stratton Dam and Algonquin (ALQN), between Algonquin and Montgomery (MNTG), between Montgomery and Yorkville (YRKV), and between Yorkville and Dayton (DAYT).

Effluent discharges for each of the six river reaches were computed using the ratios of effluent discharges to average annual effluent amount and probabilities of simulated streamflow exceedence at the effluent outlets. Figure 3.10 shows the relationship between the effluent discharge ratio and the probability of exceedence for flows in the Fox River, with the highest effluent amounts coinciding with high streamflow conditions (low exceedence probability) and the lowest effluent amounts coinciding with low streamflow conditions. The computed daily effluent discharges were then adjusted proportionally to the observed annual average values. Figure 3.11 displays the average annual effluent discharges, indicating a temporal increase in all locations. The estimated effluents for the reach between Algonquin and Montgomery (MNTG) also include the effects of water supply withdrawals for the cities of Elgin and Aurora.

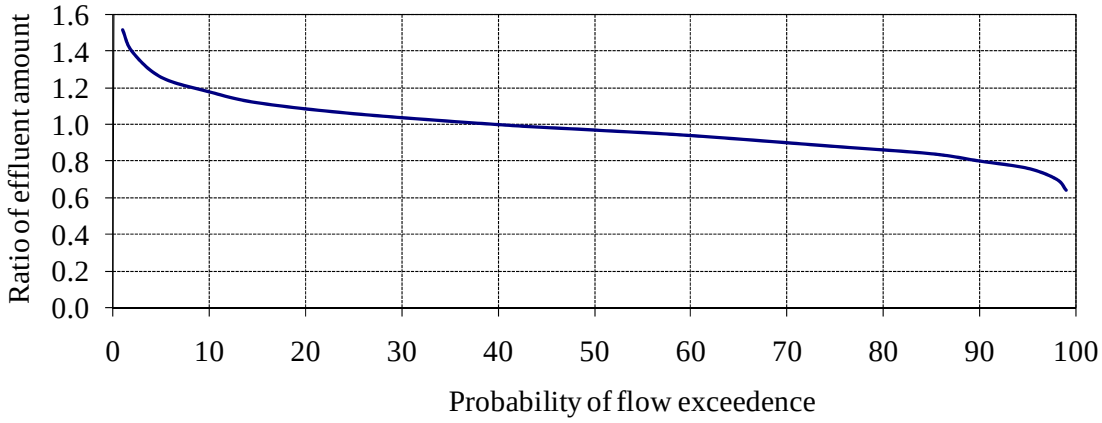

Figure 3.10. Ratio of effluent amount versus streamflow exceedence probabilities

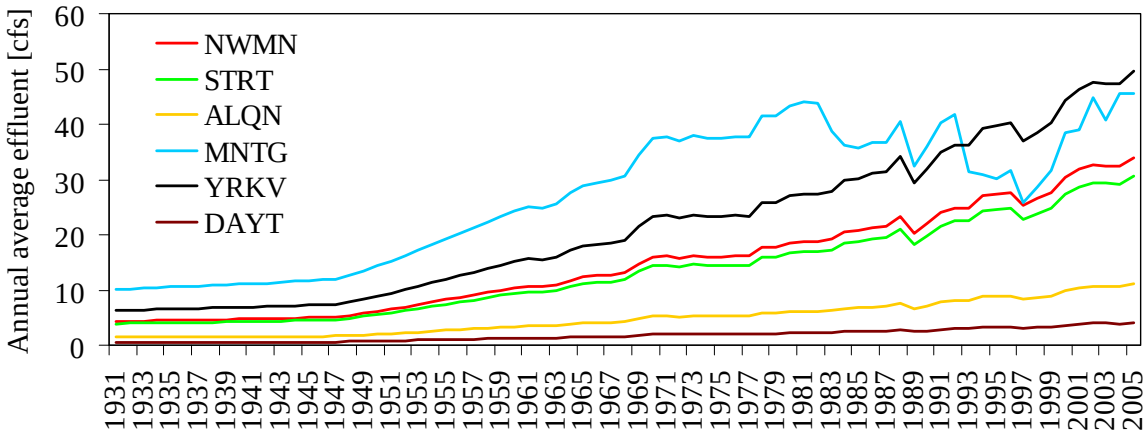

Figure 3.11. Annual average effluent discharges by river reaches

Lakes and Reservoirs

The Fox River flows through the Chain of Lakes and Stratton Dam near McHenry, whose main purpose is to maintain minimum lake levels. These interconnected lakes have a combined surface area of 7,700 acres and a storage capacity of 44,000 acre-feet at the normal pool level of 736.8 feet. Table 3.2 lists the storage capacity of the Chain of Lakes for a range of pool levels. In modeling with SWAT, the Chain of Lakes is represented as a reservoir controlled at Stratton Dam.

To account for the impact of a reservoir on the streamflow downstream, SWAT performs reservoir routing using a simple water balance method as indicated in equation (2.15). The model requires some sort of observed outflow data in order to compute daily reservoir outflows or it directly reads observed daily outflows. Since the purpose of the hydrologic model being developed is to evaluate the availability of future surface water supplies, it should be possible to simulate future climate scenarios. This excludes the use of measured outflow data during reservoir routing. Therefore, a modification has been made to a SWAT original source code by incorporating a level pool reservoir routing technique. A storage-outflow relationship has been developed based on storage data from the Chain of Lakes and daily outflows from Stratton Dam. This storage-outflow relationship is presented in Table 3.2.

Table 3.2. Storage-Outflow Relationship for Fox Chain of Lakes

Elevation of Pool level (feet) [NGVD[1]]	*Water Surface Area (acres)*	*Water Storage Capacity (acre-feet)*	*Outflow at Stratton Dam (cfs)*
735.00	6,100	31,000	1,073
736.80	7,700	44,000	1,810
738.00	10,000	54,000	2,250
740.55	11,900	82,000	4,914

Note: [1]National Geodetic Vertical Datum

It must be noted that the level pool routing is performed only when the daily inflow to the Chain of Lakes is larger than 2,250 cfs. Based on information obtained from a previous study on the operation of Stratton Dam (Knapp and Ortel, 1992), the minimum outflow from Stratton Dam is fixed at 89 cfs and the outflow is considered to be equal to the inflow when inflow to the Chain of Lakes is between 89 and 2,250 cfs. For simulation years before 1970, which had several drought periods, the minimum outflow from Stratton Dam is assumed to be 50 cfs.

4. Model Calibration and Validation

Calibration and validation of models should be carefully performed before applying them for operational predictions. This recommendation is based on the premise that reliability depends on how well the model is calibrated and validated with sufficient data. Calibration is the process of adjusting model parameters to closely match model outputs with observed or measured data. Hydrologic models are generally intended to be applicable to watersheds with various physical characteristics. These models consist of parameters that can be obtained by direct measurement of the physically observable characteristics, such as area of the watershed, and also include other parameters that are not directly observable, in which case they are determined by matching the model's hydrologic characteristics to that of the watershed of interest. Calibration should always be followed by validation. Model validation enables one to see if there is a need for further calibration refinement. The operational validity of a model should be primarily concerned with the accuracy of its output behavior over the domain of its intended applicability (Sargent, 1991).

It is a common practice to manually calibrate a model using a trial-and-error adjustment of parameters by visually comparing simulated and observed outputs. The feasibility of manual calibration, however, depends on the number of free model parameters in the model being calibrated and the degree of parameter interaction. For example, a semi-distributed hydrologic model such as SWAT requires that many model parameters be specified in order to incorporate the spatial heterogeneity of watershed characteristics into a simulation. Consequently, manual calibration of such a huge number of parameters would be a tedious and daunting task. To circumvent this problem, a combination of automatic and manual calibration approaches have been employed in this study.

Automatic Calibration Routine

An automatic calibration routine uses optimization techniques to search for optimal model parameters and objective functions as calibration criteria. It involves searching for a set of model parameters that result in a close match between measured and simulated outputs with a certain prescribed accuracy. In this application, the calibration routine is developed using genetic algorithms (GAs), first proposed by John Holland (1975) and further developed by David Goldberg (1989). GAs model natural selection and random variation, allowing a population of individuals to evolve under specified rules to a state that maximizes objectives or fitness. GAs exhibit the following three properties: (1) they use a population of individuals, which represents decision alternatives in a problem's solution, and utilize the collective learning process of these individuals; (2) they explore the solution space in two ways; the first is through a randomized mutation process and the second is recombination, which involves the exchange of information between two or more existing individuals; and (3) they assign a measure of fitness or quality for each individual, upon which potential solutions are compared and selected for further recombination.

GAs start by defining a manner to represent a potential solution, an objective function that measures the fitness of an individual solution, and fitness. In the context of GAs, a potential solution for a particular problem (e.g., a set of streamflow parameters in this particular

application) is known as a chromosome, which is a unique combination of genes or decision variables represented by either binary or real-valued parameters. A population of chromosomes is then randomly generated within the parameters space. To ensure efficient sampling of the parameter space, a Latin Hypercube Sampling (LHS) (McKay et al., 1979) has been used instead. LHS is a stratified sampling technique that is capable of exploring and efficiently sampling the distribution of model parameters within their acceptable ranges. The fitness of each chromosome is assigned to be its corresponding residual variation (*RSR*), which is computed as the ratio of root mean square error (*RMSE*) to the standard deviation of observed data (Moriasi, et al., 2007). The *RSR* incorporates the benefits of error index statistics and also has a normalization factor so that the resulting statistic can apply to various constituents (Moriasi, et al., 2007). The *RSR* is given as

$$RSR = \frac{\sqrt{\sum_{j=1}^{N}\left(O_j - S_j\right)^2}}{\sqrt{\sum_{j=1}^{N}\left(O_j - \overline{O}\right)^2}} \tag{4.1}$$

where O_j and S_j are the j^{th} observed and simulated data, respectively, $\overline{O}$ is the mean of observed data, and *N* is the total number of data used during calibration. The value of *RSR* ranges from an optimal value of zero for a perfect model to a very large positive number for a poor model. The lower the value of RSR, the better the model performance or the fitness of a chromosome will be. Based on fitness, mating couples are selected and undergo crossover, or recombination, in hopes of creating offspring with better fitness. The newly created chromosomes replace solutions with worse fitness. To avoid premature convergence to local, instead of global, optimum, and fully explore the solution space, some variations in the genetic makeup of the chromosomes are induced using mutation operators. Finally, the fitness of new offspring and mutated chromosomes are evaluated, and convergence criteria will then be checked. User-specified error tolerance, a maximum number of generations, or both can be used as convergence criteria. For further detailed account of the algorithm, refer to Haupt and Haupt (1998).

Model Performance Evaluation Metrics

Based on thorough review of model applications and evaluation methods, Moriasi et al. (2007) recommended three quantitative statistics be used in model performance evaluation in watershed simulations: the Nash-Sutcliffe efficiency (*NSE*), percent bias (*PBIAS*), and ratio of the root mean square error to the standard deviation of measured data (*RSR*). These three numerical model performance metrics have been used in evaluating SWAT's simulation of streamflows. Note that the *RSR* is also used as an objective function during auto-calibration to guide the search for optimal model parameters. The *NSE* is a normalized statistic that quantifies the relative magnitude of the residual variance compared to the variance of the measured data (Nash and Sutcliffe, 1970). The *NSE* shows how good a plot of observed and simulated data fits the 1:1 line and is given as

$$NSE = 1 - \left[\frac{\sum_{j=1}^{N} (O_j - S_j)^2}{\sum (O_j - \overline{O})^2} \right] \tag{4.2}$$

where O_j, S_j, $\overline{O}$, and *N* are as defined in equation (4.1). *NSE* values range from an optimal value of 1.0 for a perfect model to minus infinity. However, the values should be larger than zero to indicate minimally acceptable performance (Gupta, et al., 1999). *NSE* values less than or equal to zero show that the mean of the observed data is a better predictor than the model itself.

Percent bias (*PBIAS*) measures the average tendency of the simulated values to be larger or smaller than their observed counterparts (Gupta et al., 1999). The optimal value of *PBIAS* is zero, indicating exact simulation of observed values. In general, a lower value of *PBIAS* signifies accurate model simulation. *PBIAS*, which is the percent deviation of simulated data, is calculated as

$$PBIAS = 100 \times \left[\frac{\sum_{j=1}^{N} (O_j - S_j)}{\sum O_j} \right] \tag{4.3}$$

where O_j, S_j, and *N* are as defined in equation (4.1).

Moriasi et al. (2007) further established performance ratings for each recommended statistic. According to their analysis, in general, model simulation can be judged as satisfactory if *NSE* > 0.50 and *RSR* < 0.70, and if *PBIAS* is within ±25 percent for streamflow simulations in a monthly time-step. Table 4.1 shows the recommended performance ratings for streamflow simulations at monthly time-steps.

In addition to the aforementioned performance evaluation criteria, comparisons of observed and simulated hydrographs and daily flow duration curves are made to illustrate the model's ability in predicting ranges of flow values.

Calibration Parameters

A total of 16 model parameters that govern the hydrologic processes in SWAT have been selected for calibration. Table 4.2 lists these parameters and their ranges of variation. The first 12 parameters are among those that are responsible for the rainfall-runoff processes in the model, whereas the remaining four govern the accumulation of snow and snowmelt runoff processes. A brief description of each parameter is provided.

Table 4.1. Performance Ratings for Recommended Statistics[1]

Performance rating	*RSR*	*NSE*	*PBIAS (%)*
Very good	$0.00 \le RSR \le 0.50$	$0.75 \le NSE \le 1.00$	$\lvert PBIAS \rvert < 10$
Good	$0.50 < RSR \le 0.60$	$0.65 < NSE \le 0.75$	$10 < \lvert PBIAS \rvert \le 15$
Satisfactory	$0.60 < RSR \le 0.70$	$0.50 < NSE \le 0.65$	$15 < \lvert PBIAS \rvert \le 25$
Unsatisfactory	$RSR > 0.70$	$NSE < 0.50$	$\lvert PBIAS \rvert < 25$

Note: [1]Adapted from Moriasi et al. (2007).

Table 4.2. Selected Calibration Parameters

Parameter name	*Description of the parameters (units)*	*Ranges of values*	
		Minimum	*Maximum*
CN2	SCS runoff curve number (-)	30	70
SOL_AWC[1]	Available soil water capacity (mm/mm)	-0.04	0.04
ESCO	Soil evaporation compensation factor (-)	0.8	1
GW_REVAP	Groundwater " *REVAP* " coefficient (-)	0.02	0.2
REVAPMN	Minimum Threshold depth of water in the shallow aquifer for "*REVAP*" to occur	1	100
GWQMN	Minimum threshold depth of water in the shallow aquifer required for return flow to occur (mm)	10	100
ALPHA_BF	Base flow alpha factor (days)	0	1
RCHRG_DP	Deep aquifer percolation fraction (-)	0.0	0.25
DELAY	Groundwater delay (days)	0	100
CH_N2	Manning's "n" value for the main channels (-)	0.025	0.065
OV_N	Manning's "n" value for overland flow (-)	0.05	0.25
SURLAG	Surface runoff lag time (days)	0.5	4.0
SFTMP	Snowfall temperature (^{o}C)	-3.0	5.0
SMTMP	Snow melt base temperature (^{o}C)	0.0	5.0
SMFMX	Melt rate for snow on June 21 (mm/^{o}C day)	2.5	4.5
SMFMN	Melt rate for snow on December 21 (mm/^{o}C day)	0.0	2.5

Note: [1]Changes from its original value

Calibration parameters that affect the surface runoff include the curve number (*CN2*), available soil water capacity (*SOL_AWC*), and the soil evaporation compensation factor (*ESCO*). As indicated in equation (2.2), the *CN2* is used to calculate the depth of accumulated runoff or rainfall excess. *SOL_AWC* is the amount of water available to plants when the soil is at field capacity. It varies with the soil layer and is expressed as a fraction of the total soil water volume. *ESCO* modifies the depth distribution used to meet the soil evaporative demand, accounting for the effect of capillary action, crusting, and cracks.

One of the calibration parameters that govern the subsurface flow in SWAT is the groundwater "*REVAP*" coefficient (*GW_REVAP*). *REVAP* is the amount of water in the shallow aquifer that returns to the root zone. *GW_REVAP* controls the *REVAP* resulting from soil moisture depletion and direct groundwater uptake by deep-rooted plants. Other subsurface flow parameters include the threshold depth of water in the shallow aquifer for *REVAP* to occur (*REVAPMN*), the threshold depth of water in the shallow aquifer required for base flow to occur (*GWQMN*), the proportion of recharge percolating to the deep aquifer (*RCHRG_DP*), the groundwater delay factor (*DELAY*), and the base flow alpha factor or recession constant (*ALPHA_BF*). *ALPHA_BF* characterizes the steepness of the groundwater recession curve. Additional parameters that affect the watershed response are also considered for calibration. These include the Manning's roughness coefficients for the channel (*CH_N2*) and overland flow (*OV_N*), surface runoff lag time (*SURLAG*), snowfall temperature (*SFTMP*), snowmelt base temperature (*SMTMP*), and snow melt factors for June 21st (*SMFMX*) and for December 21st (*SMFMN*).

Out of the 16 parameters, five of them are lumped parameters and thus assume uniform values over the watershed to be modeled. The remaining are distributed parameters (i.e., they could differ from subbasin to subbasin depending on land use, soil type, and/or topographic features) and the total number of parameters to be calibrated becomes a multiple of the number of subbasins in a given watershed. This, however, results in an enormously large number of parameters to be estimated for the entire watershed. Thus, parameter reduction is inevitable, and it has been achieved by forcing the parameters to assume uniform values and by dividing the watershed into three larger subwatersheds. For example, parameters related to groundwater flow are forced to assume the same value for all subbasins in a given subwatershed. Other model parameters, such as Curve Number (*CN2*) and available soil water capacity (*SOL_AWC*), were parameterized by developing a relationship between parameters of a reference subbasin and corresponding parameters of other subbasins in the watershed using available information about the parameters. For example, the Curve Number is an index combining hydrologic soil group and land use factors. Thus, a parametric relationship based on hydrologic soil groups and land use factors is developed between the Curve Numbers of the reference subbasin and others in the watershed. Recommended values in SWAT literature are used in developing this relationship. Once the parameter value for the reference subbasin is identified, the relationship is used to determine Curve Numbers of other subbasins in the watershed.

Calibration Procedure

The calibration procedure applied in this study is a combination of manual and automatic calibration methods. During the automatic calibration process, the Fox River watershed was divided into three large subwatersheds, which are further subdivided into smaller subbasins. These include the watershed area upstream of *USGS_05545750* gauging station at New Munster (Subwatershed I), the watershed area between New Munster and *USGS_05550000* gauging station at Algonquin (Subwatershed II), and the remaining portion of the watershed downstream of Algonquin (Subwatershed III). The *USGS_05552500* gauging station at Dayton is close to the watershed outlet and is used to calibrate model parameters for Subwatershed III.

The subdivision of the watershed into three components during automatic calibration serves two important purposes. First, it ensures distributed parameter calibration while reducing dimensionality of the auto-calibration problem. This, in turn, results in less computational demand for a given auto-calibration model run. In addition, it enables better sampling of model parameters between their acceptable ranges as the number of calibration parameters becomes smaller. Second, more observed data (e.g., measured discharges from upstream subwatershed) can be used in the process of parameter estimation. Three independent hydrologic models are thus developed based on a single model input's database, and calibration of each model is then conducted separately.

Calibration Scenarios

The purpose of developing the hydrologic simulation model is to analyze the potential impact of climate change on low flow hydrology and surface water availability. In this regard, Bekele and Knapp (2008) developed a hydrologic simulation model for the Fox River watershed. This model is calibrated and validated with periods of daily streamflow records from 1990 to 2003, which is representative of average conditions. Testing the model with drought periods, however, resulted in poor model performance with higher overestimation of streamflows. The average annual precipitation and flows in the Fox River watershed during climate periods of 1931-1960 and 1971-2000 shows considerable variations. Figure 4.1 shows average annual precipitation in the watershed for these two climate periods. The 30-year average annual precipitation during 1931-1960 is about 2 inches below that of the 1971-2000 period. Comparison of average annual flows during the same periods for *USGS_05552500* at Dayton, which is close to the watershed outlet, is presented in Figure 4.2. The 30-year average annual flow for the drier climate period was 4.6 inches lower than that of 1971-2000. The hydrologic response to these different climate conditions affects model calibration, and a single set of model parameters could not fairly simulate both the drought and average conditions. In this regard, Wu and Johnston (2007) conducted a case study looking into the hydrologic response to climate variability in a watershed using the SWAT model. Their findings indicate that model parameters related to evapotranspiration and snowmelt differ with varying climate conditions.

In order to develop a hydrologic model that is capable of simulating the response in streamflows to various climate conditions, two calibration scenarios representing drought (i.e., Calibration Scenario I) and average conditions (i.e., Calibration Scenario II) were considered. The periods of calibration and validation for Calibration Scenario I (CS-I) run from 1960 to 1969 and 1950 to 1959, respectively. Note that in this scenario, the validation period has more drought

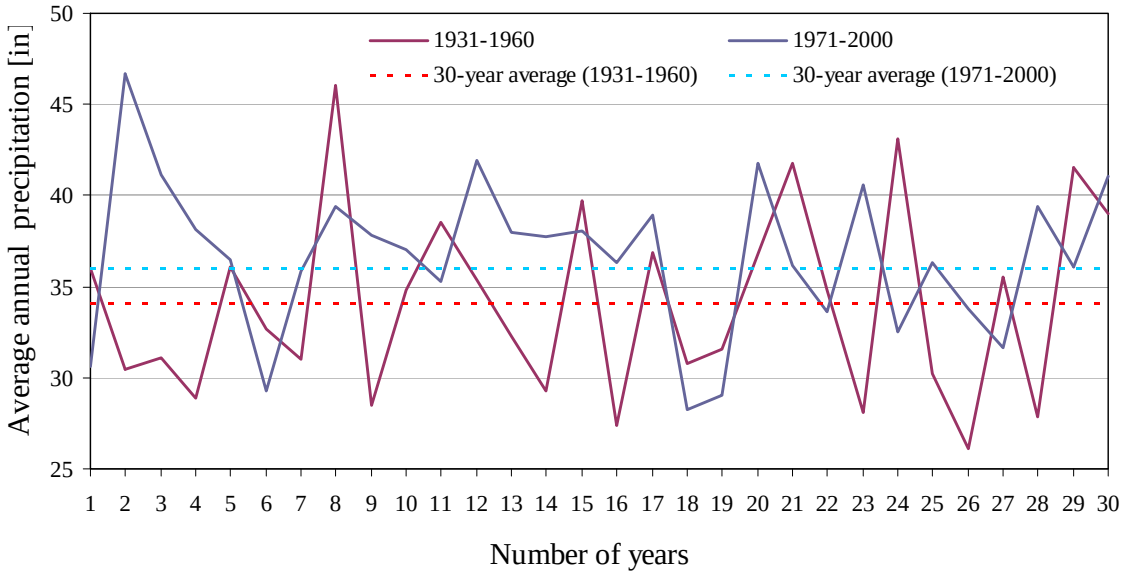

Figure 4.1. Average annual precipitation in the watershed

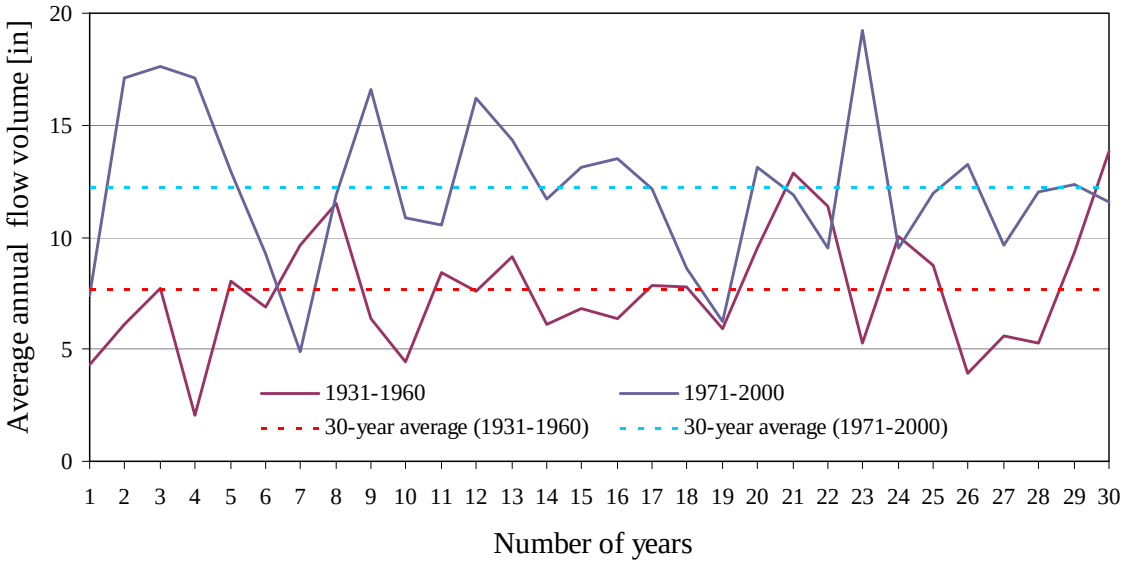

Figure 4.2. Average annual flows for *USGS_055525000* at Dayton

years than the calibration period. In addition, the model performance is evaluated using a long-term drought period spanning from 1931 to 1960. Calibration Scenario II (CS-II), which represents average conditions, has periods of calibration and validation spanning from 1990 to 1999 and from 2000 to 2005, respectively. In this case, the model performance is further evaluated for a 30-year period from 1971 to 2000, which is considered a baseline period for simulation of climate change scenarios.

Subwatershed I: Calibration and Validation of Streamflows

As indicated earlier, the entire Fox River watershed was divided into 207 subbasins or hydrologic response units (HRUs). Using the ArcView interface of SWAT (AVSWAT2000), Subwatershed I is delineated by selecting the streamflow gauging station at New Munster (i.e., *USGS_05545750*) as its watershed outlet, resulting in 49 subbasins as shown in Figure 4.3. The digital land use and soil maps are clipped to the watershed area to determine the land use and soils of each HRU. About 65 percent of Subwatershed I is agricultural lands and urban areas constitute nearly 30 percent of the watershed. The remaining 5 percent of the watershed areas has either wetlands or forest land use. The soils in this part of the watershed belong to the hydrologic soil group B and C with percentages equal to 45 and 55, respectively, exhibiting low to moderate runoff potential. A very small portion of Subwatershed I has soils of hydrologic group A with high infiltration capacity.

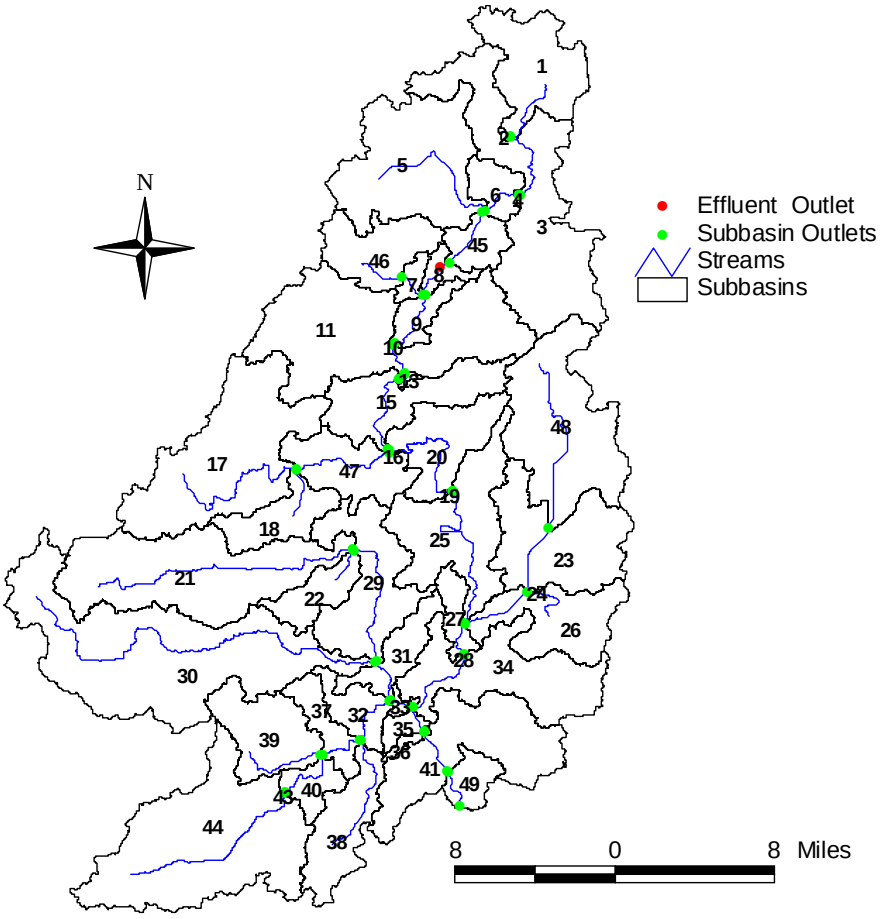

Figure 4.3. Delineation of Subwatershed I into 49 subbasins

In simulating Subwatershed I, climate inputs, including precipitation and temperature, from six weather stations that are close to or within the watershed were used. The weather stations are Germantown (*473058*), Waukesha (*478937*), Whitewater (*479190*), Burlington (*471205*), Union Grove (*478723*), and Lake Geneva (*474457*), which are all located in the Wisconsin portion of the watershed. As indicated earlier, solar radiation, relative humidity, and wind speed are generated based on their corresponding average monthly values using SWAT's weather generator, and the potential evapotranspiration is estimated using the Penman-Monteith method. While setting up the hydrologic simulation model using the ArcView interface of SWAT, input files representing the physical characteristic of the watershed and default parameter estimates for various model processes are automatically generated. These input files can be used to simulate the watershed using the FORTRAN version of SWAT. The FORTRAN version of SWAT is an open source code and thus, allows making modifications and/or adding other model process algorithms as required.

In this study, an automatic calibration tool that employs a genetic algorithm for optimization of model parameter values is developed and integrated into SWAT. The calibration tool is used to automatically adjust the 16 model parameters based on the objective function given in equation (4.1). In executing the automatic calibration routine, the following set of algorithm parameters was adopted: an initial population of 100 chromosomes selected from 1,000 Latin Hypercube samples, a maximum of 20 generations, which is also considered as a convergence criterion, uniform crossover with a probability of 0.5, and a mutation rate of 0.25 with a probability of 1/*l*, where *l* is the chromosome length (i.e., equal to the number of calibration parameters). At the final generation, the chromosome with the minimum *RSR* for daily streamflow is considered to be the optimal set of parameter values. Further manual adjustment of optimal parameter values has been done to ensure satisfactory simulations of all ranges of flows. In this regard, a comparison of observed and simulated daily flow duration curves was made. In addition, observed annual and monthly flow volumes were compared with their corresponding simulated values while adjusting parameter values.

Results for Calibration Scenario I (CS-I)

As indicated earlier, the hydrologic simulation model for Subwatershed I was calibrated for daily streamflows at *USGS_05545750* using automatic and manual calibration methods. The performance evaluation statistics obtained for model calibration and validation at daily, monthly, and annual time-steps are shown in Table 4.3. During calibration, validation and drought periods considered, values of model efficiency (*NSE*) for daily, monthly, and annual simulations were at least 0.65, 0.67, and 0.82, respectively. The maximum *RSR* (i.e., the ratio of root mean square error to the standard deviation of observed data) value and percent bias (*PBIAS*) obtained during all periods and at all time-steps considered were 0.59 and 11.4, respectively. For monthly simulations, an *NSE* value of at least 0.67, a maximum value of 0.57 for *RSR*, and a *PBIAS* of less than 15 percent indicate good model performance. The values of the performance evaluation statistics obtained for daily simulations satisfy the stricter ratings adopted for monthly time-steps and thus, daily simulations can also be judged as good in this particular case.

Table 4.3. Performance Statistics for Flow Simulations at *USGS_05545750* under CS-I

Performance statistic	*Calibration (1960-1969)*	*Validation (1950-1959)*	*Drought period (1940-1960)*
PBIAS (%)	11.4	4.0	5.0
Daily			
RSR (-)	0.59	0.57	0.55
NSE (-)	0.65	0.67	0.70
Monthly			
RSR (-)	0.57	0.51	0.49
NSE (-)	0.67	0.74	0.76
Annual			
RSR (-)	0.42	0.38	0.38
NSE (-)	0.82	0.85	0.86

In addition to the above performance evaluation statistics, graphical comparisons of observed and simulated flows at all time-steps are made. Figures 4.4a and 4.4b illustrate observed and simulated daily hydrographs and flow duration curves for calibration and validation periods. Both figures indicate that model outputs and observed values are generally in good agreement with slight underestimation of flows having less than 20 percent exceedence. The *PBIAS*, which ranges from 4.0 percent to 11.4 percent during all periods considered, also shows that the model tends to slightly underestimate flows. Figures 4.4c and 4.4d show good matches between observed and simulated monthly flow and annual flow volumes, respectively. This is also evident from the performance statistics obtained for each of these flow parameters. For example, the *NSE* values obtained for annual flow volumes is at least 0.82. A graphical comparison of observed and simulated annual base flow volumes was shown in Figure 4.4e. The *NSE* values obtained for annual base flow simulations during the calibration and validation periods were 0.50 and 0.65, respectively. Note that observed base flow volumes are determined using a base flow separation program. The base flow proportions computed using observed and simulated flows were 0.62 and 0.55, respectively, indicating the model's biases towards underestimation of annual base flows.

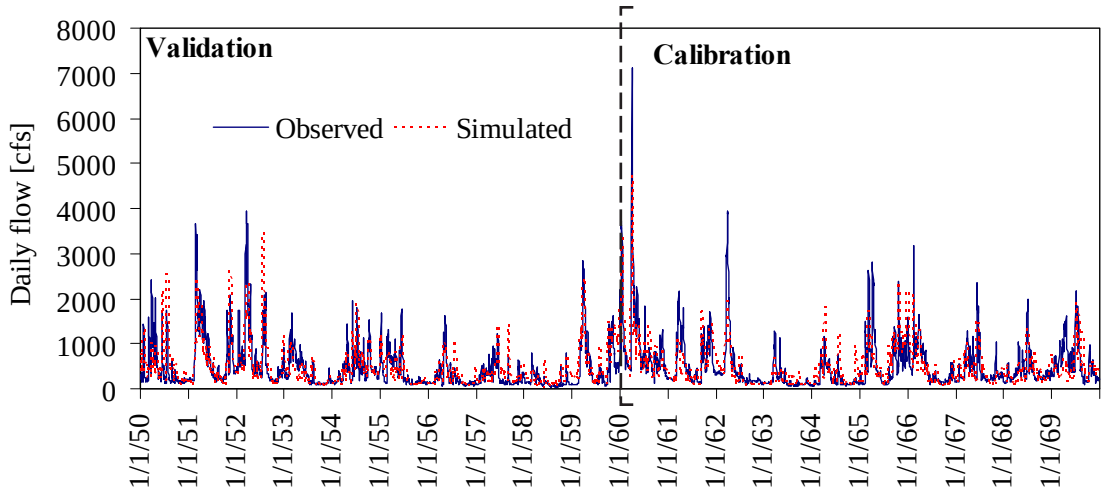

Figure 4.4a Comparison of daily flows for *USGS_05545750* (CS-I)

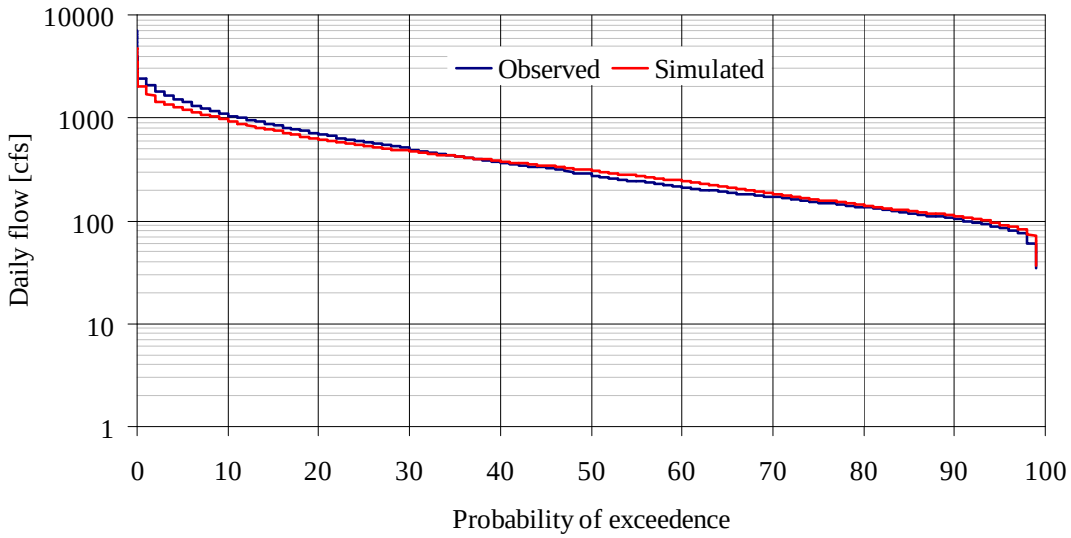

Figure 4.4b. Comparison of daily flow duration curves for *USGS_05545750* (1950-1969)

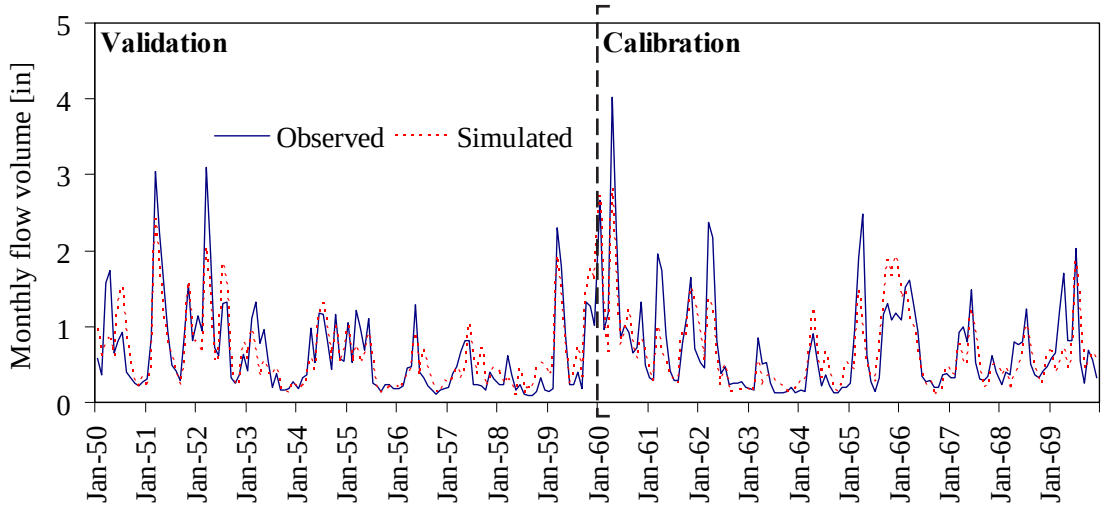

Figure 4.4c. Comparison of monthly flow volumes for *USGS_05545750* (CS-I)

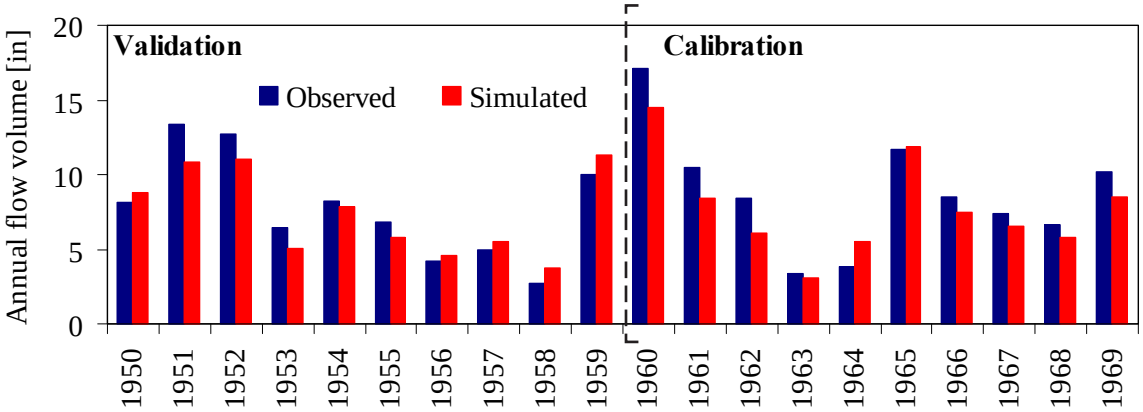

Figure 4.4d. Comparison of annual flow volumes for *USGS_05545750* (CS-I)

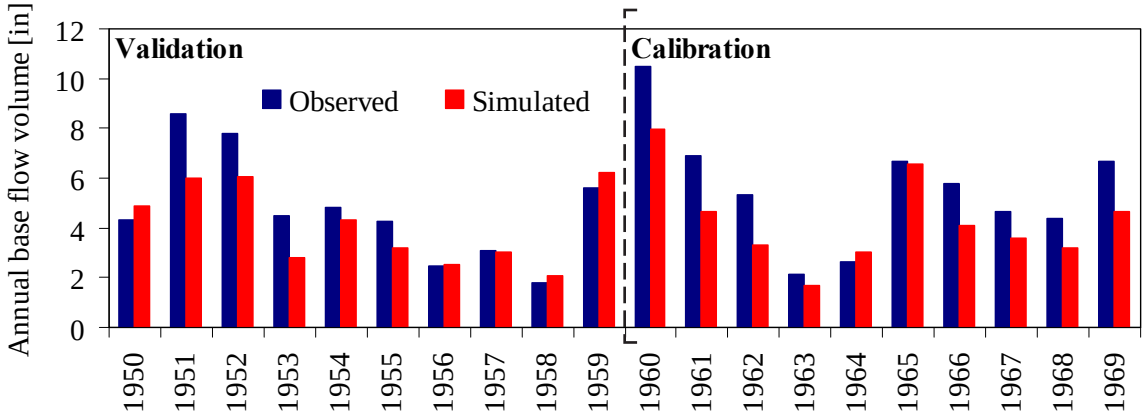

Figure 4.4e. Comparison of annual base flow volumes for *USGS_05545750* (CS-I)

Performance evaluation statistics obtained for flow simulations from 1940 to 1960 confirm that the hydrologic model for Subwatershed I is suitable for simulation of drought periods in future climate change scenarios. The *NSE* values obtained for daily, monthly, and annual simulations were 0.70, 0.76, and 0.86, respectively, indicating the model's good performance in the drought period. Figure 4.4f illustrates the daily flow duration curves for the drought period from 1940 to 1960. The figure generally shows good agreement between observed and simulated flow trends with biases towards overestimation of flows. The *PBIAS* obtained for this period was 5 percent, which is within recommended limits for a very good simulation.

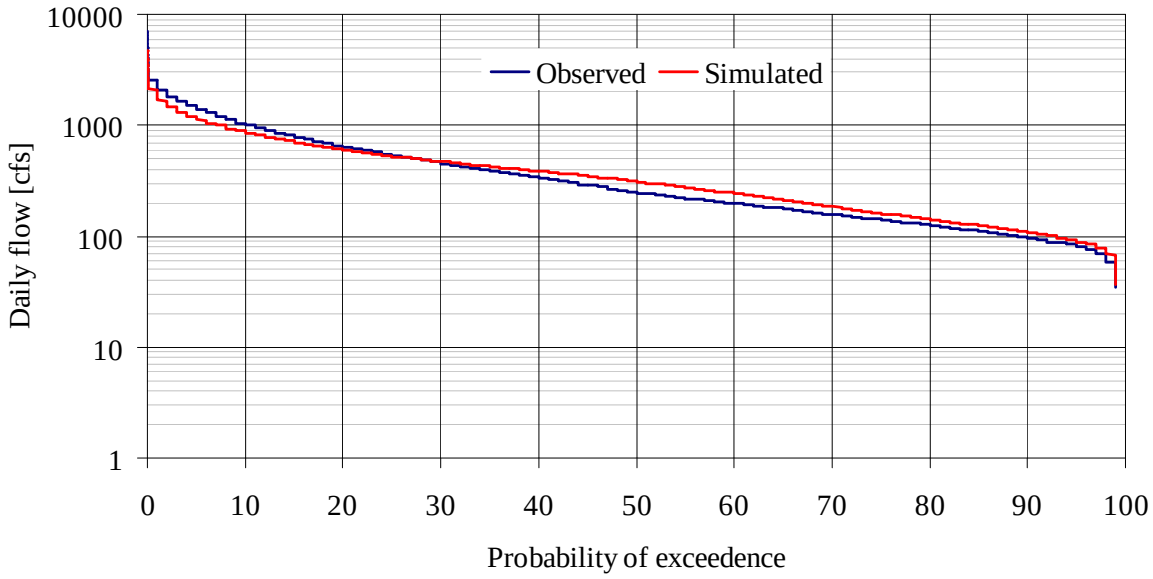

Figure 4.4f. Comparison of daily flow duration curves for *USGS_05545750* (1940-1960)

Results for Calibration Scenario II (CS-II)

Under Calibration Scenario II, the hydrologic model for Subwatershed I is calibrated for 10 years of daily flow records from 1990 to 1999 and is validated using daily flow data from 2000 to 2005. The performance statistics for daily, monthly, and annual flow simulations using CS-II, which represent the present and average conditions, are presented in Table 4.4. The worst *NSE* values obtained during calibration and validation periods were 0.57, 0.62, and 0.78 for daily, monthly, and annual flow simulations, respectively. During the same period, the maximum *RSR* was 0.65 and the maximum absolute *PBIAS* obtained was 7.3 percent. Based on the *RSR* and *NSE* values, the daily and monthly simulations were good in the validation and baseline period, but satisfactory in the calibration period. An absolute *PBIAS* of less than 10 percent in all cases indicates the model's very good performance in simulating average flow trends.

Comparisons of observed and simulated daily flows are presented in Figures 4.5a for calibration and validation periods. Daily flow duration curves constructed using observed and simulated flows were also compared in Figure 4.5b. Both figures show that the model was able to fairly simulate nearly all ranges of flows. The low flows are very well simulated and flows with less than 10 percent exceedence are slightly underestimated. Monthly and annual flow volumes are compared in Figures 4.5c and 4.5d, respectively. The figures generally show good agreement between observed and simulated flow volumes with the exception of years 1993 and 2004. The model overestimated flows in 2004 as also indicated in the *PBIAS* value of -7.3 percent in the validation period, whereas the model underestimated flows in 1993 when record flooding occurred in the Midwest. A graphical comparison of observed and simulated annual base flow volumes are presented in Figure 4.5e. The *NSE* values obtained for annual base flow simulations were 0.38 for calibration and 0.80 for validation. Although the base flow simulations in the validation period were better than in the calibration period, the model generally shows biases towards underestimation under CS-II. The base flow proportions for observed and simulated flows were 0.64 and 0.55, respectively.

Table 4.4. Performance Statistics for Flow Simulations at *USGS_05545750* under CS-II

Performance statistic	*Calibration (1990-1999)*	*Validation I (2000-2005)*	*Baseline Period (1971-2000)*
PBIAS (%)	5.3	-7.3	0.4
Daily			
RSR (-)	0.65	0.61	0.60
NSE (-)	0.57	0.63	0.64
Monthly			
RSR (-)	0.61	0.57	0.54
NSE (-)	0.62	0.68	0.70
Annual			
RSR (-)	0.47	0.40	0.49
NSE (-)	0.78	0.84	0.76

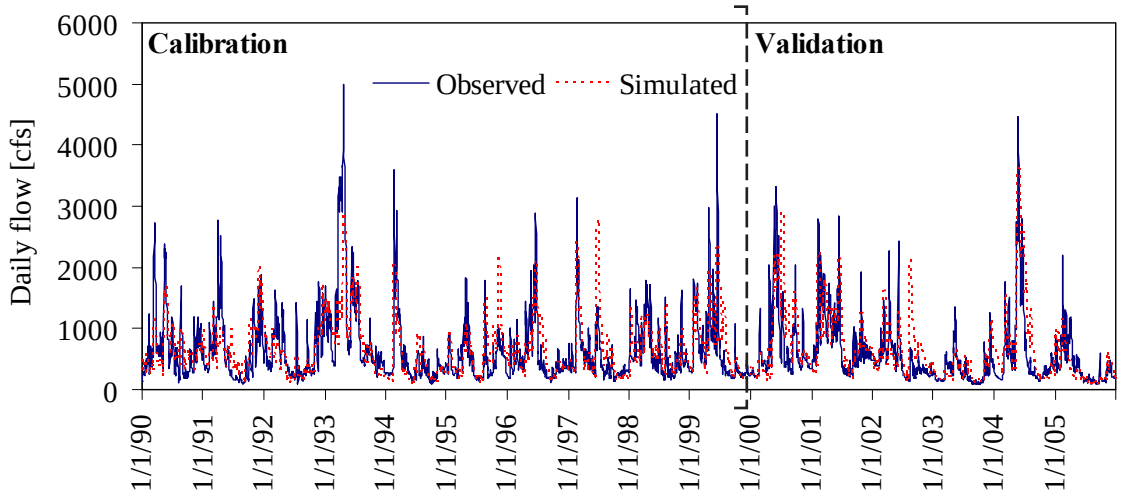

Figure 4.5a. Comparison of daily flows for *USGS_05545750* (CS-II)

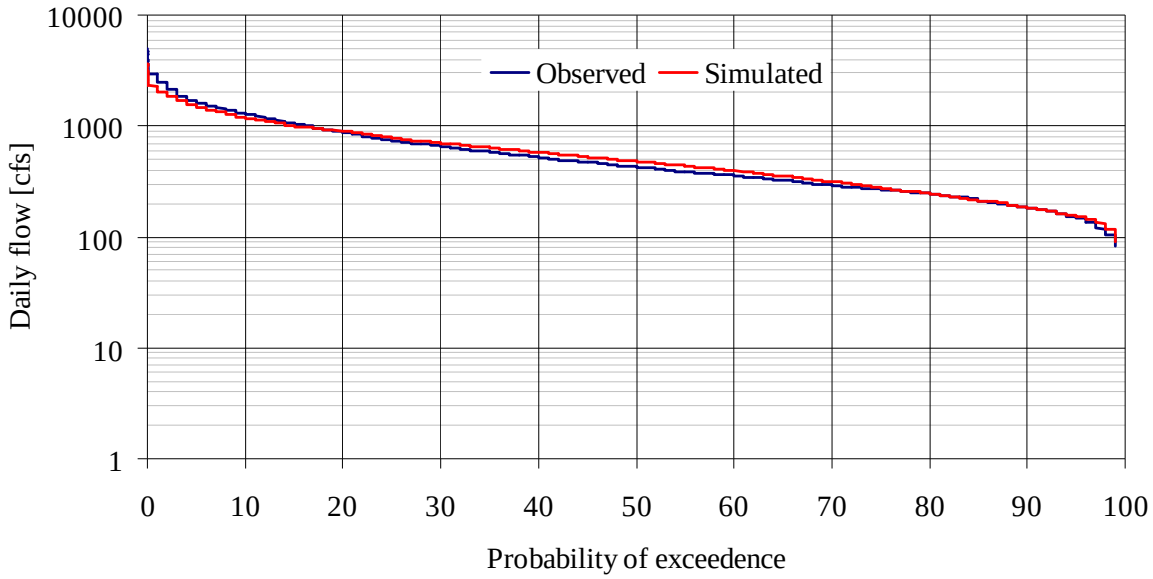

Figure 4.5b. Comparison of daily flow duration curves for *USGS_05545750* (1990-2005)

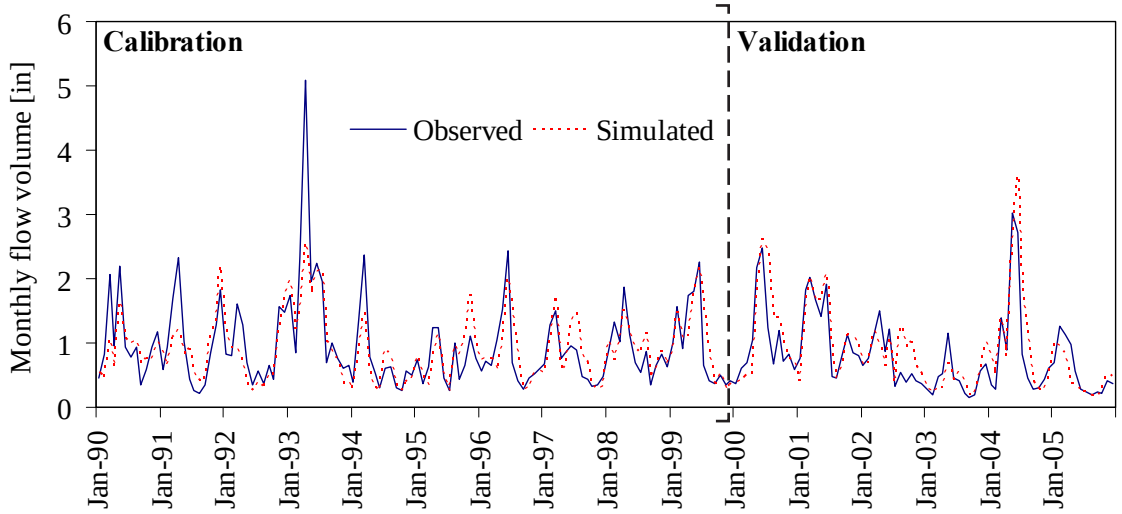

Figure 4.5c. Comparison of monthly flow volumes for *USGS_05545750* (CS-II)

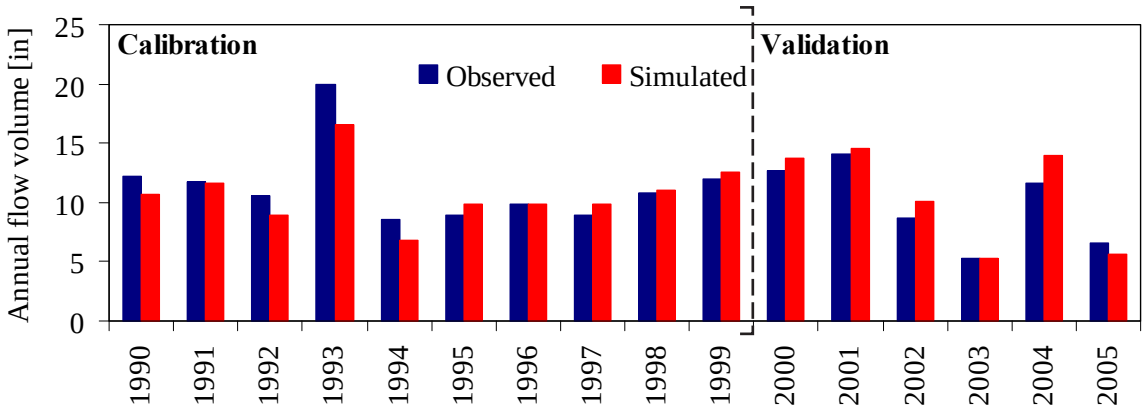

Figure 4.5d. Comparison of annual flow volumes for *USGS_05545750* (CS-II)

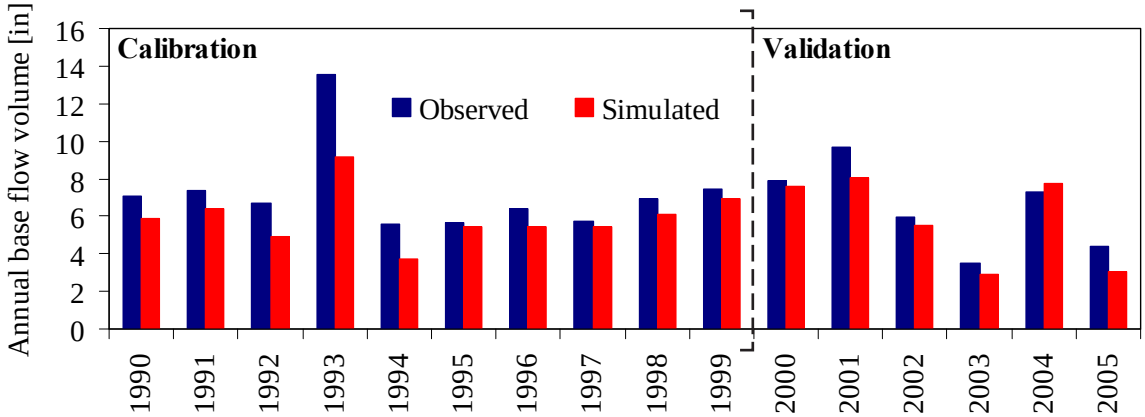

Figure 4.5e. Comparison of annual base flow volumes for *USGS_05545750* (CS-II)

The *NSE* values obtained for daily, monthly, and annual flows are 0.64, 0.70, and 0.76, respectively, and the *PBIAS*, which shows the percent deviation of simulated flows, is 0.4 percent. For the baseline period, a comparison of observed and simulated daily flow duration curves is presented in Figure 4.5f. The simulated flow duration curve and the performance evaluation statistics show that the hydrologic model for Subwatershed I has generally performed better in the baseline period as compared to the calibration and validation periods.

Subwatershed II: Calibration and Validation of Streamflows

The second portion of the larger Fox River watershed is designated as Subwatershed II, and it encompasses the drainage area between the USGS gauging stations at New Munster in Wisconsin (*USGS_05545750*) and Algonquin in Illinois (*USGS_05550000*) with its outlet at Algonquin. This portion of the watershed is divided into 61 subbasins as shown in Figure 4.6. The figure also shows the stream networks, outlets for subbasins and effluent discharge, location of Stratton Dam, and inlet for upstream draining watershed (i.e., outlet of Subwatershed I). The major land uses in this section of the watershed are composed of agriculture (61percent), forest (16 percent), and urban areas (20 percent). Wetlands and water bodies account for about 3 percent of the watershed. More than 80 percent of the soils in Subwatershed II belong to hydrologic group B, having limited runoff potential.

Five weather stations with precipitation and temperature data have been used during simulation of Subwatershed II. The weather stations are Burlington (*471205*), Union Grove (*478723*), Lake Geneva (*474457*), McHenry (*115493*), and Elgin (*112736*), which are close to or within the extent of Subwatershed II. Other climatic input such as solar radiation, relative humidity, and wind speed were generated by the model based on long-term monthly values. Potential Evapotranspiration was estimated using the Penman-Monteith method.

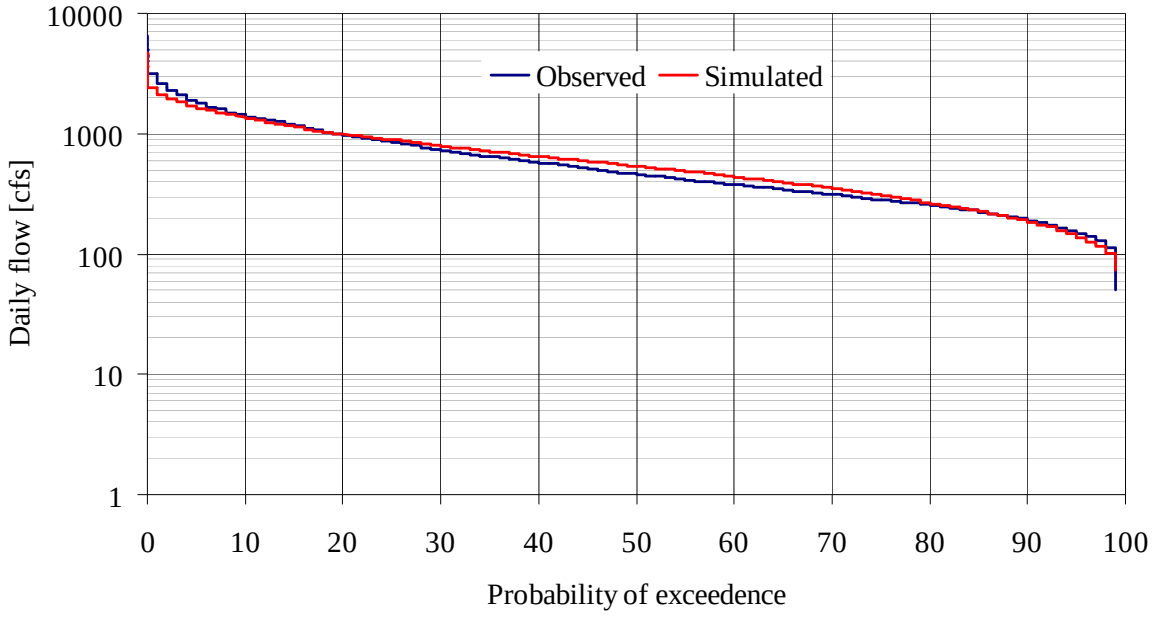

Figure 4.5f. Comparison of daily flow duration curves for *USGS_05545750* (1971-2000)

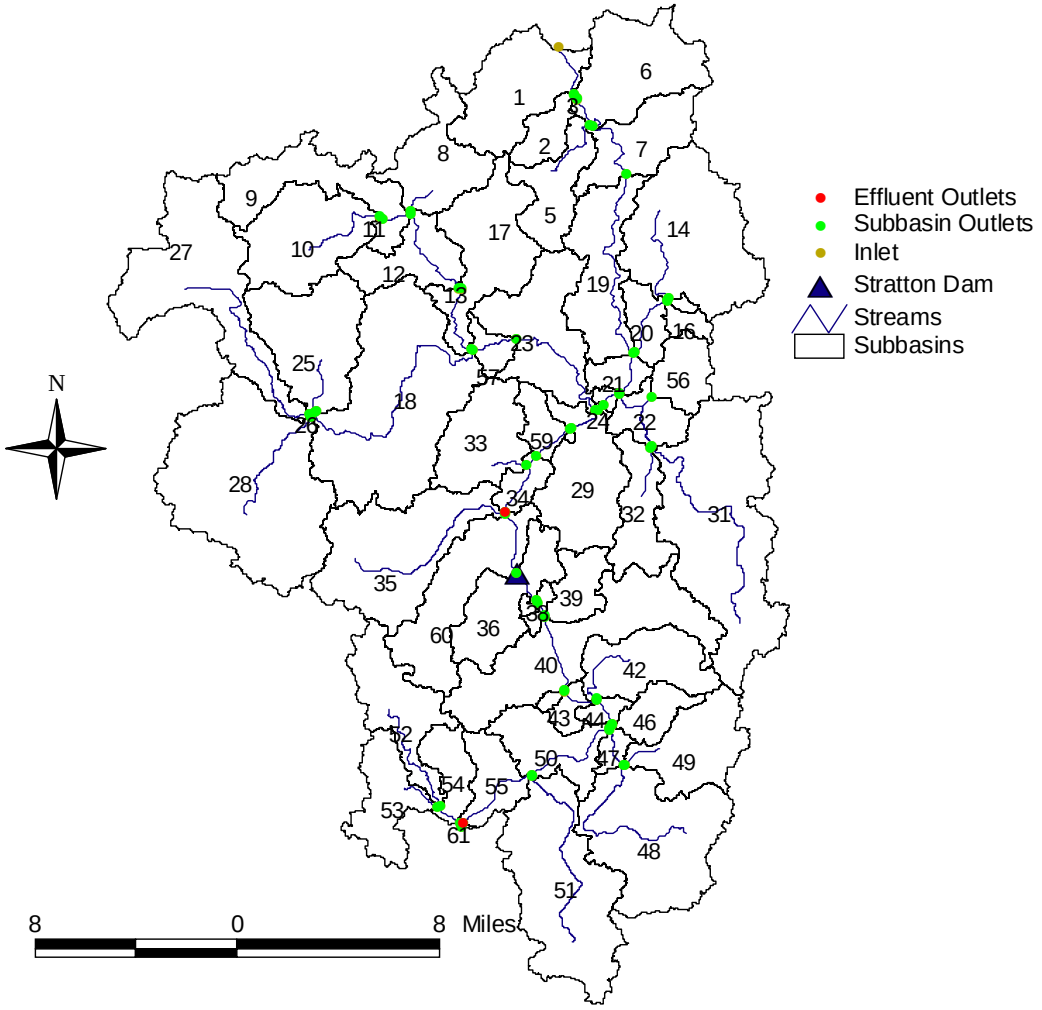

Figure 4.6. Delineation of Subwatershed II into 61 subbasins

During the modeling exercise, the Fox Chain of Lakes is represented as a reservoir controlled at Stratton Dam. Since Subwatershed I drains into Subwatershed II, observed daily flows at *USGS_05545750* near New Munster were used as inflows at the upstream end of this watershed. Once the input files containing the watershed physical characteristics and default parameter estimates of model processes were generated using the ArcView interface of SWAT, the hydrologic model was calibrated for streamflows at *USGS_05550000* using the auto-calibration tool developed in this study. During auto-calibration, the same parameter settings were used for the optimization algorithm. The optimal values of model parameters obtained at the end of the automated calibration were further manually adjusted by comparing duration curves of simulated and observed daily flows. Additionally, simulated annual and monthly flow volumes were compared with their observed counterparts while adjusting these parameter values.

As indicated previously, the level pool reservoir routing method is incorporated into SWAT to determine the daily outflows from Stratton Dam. The routing procedure was able to fairly simulate daily outflow trends from Stratton Dam with *NSE* equal to 0.77, an absolute *PBIAS* of 3.8 percent, and an *RSR* value of 0.48. Figures 4.7a and 4.7b illustrate graphical comparisons of observed and simulated daily hydrographs and duration curves, respectively. The daily duration curves, which were also plotted using outflows from 1991 to 2003, indicate that all flow ranges are simulated very well, and outflows with more than 70 percent exceedence were slightly overestimated.

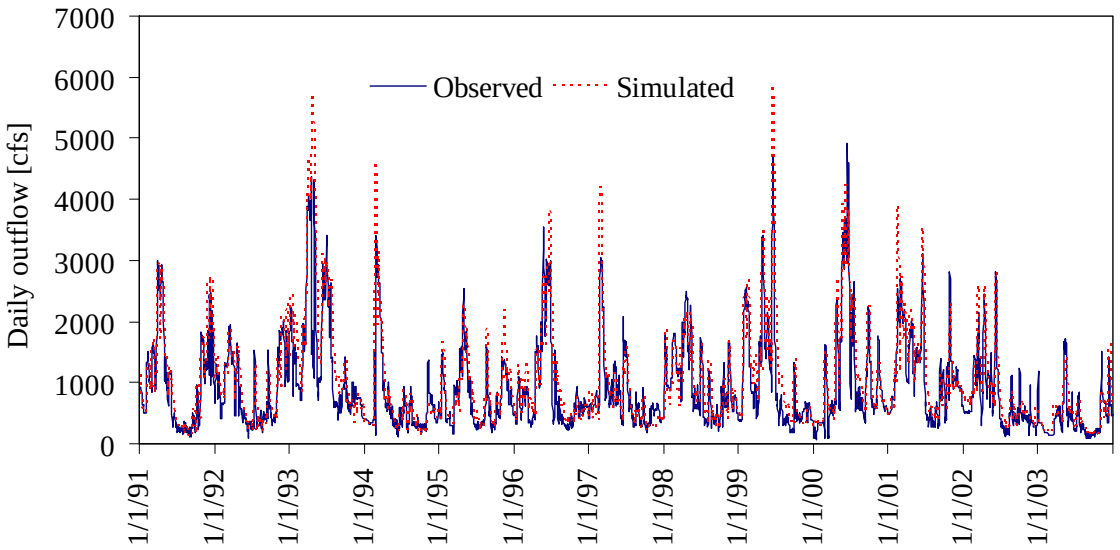

Figure 4.7a. Comparison of daily outflows from Stratton Dam

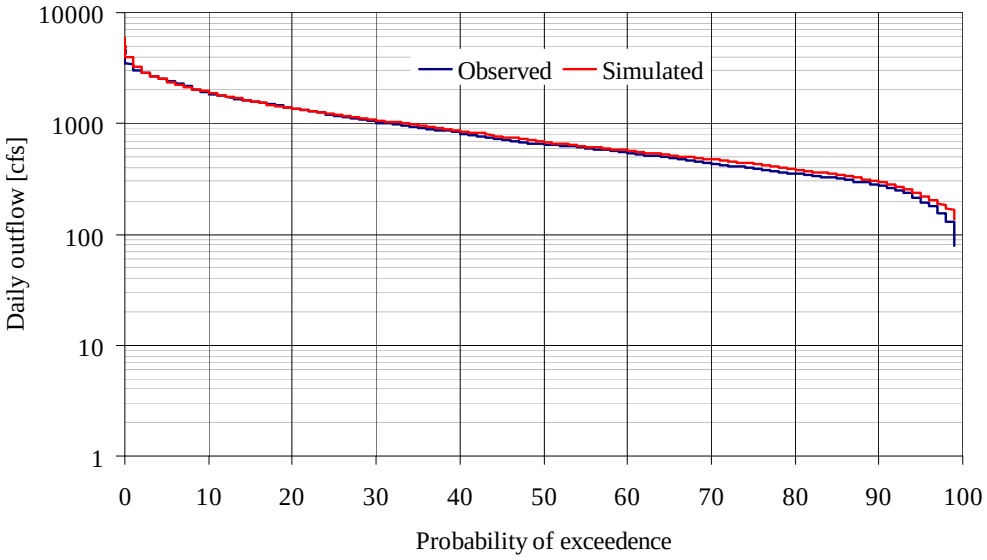

Figure 4.7b. Comparison of daily duration curves for outflows from Stratton Dam

Results for Calibration Scenario I (CS-I)

The performance evaluation statistics obtained for model calibration and validation at daily, monthly, and annual time-steps are presented in Table 4.5. In the calibration and validation periods, values of model efficiency (*NSE*) for daily, monthly, and annual simulations were at least 0.84, 0.92, and 0.96, respectively. The maximum *RSR* value and maximum absolute *PBIAS* obtained during these periods and for all time-steps were 0.4 and 3.2 percent, respectively. Using the same performance rating for daily and monthly simulations, *NSE* values of at least 0.84, a maximum value of 0.4 for *RSR*, and a *PBIAS* of less than 10 percent show that the model performance was very good at both time-steps.

Graphical comparisons of observed and simulated daily hydrographs and flow duration curves are presented in Figures 4.8a and 4.8b, respectively. Both figures illustrate the very good agreement between observed and simulated daily flows as also shown with the values of the performance evaluation statistics. Although the model's bias towards either overestimation or underestimation of flows is minimal with an absolute maximum of *PBIAS* of 3.2 percent, the flow duration curves show slight underestimation of low flows with around 85 percent probability of exceedence.

Graphical comparisons of monthly and annual flow volumes are presented in Figures 4.8c and 4.8d, respectively, and they both show good matches between observed and simulated ones as also evidenced by the performance evaluation statistics obtained. The annual base flow volumes are also compared in Figure 4.6e, and the *NSE* values obtained during the calibration and validation periods were 0.97 and 0.86, respectively. Furthermore, the base flow proportions computed from observed and simulated annual flows were 0.65 and 0.61, respectively, indicating the model's good performance in simulating base flows.

Table 4.5. Performance Statistics for Flow Simulations at *USGS_05550000* under CS-I

Performance statistic	*Calibration (1960-1969)*	*Validation (1950-1959)*	*Drought period (1931-1960)*
PBIAS (%)	-2.5	3.2	-1.9
Daily			
RSR (-)	0.40	0.39	0.52
NSE (-)	0.84	0.85	0.73
Monthly			
RSR (-)	0.28	0.25	0.43
NSE (-)	0.92	0.94	0.81
Annual			
RSR (-)	0.15	0.21	0.36
NSE (-)	0.98	0.96	0.87

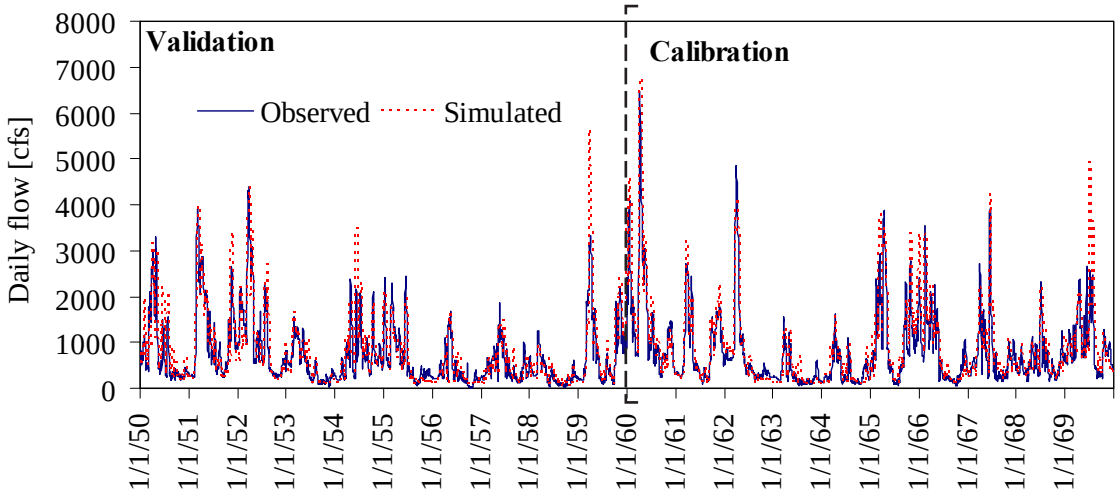

Figure 4.8a. Comparison of daily flows for *USGS_05550000* (CS-I)

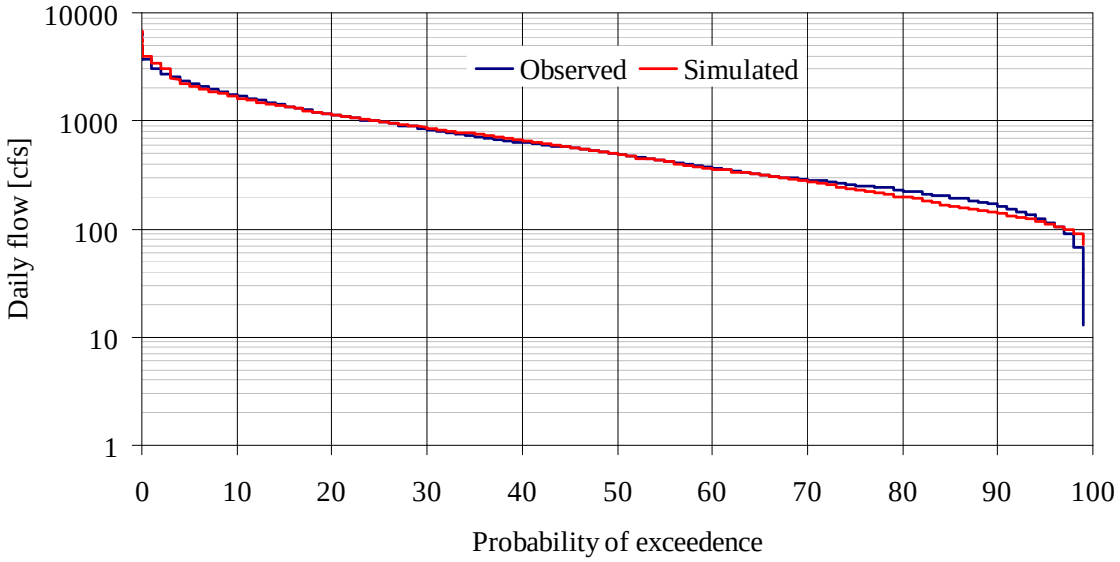

Figure 4.8b. Comparison of daily flow duration curves for *USGS_05550000* (1950-1969)

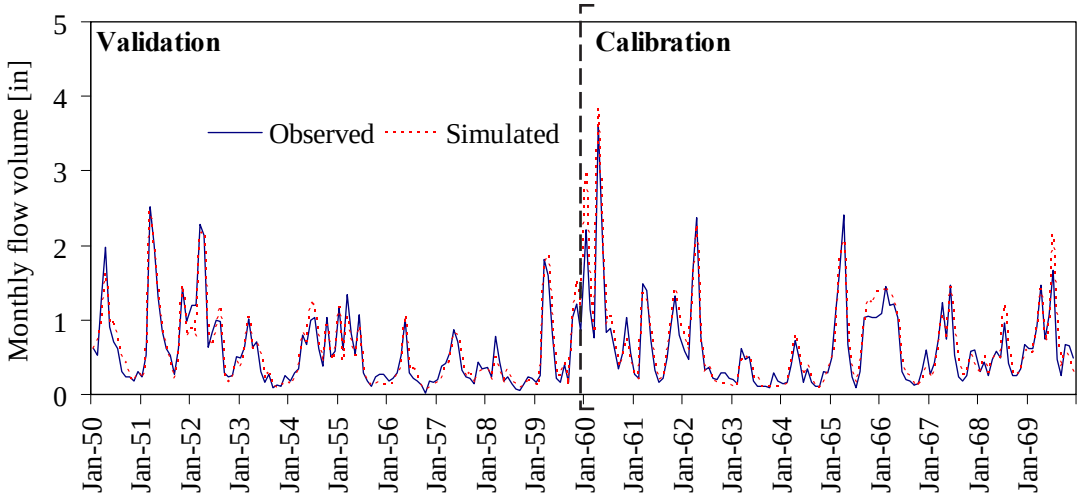

Figure 4.8c. Comparison of monthly flow volumes for *USGS_05550000* (CS-I)

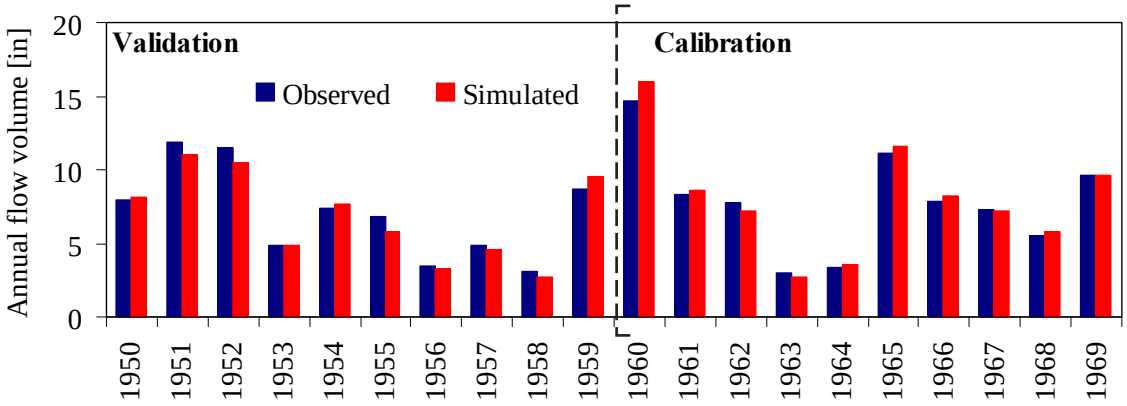

Figure 4.8d. Comparison of annual flow volumes for *USGS_05550000* (CS-I)

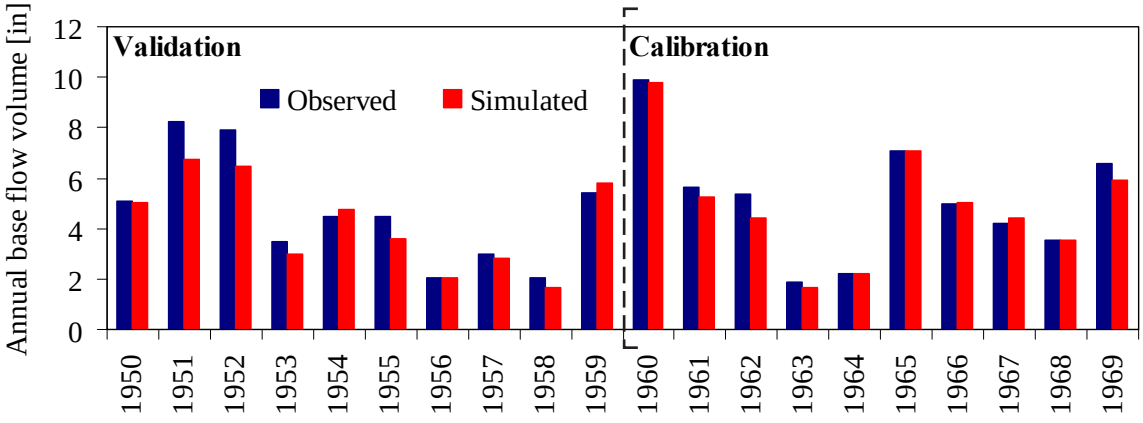

Figure 4.8e. Comparison of annual base flow volumes for *USGS_05550000* (CS-I)

In addition, the hydrologic simulation model for Subwatershed II was evaluated for the drought period from 1931 to 1960, and good simulation results were obtained as shown in the values of the performance statistics presented in Table 4.5. The associated *NSE* values obtained for daily, monthly, and annual simulations were 0.73, 0.81, and 0.87, respectively. Figure 4.8f illustrates the daily flow duration curves for the drought period from 1931 to 1960. The figure generally shows good agreement between observed and simulated flow trends with biases towards overestimation of flows with more than 90 percent exceedence. A *PBIAS* of 1.9 percent was obtained for this period, which is within recommended limits for very good simulation.

Results for Calibration Scenario II (CS-II)

Calibration Scenario II, which could be representative of the average climate period, was employed to calibrate the hydrologic simulation model for Subwatershed II. As indicated before, the calibration period covers 10 years from 1990 to 1999, followed by a validation period of six years from 2000 to 2005. Results of model calibration and validation are presented in Table 4.6, showing the performance statistics for daily, monthly, and annual flow simulations. The table also provides the associated performance evaluation statistics for the baseline period. The *NSE* values obtained for all time-steps and in all periods considered were at least 0.77. The maximum *RSR* value obtained was 0.49 and the maximum absolute *PBIAS* obtained was 7.9 percent. The *RSR*, *NSE*, and *PBIAS* values show that daily, monthly, and annual flow trends were very well simulated in the calibration, validation, and baseline period.

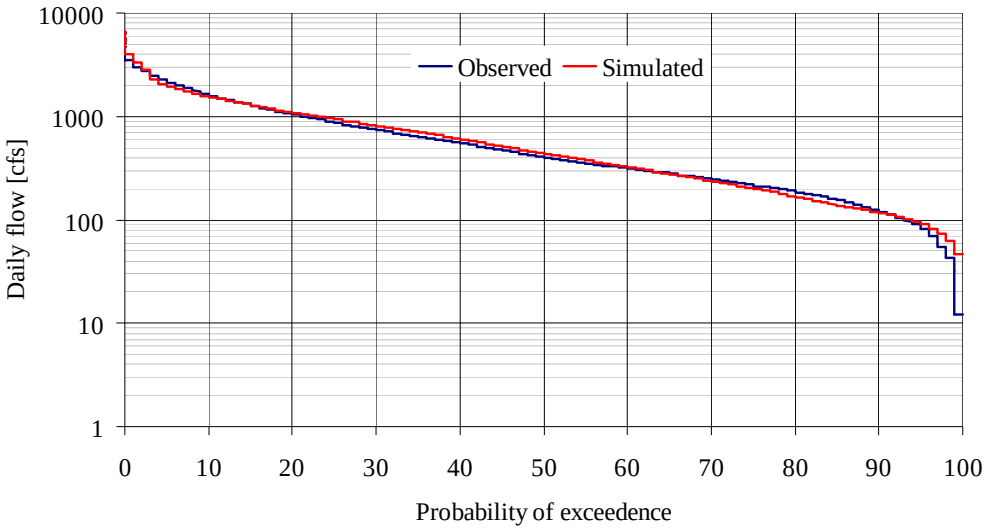

Figure 4.8f. Comparison of daily flow duration curves for *USGS_05550000* (1931-1960)

Table 4.6. Performance Statistics for Flow Simulations at *USGS_05550000* under CS-II

Performance statistic	*Calibration (1990-1999)*	*Validation (2000-2005)*	*Baseline period (1971-2000)*
PBIAS (%)	-4.9	-3.9	-7.9
Daily			
RSR (-)	0.48	0.47	0.44
NSE (-)	0.77	0.78	0.81
Monthly			
RSR (-)	0.38	0.35	0.34
NSE (-)	0.86	0.88	0.89
Annual			
RSR (-)	0.49	0.25	0.40
NSE (-)	0.76	0.94	0.84

Figure 4.9a shows comparisons of observed and simulated daily flows in the calibration and validation periods. The corresponding flow duration curves are presented in Figure 4.9b, and flows with more than 80 percent exceedence are slightly overestimated, which could be due to assumed outflows from Stratton Dam during periods of low and average flow conditions. Flow volumes at monthly and annual time-steps are compared graphically and are presented in Figures 4.9c and 4.9d, respectively. In general, the figures show good matches between observed and simulated values, except for 1993, in which case the model overestimated the annual flows by almost 18 percent.

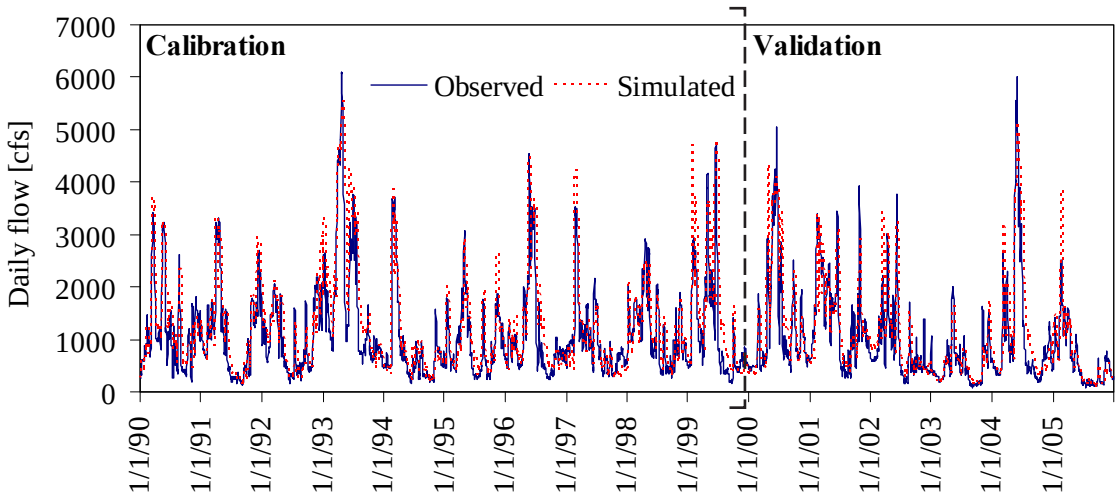

Figure 4.9a. Comparison of daily flows for *USGS_05550000* (CS-II)

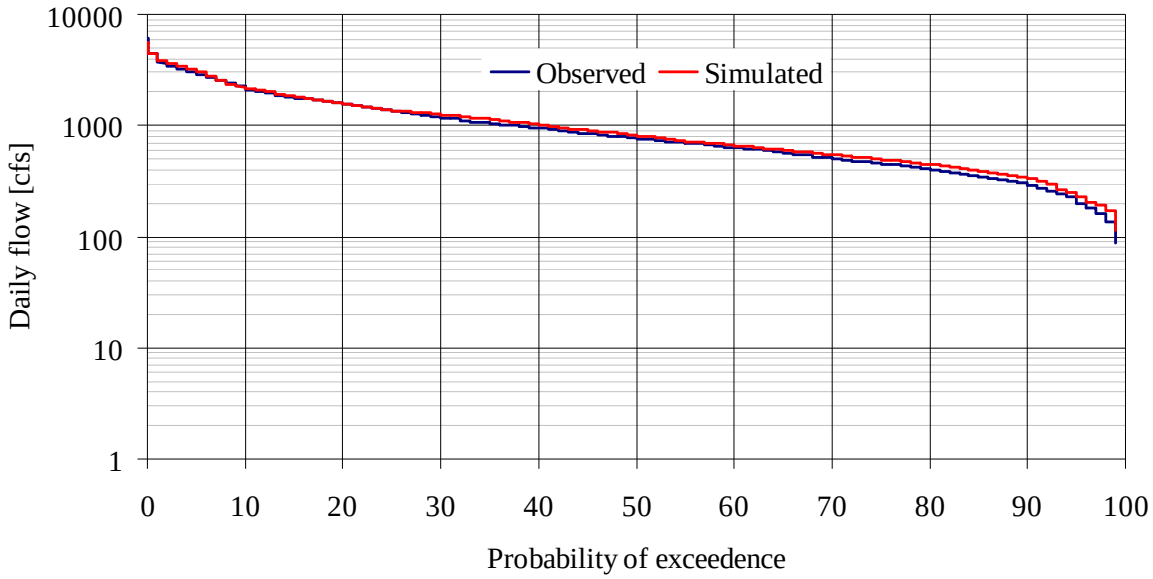

Figure 4.9b. Comparison of daily flow duration curves for *USGS_05550000* (1990-2005)

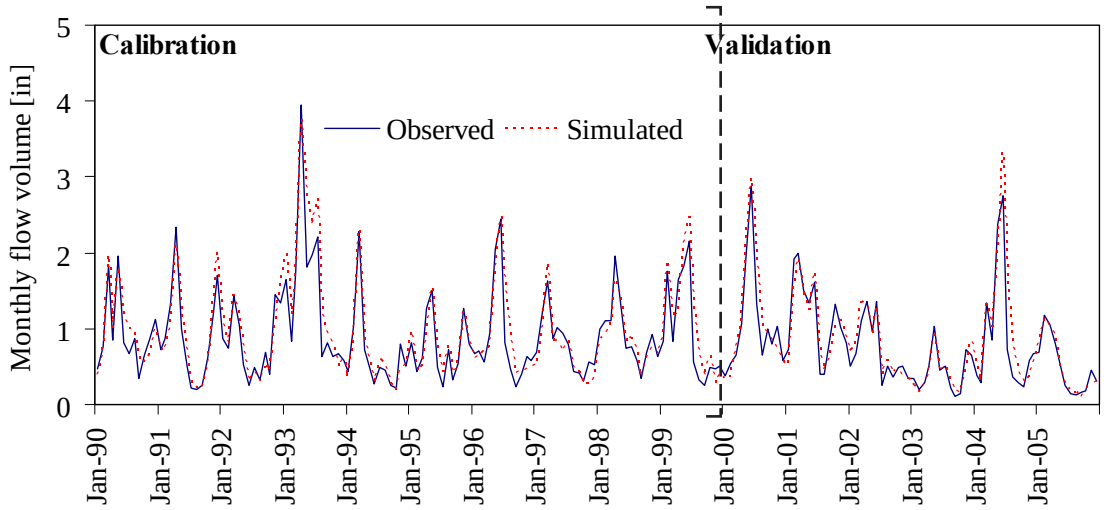

Figure 4.9c. Comparison of monthly flow volumes for *USGS_05550000* (CS-II)

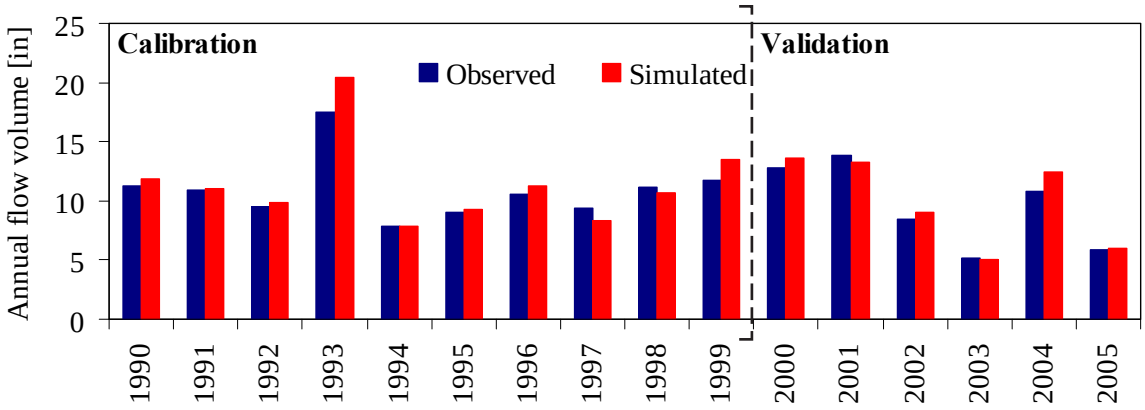

Figure 4.9d. Comparison of annual flow volumes for *USGS_05550000* (CS-II)

A graphical comparison of observed and simulated annual base flow volumes is presented in Figure 4.9e. Base flow proportions computed using observed and simulated values were 0.65 and 0.61, respectively, and the *NSE* values for calibration and validation periods were 0.84 and 0.90, respectively. The figure, the base flow proportions computed, and the *NSE* values all demonstrate the model's good performance in base flow simulations. For the baseline period, *NSE* values of 0.81, 0.89, and 0.84 were obtained for daily, monthly, and annual flow simulations, respectively, and the average deviation of simulated flows (*PBIAS*) was -7.9 percent, showing the model's bias toward overestimation of flows. A graphical comparison of observed and simulated daily flow duration curves is presented in Figure 4.9f. Results for calibration, validation, and baseline periods indicate that the hydrologic model for Subwatershed II is capable of simulating ranges of flows with good accuracy.

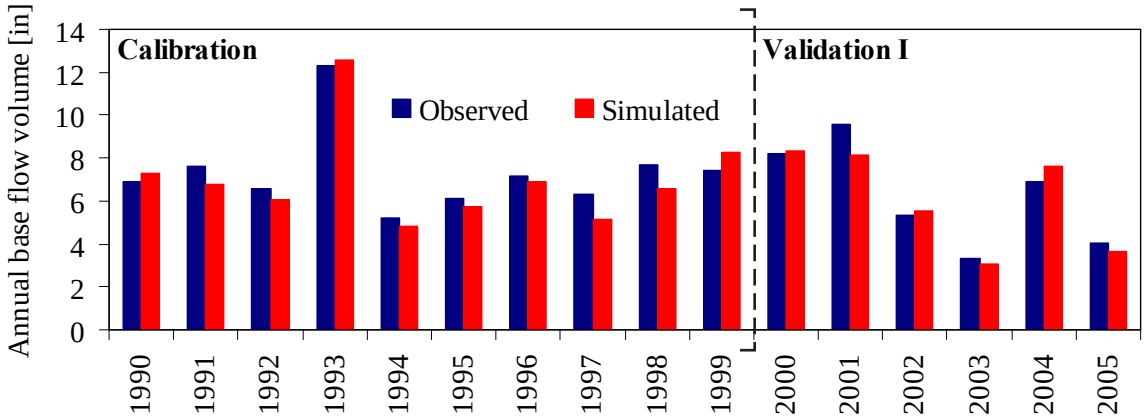

Figure 4.9e. Comparison of annual base flow volumes for *USGS_05550000* (CS-II)

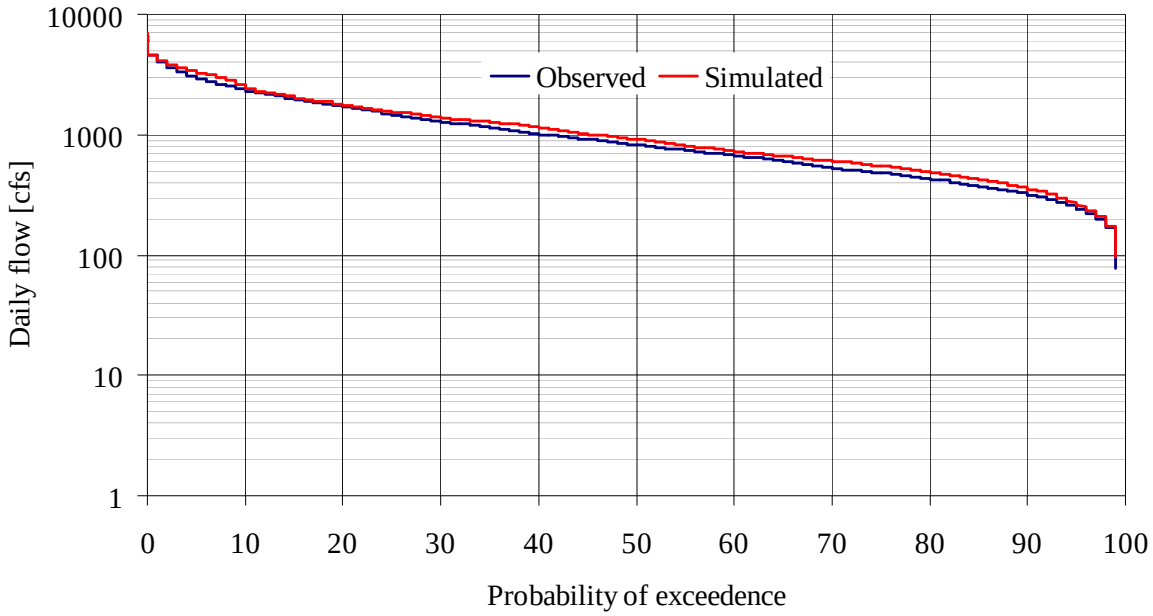

Figure 4.9f. Comparison of daily flow duration curves for *USGS_05550000* (1971-2000)

Subwatershed III: Calibration and Validation of Streamflows

Subwatershed III is the watershed area downstream of the *USGS_05550000* at Algonquin, and it is the largest of the three subwatersheds with an area of 1216 square miles. The *USGS_05552500* at Dayton is close to the watershed outlet and is, therefore, used for calibration and validation of streamflows. As shown in Figure 4.10, Subwatershed III is divided into 97 subbasins with slopes ranging from 0.7 to 8.2 percent, with its average at 2.5 percent. Agriculture is the major land use in this section of the Fox River watershed, accounting for 82 percent. The remaining portion of the watershed has urban areas (17 percent) and forest (1 percent). The soils in this portion of the watershed have moderate infiltration capacity with more than 85 percent belonging to hydrologic soil group B. The remaining portion of the watershed belongs to hydrologic soil group C (11 percent) and D (1 percent), having soils with a slow infiltration capacity or good runoff potential.

During simulation of Subwatershed III, precipitation and temperature data obtained from four weather stations that are located within the watershed or in a closer proximity were used. These stations are Elgin (*112736*), Aurora (*110338*), Paw Paw (*116661*), and Ottawa (*116526*). Climate inputs such as solar radiation, relative humidity, and wind speed were automatically generated by the SWAT model using long-term average monthly values. Potential evapotranspiration was estimated by the Penman-Monteith method. Observed streamflow data for *USGS_05550000* at Algonquin were used as inflows since upstream subwatersheds drain into Subwatershed III. The automatic calibration routine using the same parameter setting was used to calibrate daily streamflows for *USGS_05552500* at Dayton, which is very close to the outlet of Subwatershed III. Both calibration scenarios for drought and average conditions were employed.

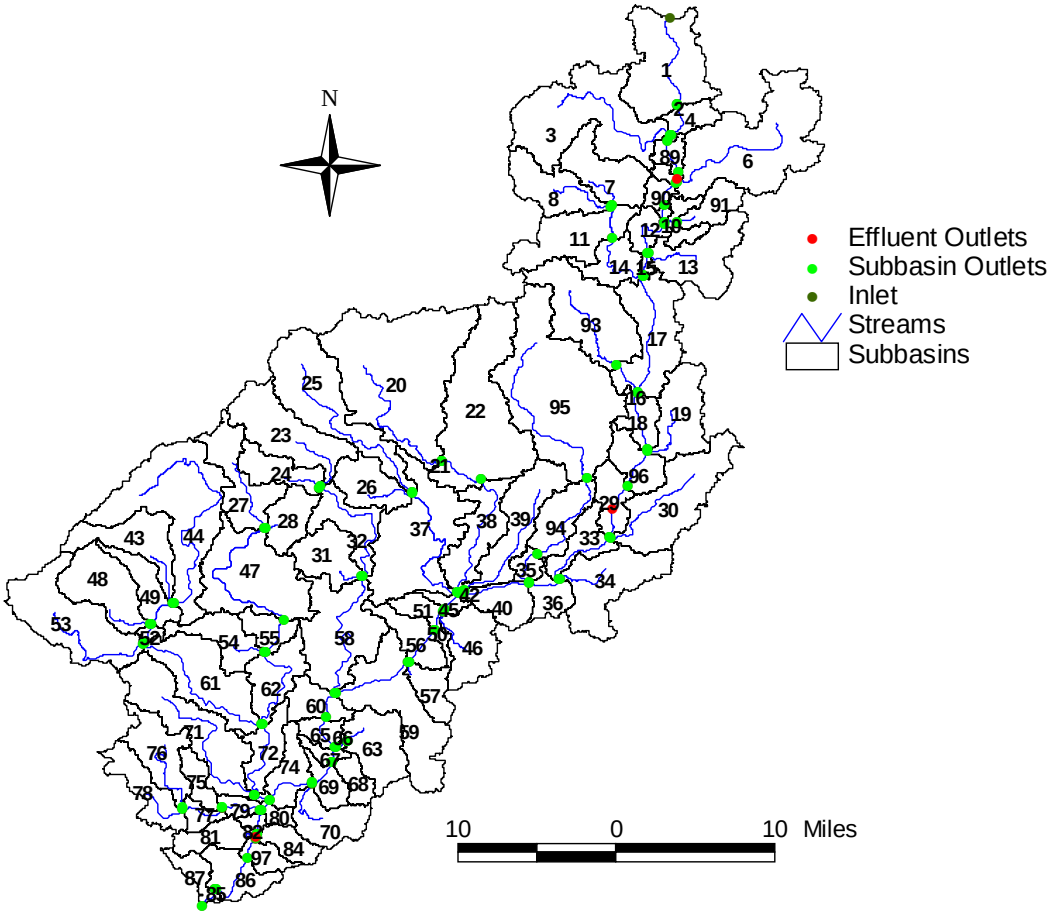

Figure 4.10. Delineation of Subwatershed III into 97 subbasins

Results for Calibration Scenario I (CS-I)

Under Calibration Scenario I, the hydrologic simulation model for Subwatershed III was calibrated for streamflows from 1960 to 1969, and it was validated using flows from 1950 to 1959. Further model evaluation was performed in severe drought periods from 1931 to 1960. The model performance under this calibration scenario was quantified using evaluation statistics (i.e., *RSR*, *NSE*, and *PBIAS*) as presented in Table 4.7. The calibration *NSE* values obtained for daily, monthly, and annual flow simulations were 0.63, 0.84, and 0.93, respectively; comparable *NSE* values were also obtained for the validation period. In the calibration and validation period, the maximum residual variations (*RSR*) obtained for daily, monthly, and annual simulations were 0.65, 0.40, and 0.28, respectively, and the *PBIAS* was less than 5 percent in all cases. Based on the evaluation statistics, the monthly simulations were very good. Applying the same performance ratings, daily simulations can be judged as satisfactory, although a less stringent guideline should apply.

Table 4.7. Performance Statistics for Flow Simulations at *USGS_05552500* under CS-I

Performance statistic	*Calibration (1960-1969)*	*Validation I (1950-1959)*	*Drought period (1931-1960)*
PBIAS (%)	4.4	3.7	2.5
Daily			
RSR (-)	0.61	0.65	0.61
NSE (-)	0.63	0.57	0.62
Monthly			
RSR (-)	0.40	0.40	0.38
NSE (-)	0.84	0.84	0.85
Annual			
RSR (-)	0.27	0.28	0.26
NSE (-)	0.93	0.92	0.93

Graphical comparisons were made between simulated and observed daily flows and duration curves in Figures 4.11a and 4.11b, respectively. The daily duration curve constructed using simulated flows matches very well with that of observed ones, showing the model's ability to simulate a range of flows. As it is reflected in the positive values of *PBIAS*, underestimation of high flows is evident in the simulated daily hydrograph or duration curve.

Figures 4.11c and 4.11d illustrate good matches between observed and simulated monthly flow and annual flow volumes, respectively. A graphical comparison of observed and simulated annual base flow volumes was also made in Figure 4.11e. The *NSE* values obtained for annual base flow simulations during the calibration and validation periods were 0.76 and 0.75, respectively, and the proportions of observed and simulated base flows were 0.63 and 0.57, respectively, indicating that simulated base flow volumes were slightly underestimated with a percentage deviation of less than 10 percent.

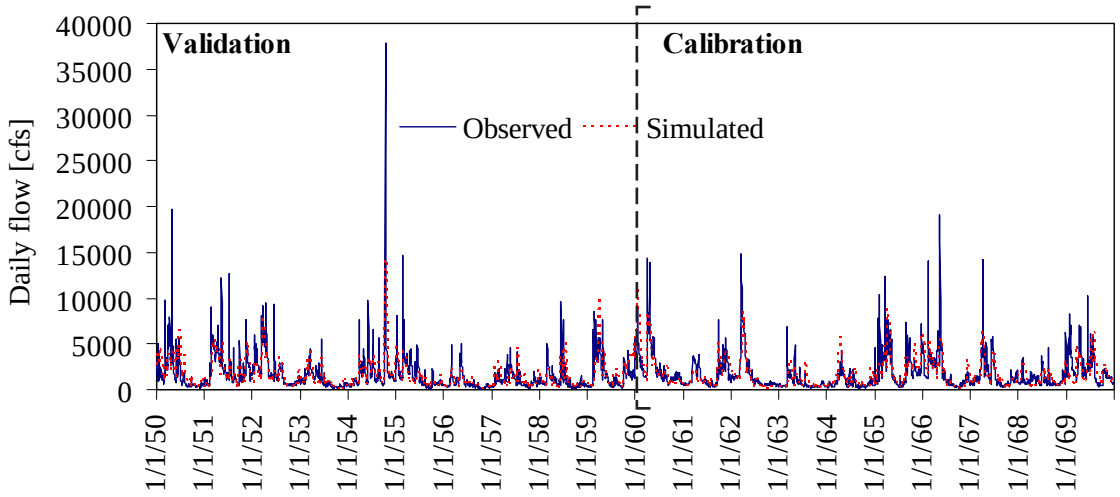

Figure 4.11a. Comparison of daily flows for *USGS_05552500* (CS-I)

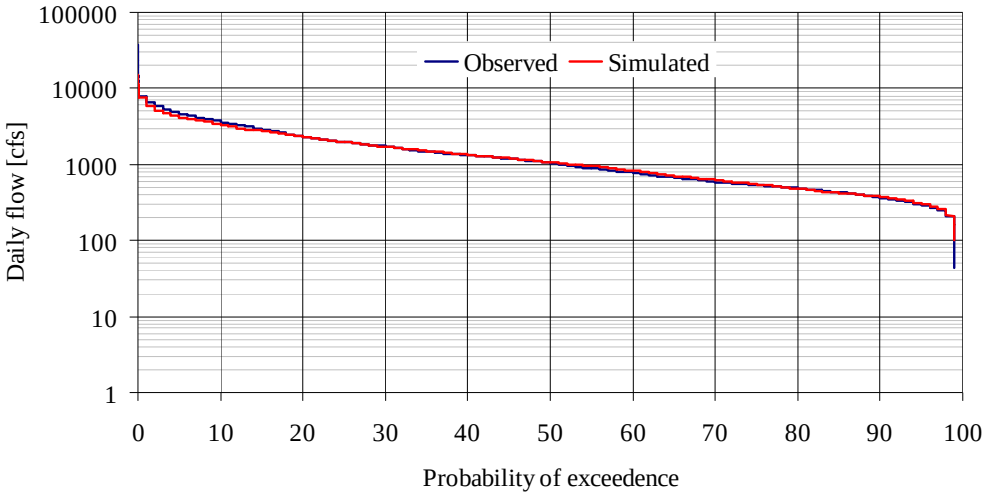

Figure 4.11b. Comparison of daily flow duration curves for *USGS_05552500* (1950-1969)

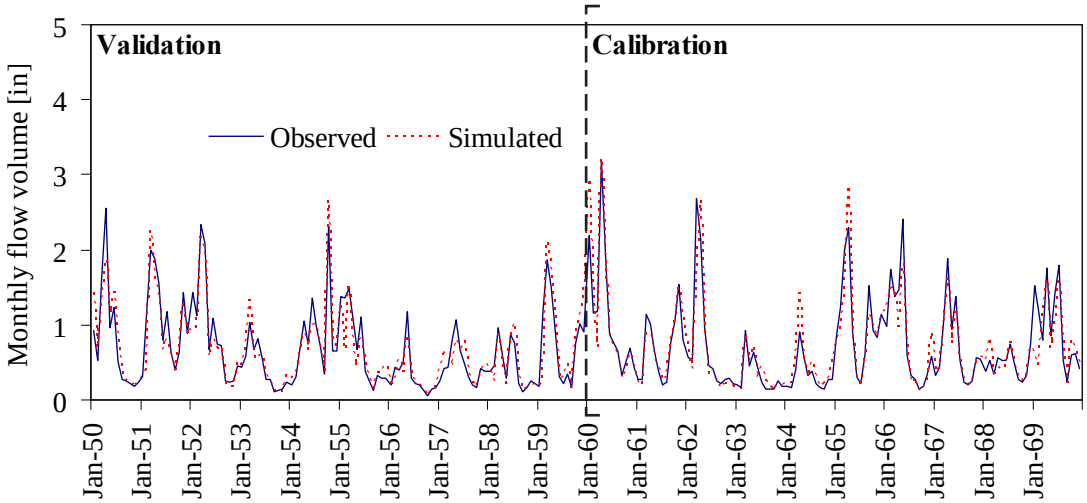

Figure 4.11c. Comparison of monthly flow volumes for *USGS_05552500* (CS-I)

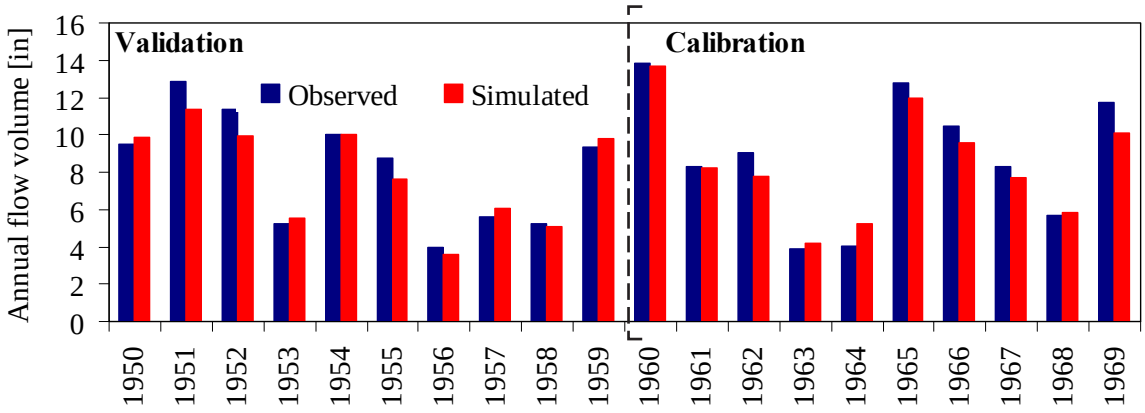

Figure 4.11d. Comparison of annual flow volumes for *USGS_05552500* (CS-I)

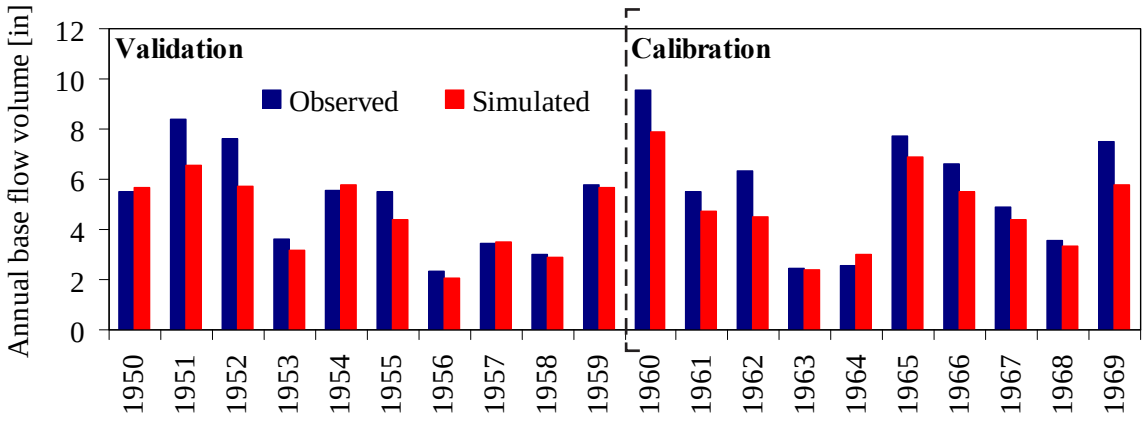

Figure 4.11e Comparison of annual base flow volumes for *USGS_05552500* (CS-I)

The hydrologic simulation model for Subwatershed III was also evaluated for the drought period from 1931 to 1960, and satisfactory to very good simulation results were obtained for daily and monthly flows as indicated in the values of the evaluation statistics presented in the last column of Table 4.7. The daily flow duration curves for this period of evaluation are illustrated in Figure 4.11f, and in general, it shows good agreement between observed and simulated flow trends with an average deviation of 2.5 percent.

Results for Calibration Scenario II (CS-II)

Values of the performance evaluation statistics obtained under Calibration Scenario II are presented in Table 4.8. The worst *NSE* values obtained for daily, monthly, and annual simulations were 0.51, 0.81, and 0.84, respectively. The maximum residual variations (*RSR*)

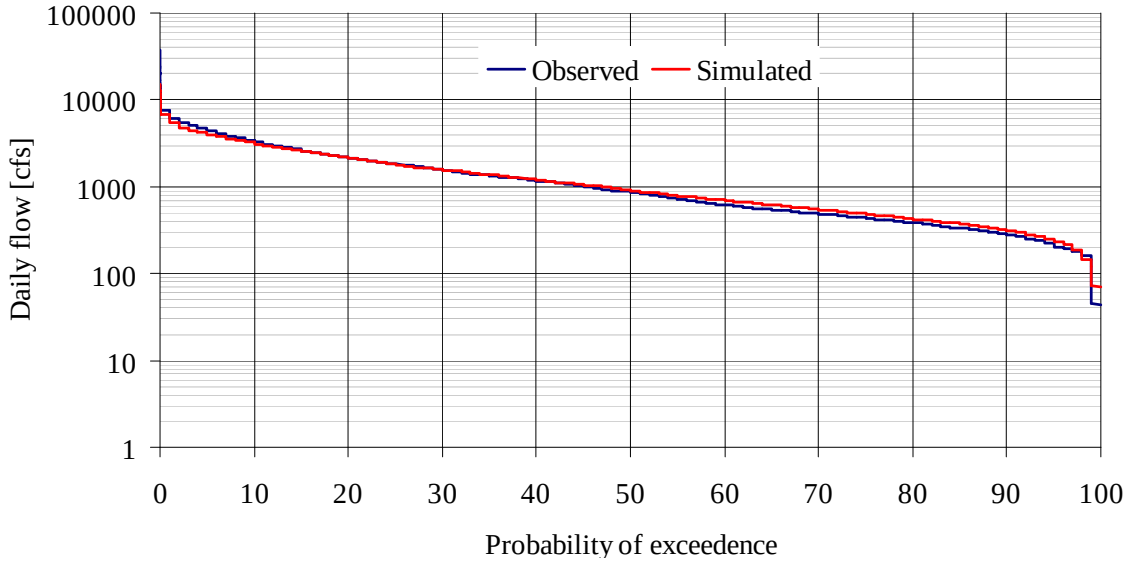

Figure 4.11f. Comparison of daily flow duration curves for *USGS_05552500* (1931-1960)

Table 4.8. Performance Statistics for Flow Simulations at USGS_05552500 under CS-II

Performance statistic	*Calibration (1990-1999)*	*Validation I (2000-2005)*	*Baseline period (1971-2000)*
PBIAS (%)	6.6	7.6	5.3
Daily			
RSR (-)	0.70	0.54	0.63
NSE (-)	0.51	0.71	0.61
Monthly			
RSR (-)	0.43	0.32	0.38
NSE (-)	0.81	0.89	0.86
Annual			
RSR (-)	0.40	0.32	0.29
NSE (-)	0.84	0.90	0.91

during calibration and validation periods were 0.70, 0.43, and 0.4 for daily, monthly, and annual simulations in that order. The *PBIAS* values were 6.6 percent and 7.6 percent for the calibration and validation periods, respectively. According to the model evaluation guidelines, the model simulated monthly streamflow trends very well in both calibration and validation periods. Model performance can be rated as satisfactory in the calibration period and good in the validation period if the same guidelines for monthly simulations were applied.

In addition to the quantitative statistics, graphical comparisons were made between observed and simulated hydrographs and duration curves. Figure 12a shows that simulated daily flows satisfactorily match that of observed ones. The daily duration curves for observed and simulated flows, as illustrated in Figure 12b, indicate that ranges of flows were adequately simulated with a slight underestimation of high flows with less than 5 percent exceedence. As the quantitative statistics indicated very good monthly simulations, Figure 12c also shows that simulated monthly flow volumes closely match their observed counterparts. Observed and simulated annual flow volumes and their base flow components are compared in Figures 12d and 12e. Simulated annual flow volumes show good agreement with observed ones, whereas the base flows were consistently underestimated. This is also evident in the lower *NSE* values of 0.32 and 0.48 obtained in the calibration and validation periods, respectively. The base flow proportions for observed and simulated flows were 0.65 and 0.57, respectively, showing an average variation of 11 percent.

For the baseline period from 1971 to 2000, *NSE* values obtained for daily, monthly, and annual flow simulations were 0.61, 0.86, and 0.91, respectively, and the average deviation of simulated flows (*PBIAS*) was 5.3 percent. According to the performance guidelines, the model simulated flow trends in the baseline period varied from good at daily to very good at annual time-steps. A graphical comparison of observed and simulated daily flow duration curves is presented in Figure 4.12f, showing slight underestimation of extreme flows. The results obtained in the calibration, validation, and baseline periods indicate that the hydrologic model for Subwatershed II simulated all ranges of flows and flow trends at all time-steps with reasonably good accuracy.

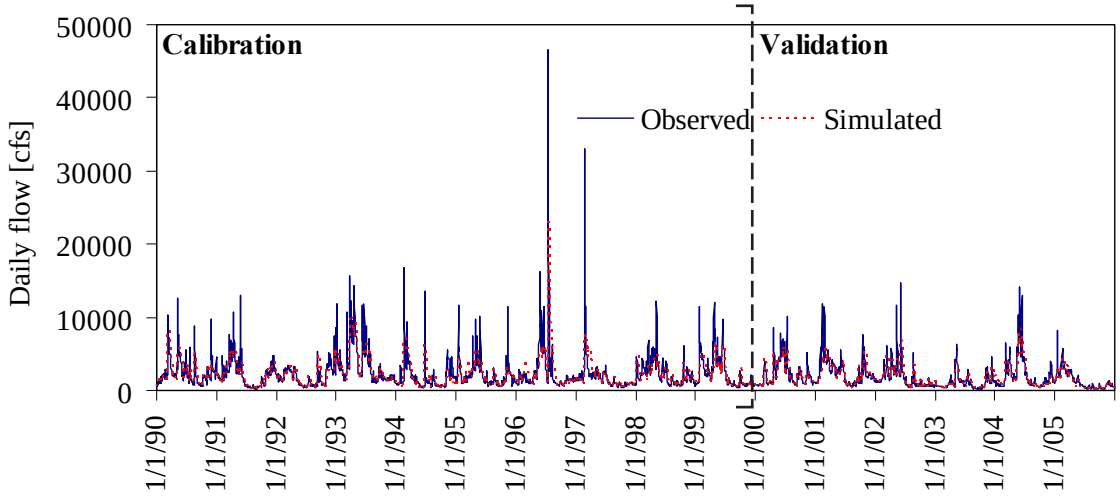

Figure 4.12a. Comparison of daily flows for *USGS_05552500* (CS-II)

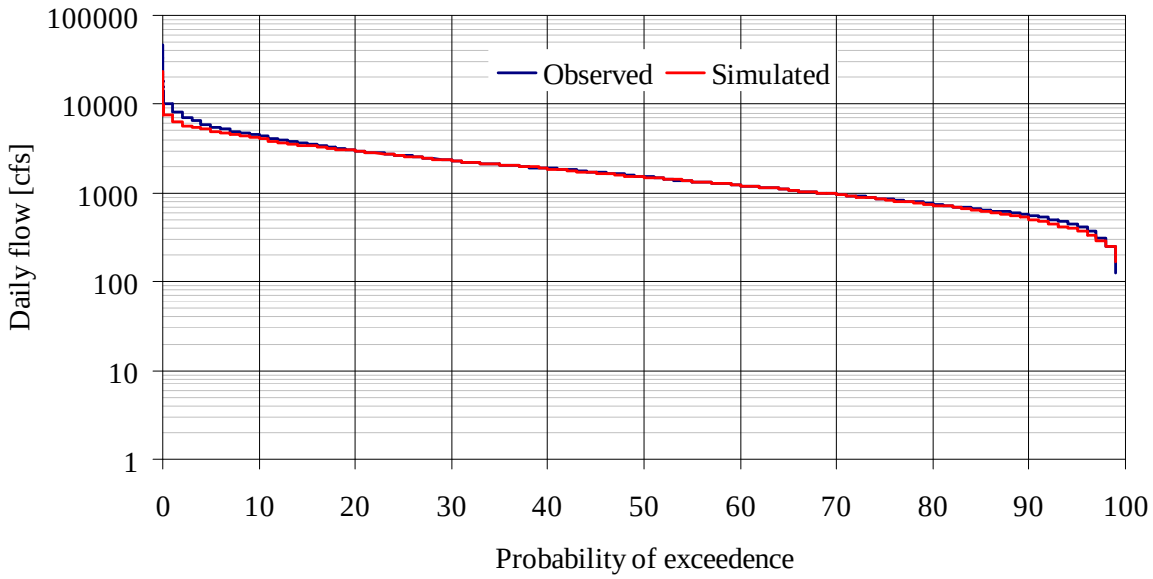

Figure 4.12b. Comparison of flow duration curves for *USGS_05552500* (1990-2005)

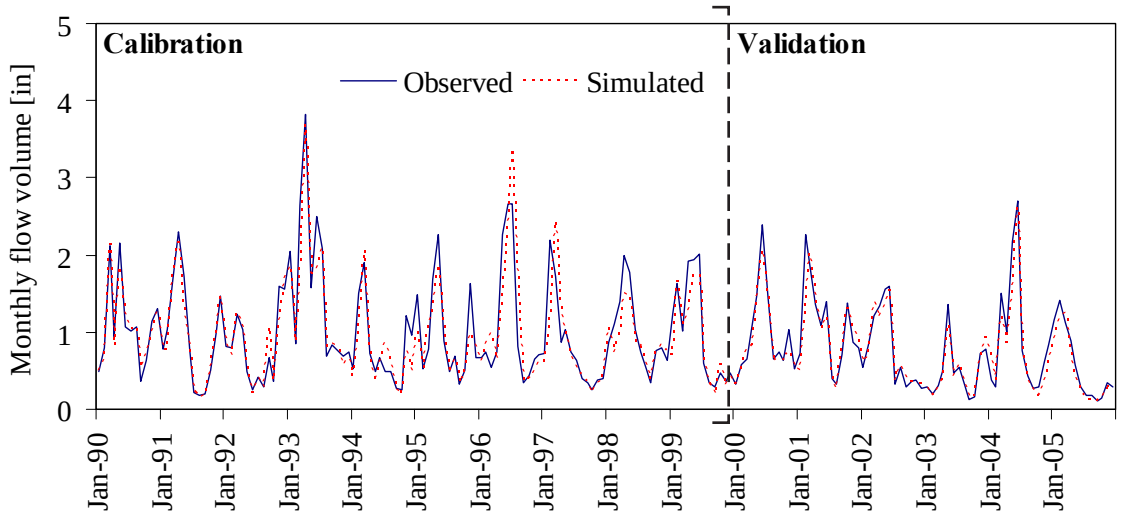

Figure 4.12c. Comparison of monthly flow volumes for *USGS_05552500* (CS-II)

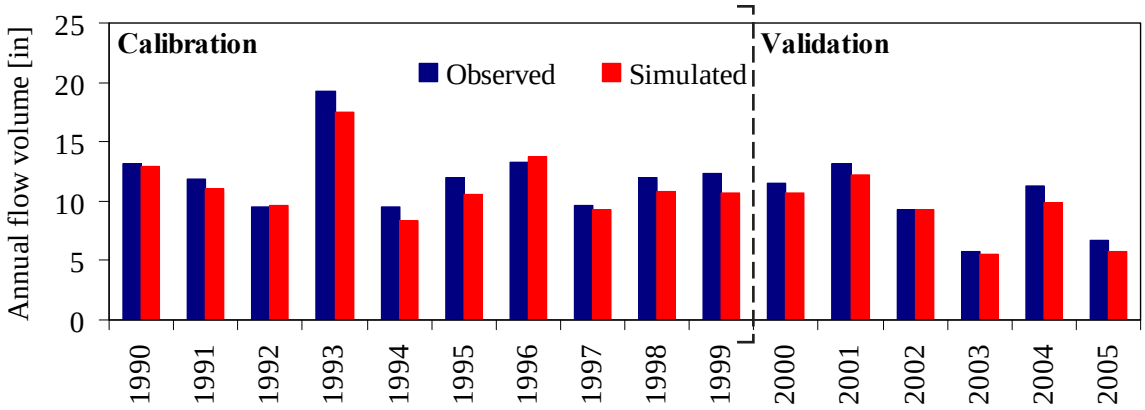

Figure 4.12d. Comparison of annual flow volumes for *USGS_05552500* (CS-II)

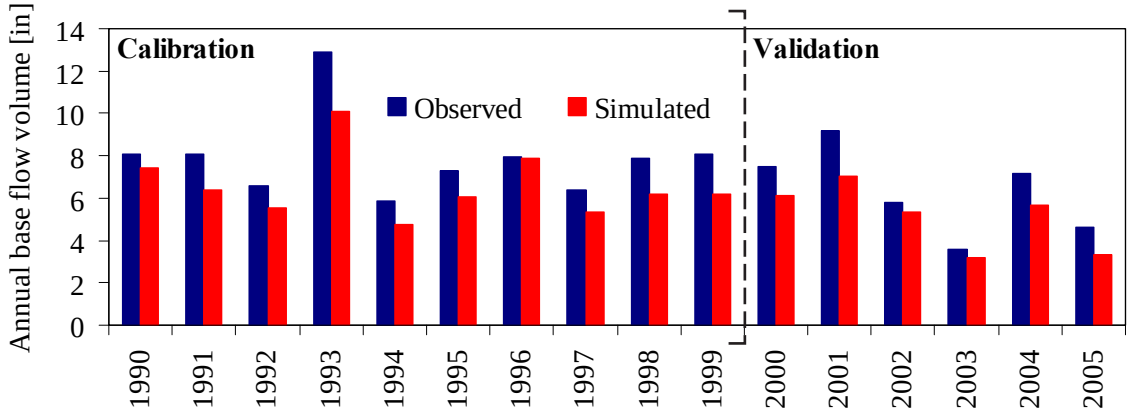

Figure 4.12e. Comparison of annual base flow volumes for *USGS_05552500* (CS-II)

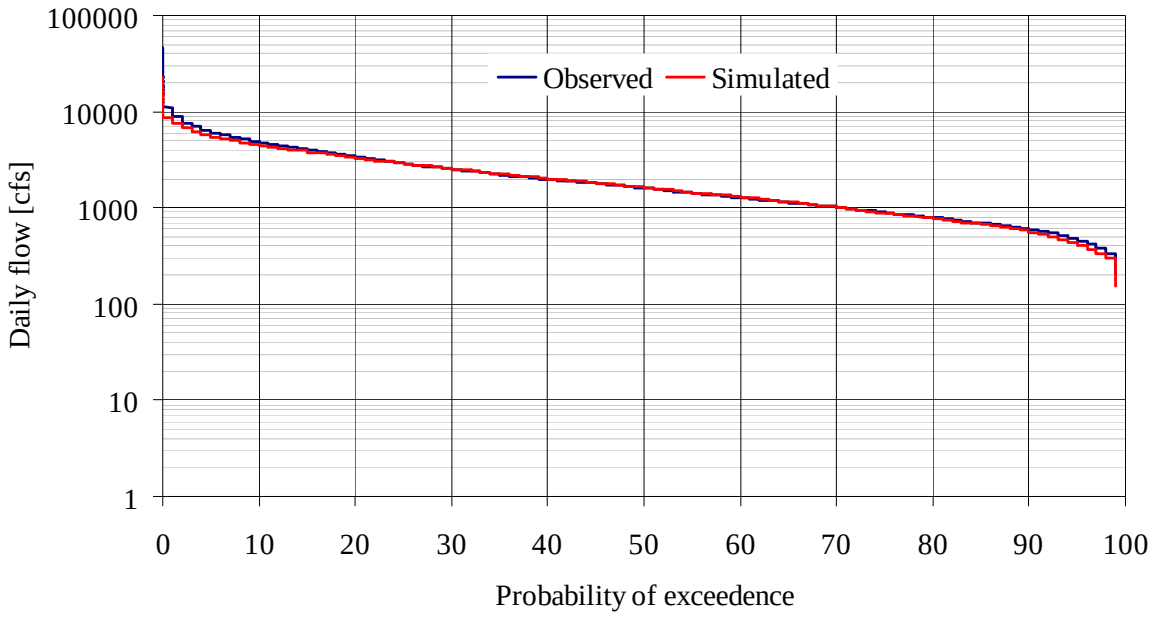

Figure 4.12f. Comparison of flow duration curves for *USGS_05552500* (1971-2000)

Hydrologic Simulation Model for the Entire Fox River Watershed

The hydrologic simulation models developed for Subwatershed I, II, and III are independent of one another as previously indicated. The model developed here is a single hydrologic simulation model for the entire Fox River watershed, which includes all three subwatersheds (i.e., Subwatershed I, II, and III). Out of the 207 subbasins in the entire Fox River watershed, the first 49 make up Subwatershed I and the next 61 subbasins are part of Subwatershed II. Subwatershed III comprises the remaining 97 subbasins. In developing the hydrologic simulation model for the entire Fox River watershed, calibrated flow parameters were accordingly assigned to each of the subbasins. It must be noted that during the modeling process, observed flows at upstream watershed outlets were used as inflows to the downstream subwatersheds (e.g., Subwatershed I drains into Subwatershed II). In this regard, observed flows for *USGS_055454750* at New Munster and flows for *USGS_05550000* at Algonquin were used as inflows to Subwatershed II and III, respectively. However, no observed inflows were required in the complete hydrologic model since the entire watershed is being modeled. Thus, this may require adjusting streamflow parameters for all subbasins downstream of Subwatershed I outlet, which is *USGS_055454750* at New Munster.

Two sets of model parameters were obtained as a result of the two calibration scenarios employed (i.e., Calibration Scenarios I and II for drought and average conditions). For each section of the watershed and both scenarios, calibrated values of model parameters are presented in Table 4.9. With the exception of the Curve Number (*CN2*) and available soil water capacity (*SOL_AWC*), all other parameters assume the same values in all subbasins of the respective subwatersheds. The *CN2* and *SOL_AWC* values are given for the reference subbasins in these subwatersheds. The *CN2* varies from subbasin to subbasin based on land use and hydrologic

Table 4.9. Calibrated Values of Flow Parameters under CS-I and CS-II

Calibration Parameter	*Subwatershed I*		*Subwatershed II*		*Subwatershed III*	
	CS-I	*CS-II*	*CS-I*	*CS-II*	*CS-I*	*CS-II*
CN2	35	45	30	45	30	45
SOL_AWC[1]	-0.0315	-0.0315	0.04	-0.025	-0.034	-0.032
ESCO	0.96	0.96	0.85	0.90	0.90	0.90
GW_REVAP	0.2	0.1	0.2	0.05	0.2	0.1
REVAPMN	0.5	29.1	34.3	34.3	7.9	7.9
GWQMN	57.7	57.7	35.4	35.4	50.0	50.0
ALPHA_BF	0.169	0.169	0.161	0.161	0.15	0.15
RCHRG_DP	0.0	0.0	0.0	0.0	0.0	0.0
DELAY	48.5	48.5	57.6	57.6	42.1	42.1
CH_N2	0.01	0.01	0.023	0.023	0.014	0.014
OV_N	0.091	0.091	0.222	0.222	0.25	0.25
SURLAG	0.5	0.5	1.5	1.5	0.5	0.5
SFTMP	-2.25	-2.25	-1.97	-1.97	1.18	1.18
SMTMP	0.0034	0.0034	0.62	0.62	2.63	2.63
SMFMX	4.24	4.24	3.08	3.08	3.70	3.70
SMFMN	0.23	0.23	0.60	0.60	0.69	0.69

Note: [1]Changes from its original value

soil group. The values of *SOL_AWC* shown in the table are variations from the default values, which are obtained from the STATSGO soil data used during watershed simulation. The change in *SOL_AWC* values is varied for each subbasin through random number generation, and optimal values are determined for each subbasin of the watershed during the calibration process. SWAT simulates groundwater recharges to shallow and deep aquifer systems. The proportion of recharge percolating to the deep aquifer, which is represented by the parameter *RCHRG_DP*, is considered to be lost from the system and thus, during calibration, this parameter is set to zero.

Comparison of parameter values obtained under the two calibration scenarios particularly shows variations in *GW_REVAP* and *CN2* values. The amount of water moving from the shallow aquifer into the overlying unsaturated zone (i.e., *REVAP*) is modeled as a function of water demand for evapotranspiration and the parameter *GW_REVAP* is a coefficient used to quantify the amount of *REVAP* from the potential evapotranspiration on a given day. Note that *REVAP* is allowed to occur only if the storage of the shallow aquifer exceeds *GWQMN*. In comparison, the *GW_REVAP* is at least twice higher under Calibration Scenario I, indicating that the movement of water from shallow aquifer to overlying unsaturated soil zone is higher in response to water deficiencies in drier periods. The *CN2* values obtained under Calibration Scenario I are smaller than those values under Calibration Scenario II, indicating lower antecedent soil moisture under the drier calibration period (i.e., Calibration Scenario I). The remaining flow parameters assume identical values under both calibration scenarios.

Results for Calibration Scenario I (CS-I)

Table 4.10 lists the performance evaluation statistics obtained for adjusted streamflow simulations for *USGS_05550000* at Algonquin and *USGS_05552500* at Dayton, which are two of the gauging stations used during model calibration. The daily *NSE* values were at least 0.5 in all cases expect for simulations at *USGS_05552500* during the validation period, in which case it was 0.46. The worst *NSE* and *RSR* values obtained for monthly simulations were 0.68 and 0.57, respectively. The *PBIAS* obtained for both gauging stations and at all time periods was less than 10 percent.

Values of the performance statistics generally show that monthly simulations were good for both gauging stations, and daily simulations were also good for *USGS_0555000* at Algonquin but only satisfactory for *USGS_05552500* at Dayton, applying the same performance guidelines as for monthly simulations. It should be noted that the performance guidelines for simulations at bigger time-steps tend to be stricter. Graphical comparisons are made between observed and simulated daily hydrographs, flow duration curves, and monthly and annual flow volumes for *USGS_05550000* at Algonquin. Figures 4.13a and 4.13b illustrate daily hydrographs and flow duration curves. Simulated monthly and annual flow volumes are compared in Figures 4.13c and 4.13d. Base flow proportions computed from observed flows and simulated flows were 0.65 and 0.61 with an average deviation of 6.3 percent, indicating a slight underestimation of base flows. Figure 4.13e illustrates a comparison of observed and simulated annual base flow volumes. *NSE*

Table 4.10. Performance Statistics for Adjusted Streamflow Simulations under CS-I

Performance statistic	*Calibration (1960-1969)*	*Validation (1950-1959)*	*Drought period (1931-1960)*
USGS_05550000 at Algonquin			
PBIAS (%)	4.2	4.8	-0.4
Daily			
RSR (-)	0.60	0.59	0.63
NSE (-)	0.64	0.65	0.61
Monthly			
RSR (-)	0.53	0.50	0.55
NSE (-)	0.72	0.75	0.70
Annual			
RSR (-)	0.26	0.43	0.44
NSE (-)	0.93	0.82	0.81
USGS_05552500 at Dayton			
PBIAS (%)	6.6	6.1	2.4
Daily			
RSR (-)	0.67	0.73	0.71
NSE (-)	0.55	0.46	0.50
Monthly			
RSR (-)	0.53	0.57	0.54
SE (-)	0.72	0.68	0.71
Annual			
RSR (-)	0.37	0.50	0.47
NSE (-)	0.86	0.75	0.78

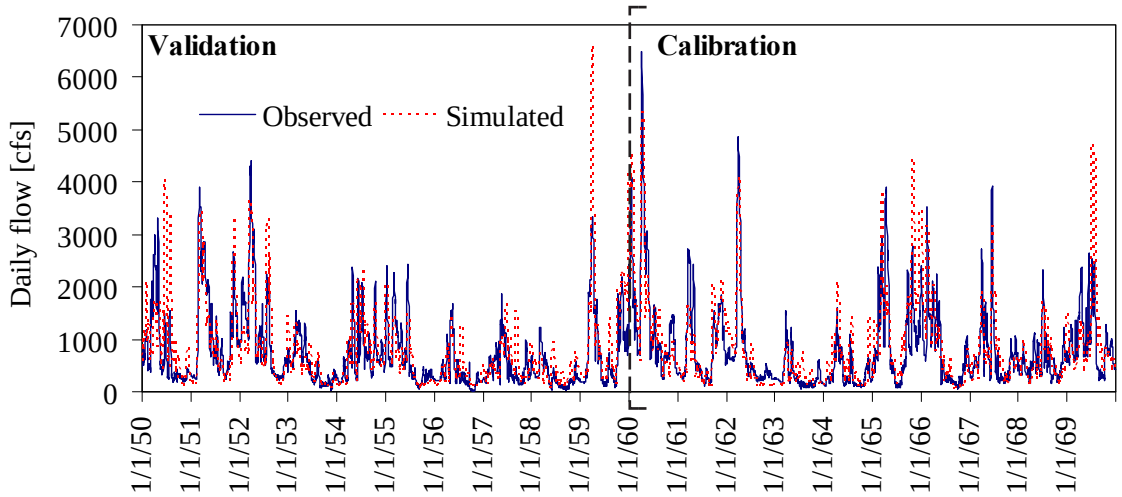

Figure 4.13a. Daily flows for *USGS_05550000* at Algonquin under CS-I

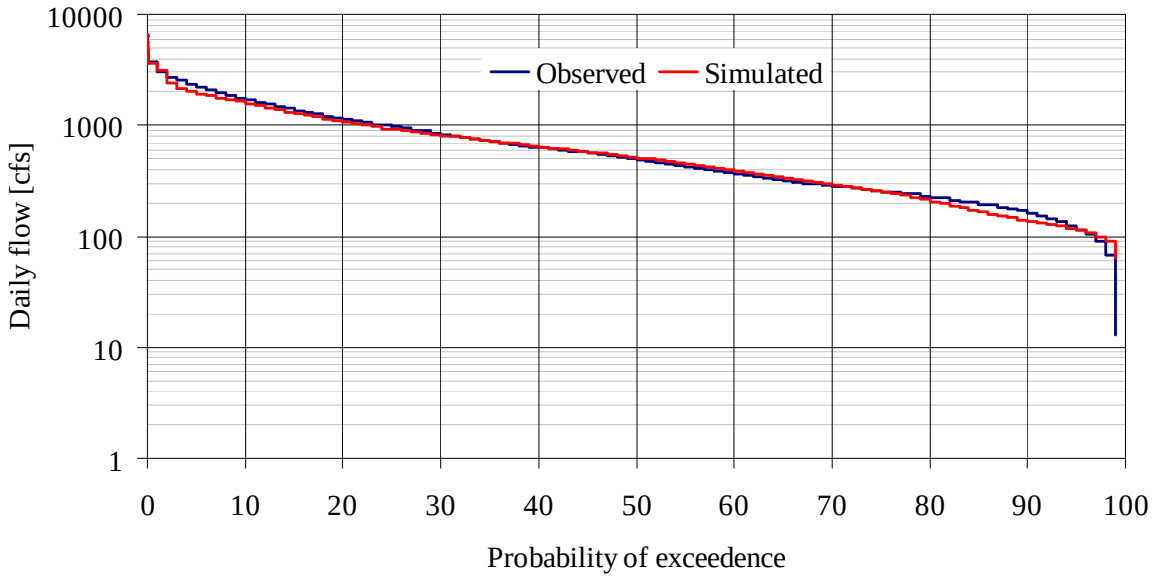

Figure 4.13b. Flow duration curves for *USGS_05550000* at Algonquin under CS-I

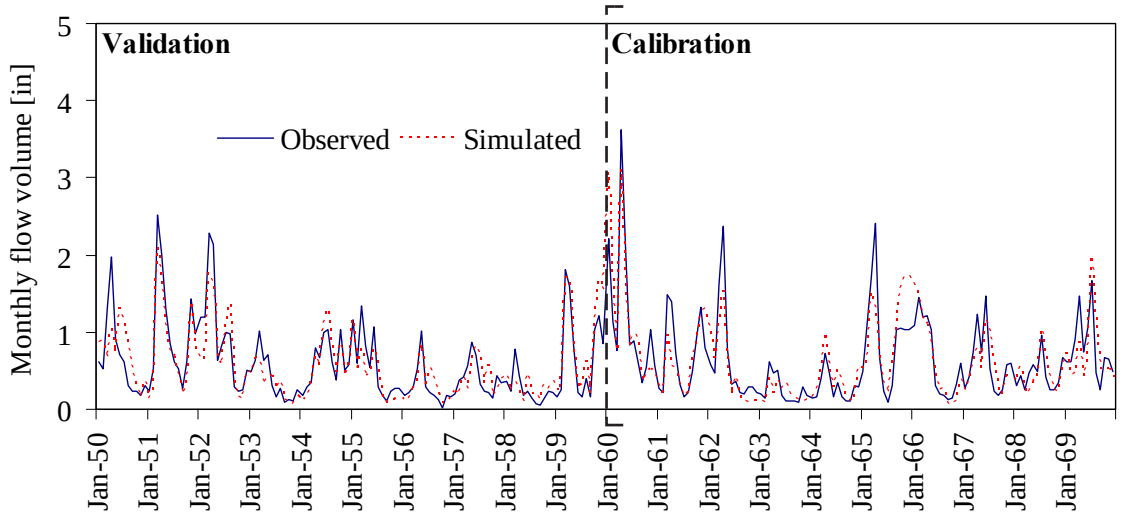

Figure 4.13c. Monthly flows for *USGS_05550000* at Algonquin under CS-I

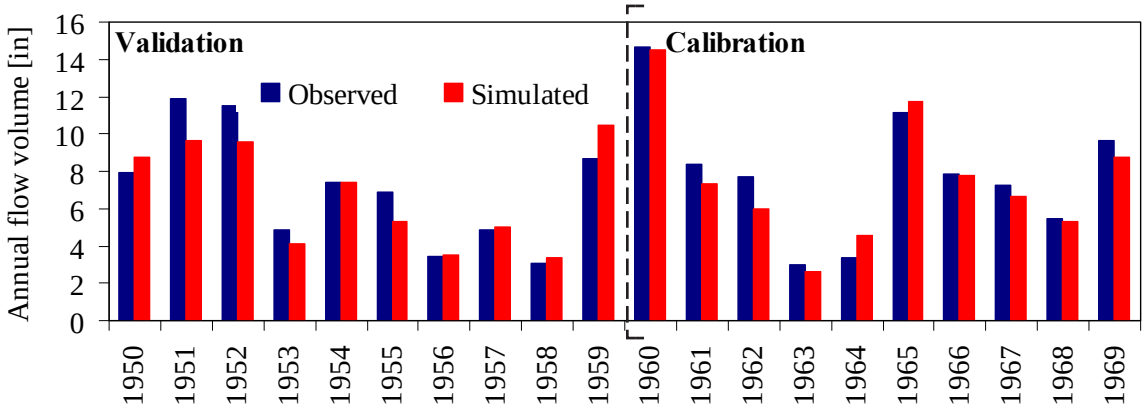

Figure 4.13d. Annual flows for *USGS_05550000* at Algonquin under CS-I

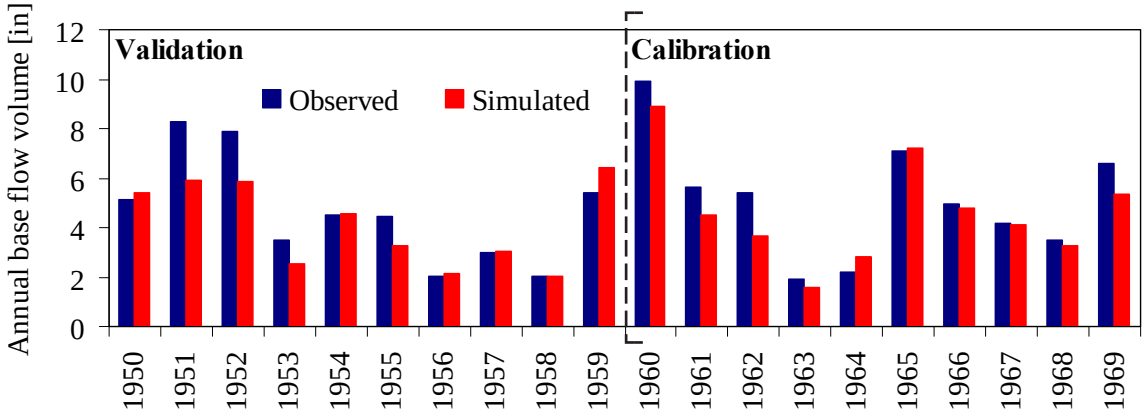

Figure 4.13e. Annual base flows for *USGS_05550000* at Algonquin under CS-I

values of 0.86 and 0.69 were obtained for annual base flow simulations during calibration and validation periods, respectively, indicating better model performance in the calibration period. In general, the figures and performance evaluation statistics indicate that the model was able to fairly simulate all ranges of flows at daily time-steps, and it exhibits good performance in simulating monthly and annual flows for *USGS_05550000* at Algonquin.

Similarly, comparisons of observed and simulated daily hydrographs, flow duration curves, and monthly and annual flow volumes were made for *USGS_05552500* at Dayton. Daily hydrographs and flow duration curves are presented in Figures 4.14a and 4.14b. Comparisons of simulated monthly and annual flow volumes with their observed counterparts are illustrated in Figures 4.14c and 4.14d. The fraction of base flows computed from simulated values was 0.57, and it was 0.63 for observed flows, showing an average deviation of 8.8 percent. The associated *NSE* values were 0.67 and 0.54 during calibration and validation periods, respectively. A graphical comparison of observed and simulated annual base flow volumes is presented in Figure 4.14e. The figures and performance evaluation statistics indicate that the model performed better in the calibration period as compared to the validation period. Overall, the hydrologic model exhibits good performance in simulating monthly and annual flows for *USGS_05552500* at Dayton and it has also satisfactorily simulated daily flows. The model was able to fairly simulate the average trends of base flows, although they were highly underestimated during the years with high annual flows.

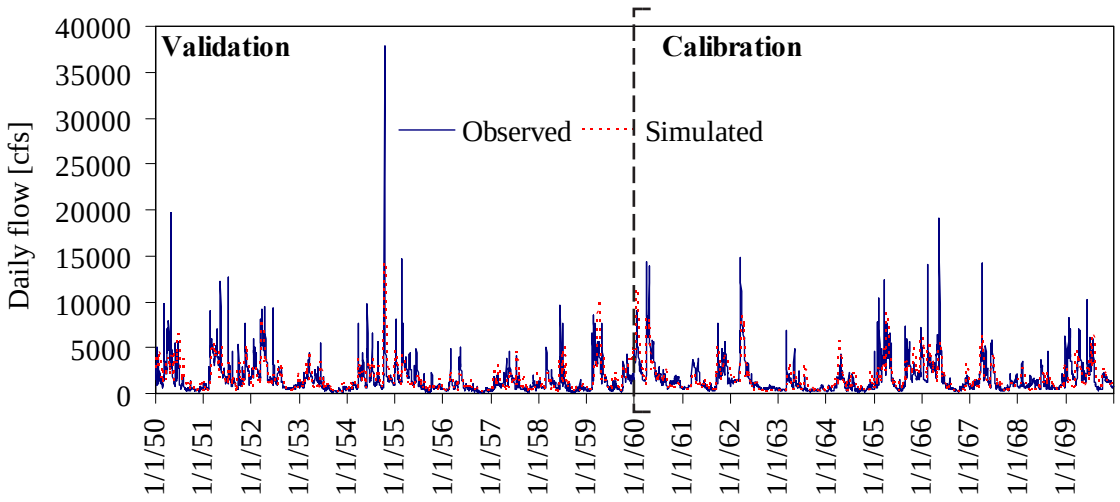

Figure 4.14a. Daily flows for *USGS_05552500* at Dayton under CS-I

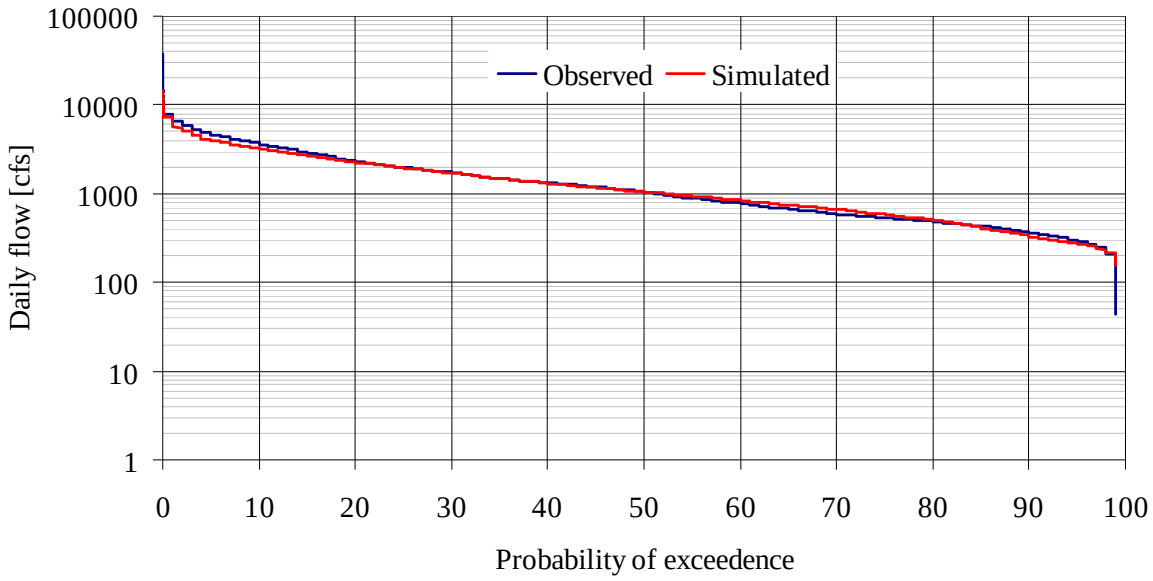

Figure 4.14b. Flow duration curves for *USGS_05552500* at Dayton under CS-I

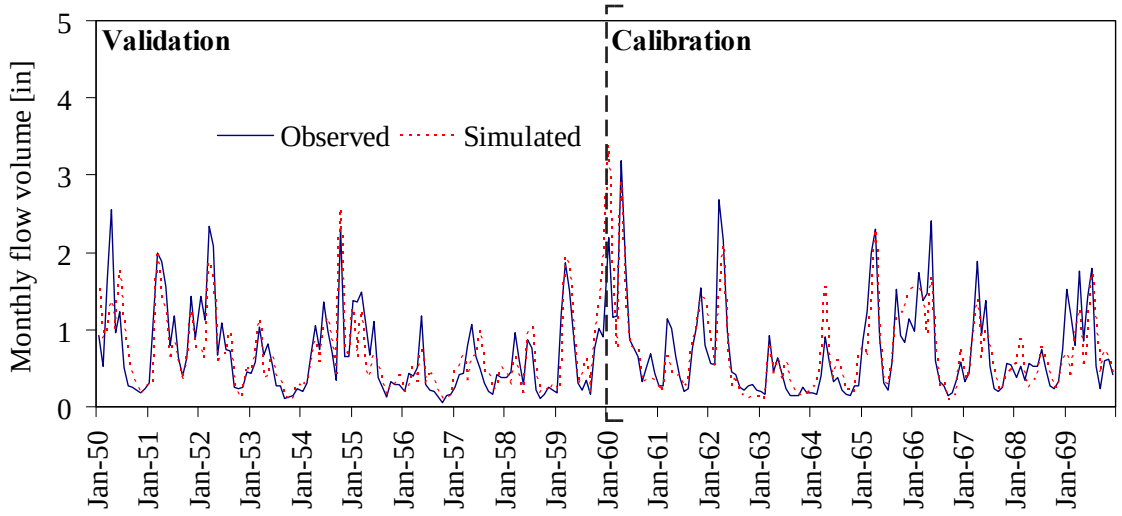

Figure 4.14c. Monthly flows for *USGS_05552500* at Dayton under CS-I

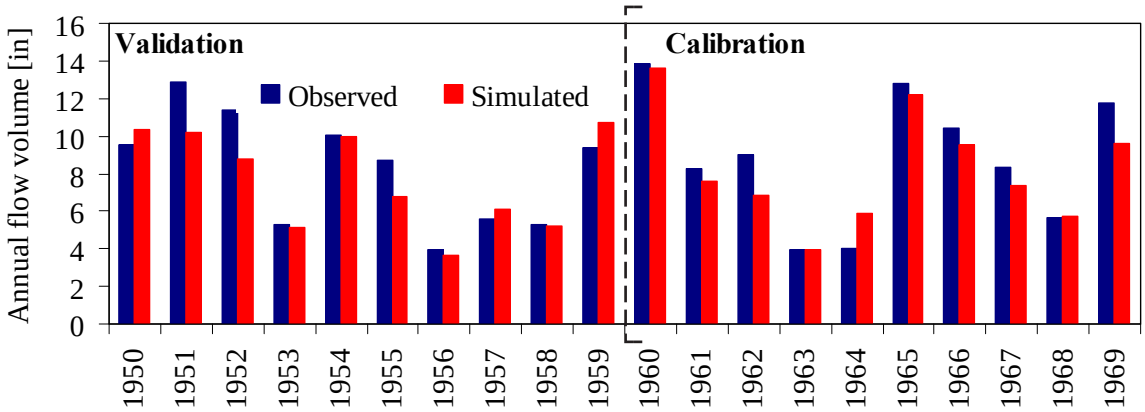

Figure 4.14d. Annual flows for *USGS_05552500* at Dayton under CS-I

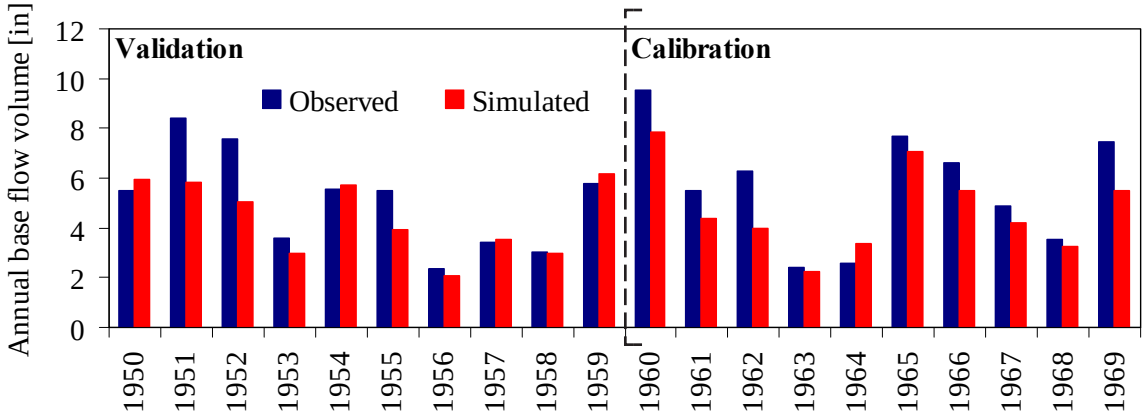

Figure 4.14e. Annual base flows for *USGS_05552500* at Dayton under CS-I

Results for Calibration Scenario II (CS-II)

The performance evaluation statistics obtained under Calibration Scenario II are presented in Table 4.11. The table lists values of *NSE*, *RSR*, and *PBIAS* obtained for adjusted streamflow simulations for *USGS_05550000* at Algonquin and *USGS_05552500* at Dayton during calibration, validation, and baseline periods. The daily *NSE* values were greater than 0.5 in all cases with the exception of flow simulations for *USGS_05552500* at Dayton in the calibration period. In this particular case, the daily *NSE* value was 0.39, but it was 0.52 in the validation period, indicating satisfactory simulation of daily flows. For monthly simulations, the worst *NSE* and *RSR* values obtained were 0.65 and 0.60, respectively. The absolute *PBIAS* obtained for both gauging stations and at all time periods was less than 10 percent, indicating a smaller bias in model estimation of flows. At both gauging stations, the daily and monthly flows were satisfactory, whereas annual flows were simulated very well at both gauging stations with an *NSE* value of at least 0.8.

Simulation results for *USGS_05550000* at Algonquin are compared with their observed counterparts using figures showing daily hydrographs, flow duration curves, and monthly and annual flow volumes. Figures 4.15a and 4.15b illustrate daily hydrographs and flow duration curves. These figures show that simulated values are in good agreement with observed ones and all ranges of flows are satisfactorily simulated. A comparison of observed and simulated monthly and annual flow volumes are made in Figures 4.15c and 4.15d, respectively. Base flow proportions calculated from observed flows and simulated flows were 0.66 and 0.61 with an average deviation of 7.9 percent, indicating a slight underestimation of base flows. *NSE* values of 0.73 and 0.81 were obtained for annual base flow simulations during calibration and validation periods, respectively, with better model performance in the validation period. Figure 4.15e illustrates the comparison of observed and simulated annual base flow volumes. Simulated annual and monthly flows show better agreement with their observed counterparts than the daily simulations as evidenced by the performance statistics and figures presented.

Table 4.11. Performance Statistics for Adjusted Streamflow Simulations under CS-II

Performance statistic	*Calibration (1990-1999)*	*Validation (2000-2005)*	*Baseline period (1971-2000)*
USGS_05550000 at Algonquin			
PBIAS (%)	0.7	-5.4	-5.0
Daily			
RSR (-)	0.67	0.65	0.59
NSE (-)	0.56	0.57	0.65
Monthly			
RSR (-)	0.62	0.65	0.53
NSE (-)	0.61	0.60	0.72
Annual			
RSR (-)	0.36	0.42	0.46
NSE (-)	0.87	0.82	0.79
USGS_05552500 at Dayton			
PBIAS (%)	6.9	4.7	2.8
Daily			
RSR (-)	0.78	0.69	0.70
NSE (-)	0.39	0.52	0.51
Monthly			
RSR (-)	0.61	0.54	0.52
NSE (-)	0.63	0.71	0.73
Annual			
RSR (-)	0.40	0.31	0.35
NSE (-)	0.84	0.91	0.88

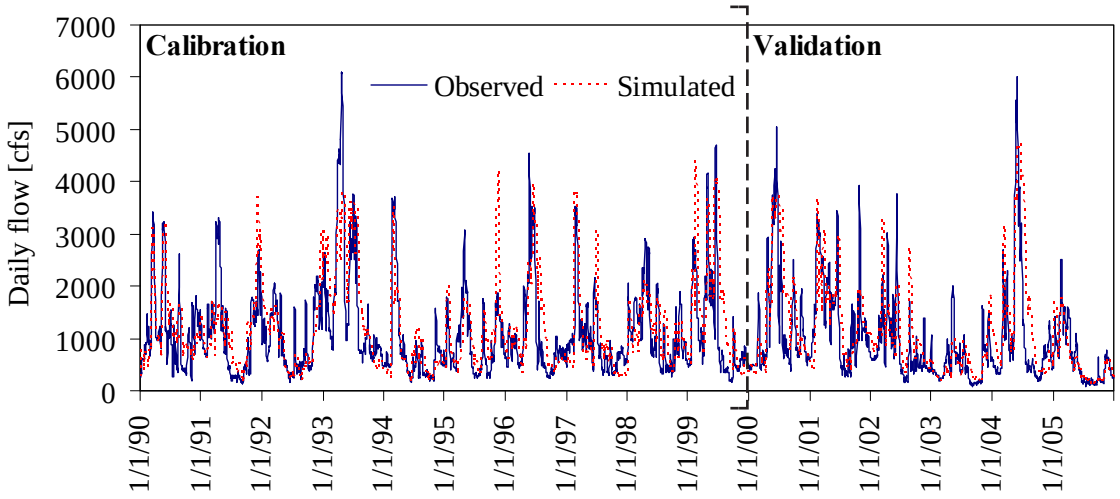

Figure 4.15a. Daily flows for *USGS_05550000* at Algonquin under CS-II

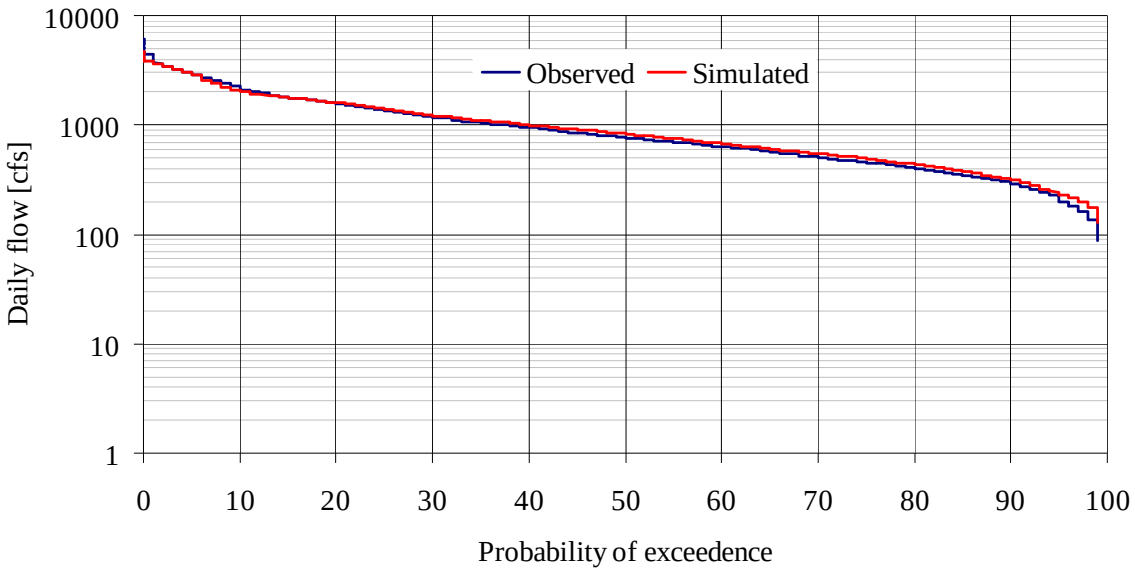

Figure 4.15b. Flow duration curves for *USGS_05550000* at Algonquin under CS-II

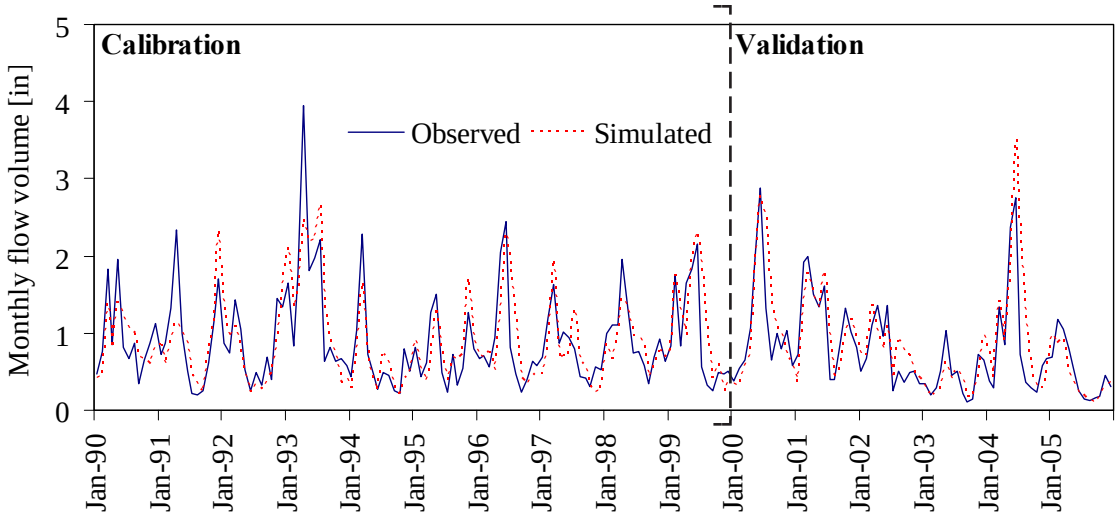

Figure 4.15c. Monthly flows for *USGS_05550000* at Algonquin under CS-II

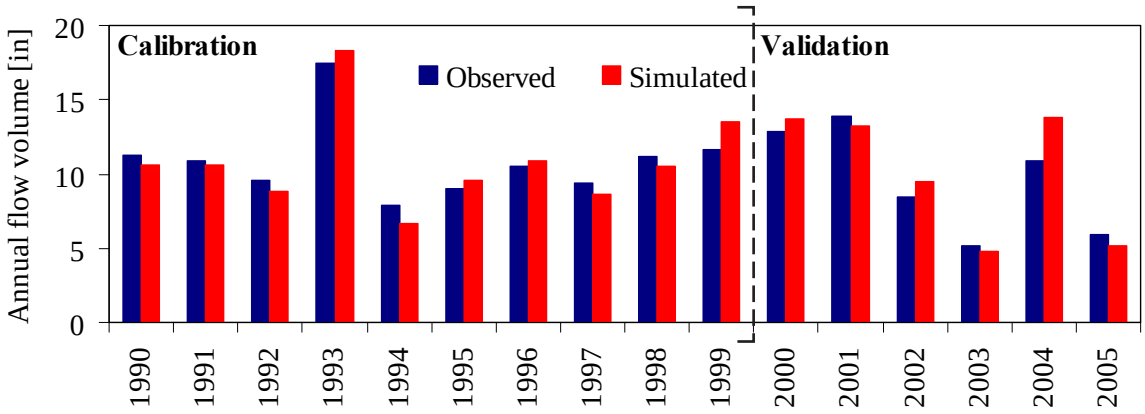

Figure 4.15d. Annual flows for *USGS_05550000* at Algonquin under CS-II

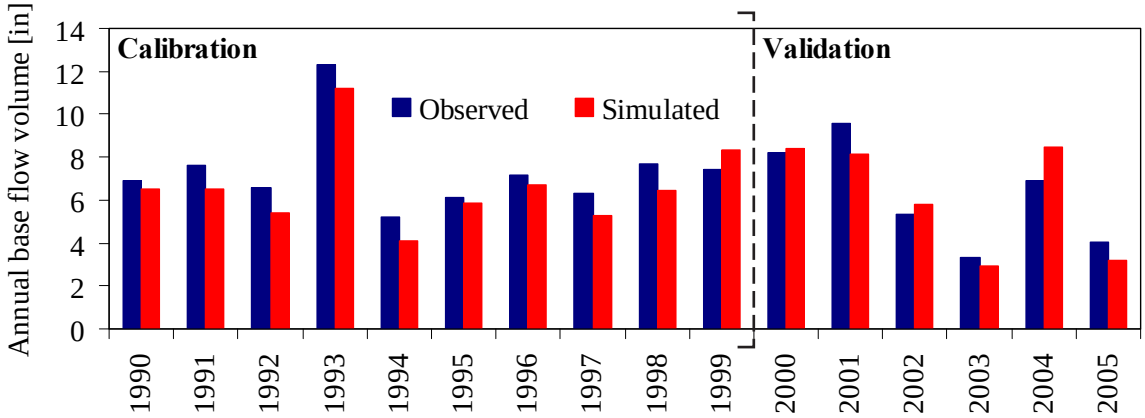

Figure 4.15e. Annual base flows for *USGS_05550000* at Algonquin under CS-II

Graphical comparisons of observed and simulated daily hydrographs, flow duration curves, and monthly and annual flow volumes were also made for *USGS_05552500* at Dayton. Observed and simulated daily hydrographs are compared in Figure 4.16a. The figure shows that average and low flows were very well simulated, but flows greater than 10,000 cfs were underestimated. A comparison of observed and simulated daily duration curves in Figure 4.16b clearly shows good agreement with the exception of flows with less than 10 percent exceedence. Simulated flows at monthly and annual time-steps are compared with their observed counterparts as shown in Figures 4.16c and 4.16d. The ratio of simulated annual base flows to total flow was 0.57, whereas it was 0.65 for observed values, showing an average deviation of 11.4 percent. The corresponding *NSE* values were 0.33 and 0.53 during calibration and validation periods, respectively. Figure 4.16e shows a graphical comparison of observed and simulated annual base flow volumes. The figures and performance evaluation statistics indicate that the model performed better in the validation period, and the baseflow simulations were unsatisfactory, particularly in the calibration period. With the exception of base flow simulations, the hydrologic model was able to fairly simulate flows at daily, monthly, and annual time-steps, and it showed biases towards underestimation of flows for *USGS_05552500* at Dayton.

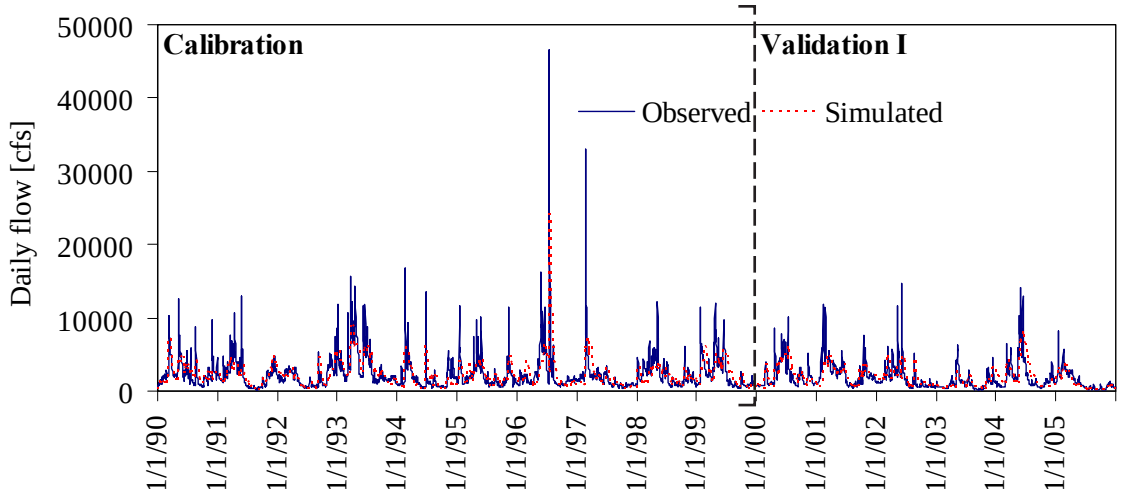

Figure 4.16a. Daily flows for *USGS_05552500* at Dayton under CS-II

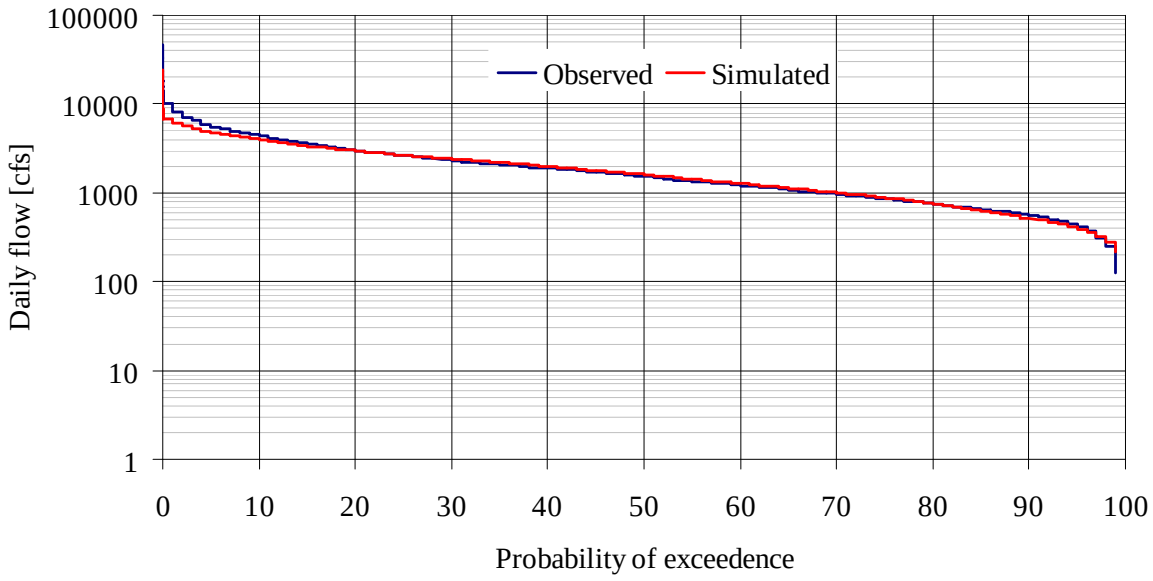

Figure 4.16b. Flow duration curves for *USGS_05552500* at Dayton under CS-II

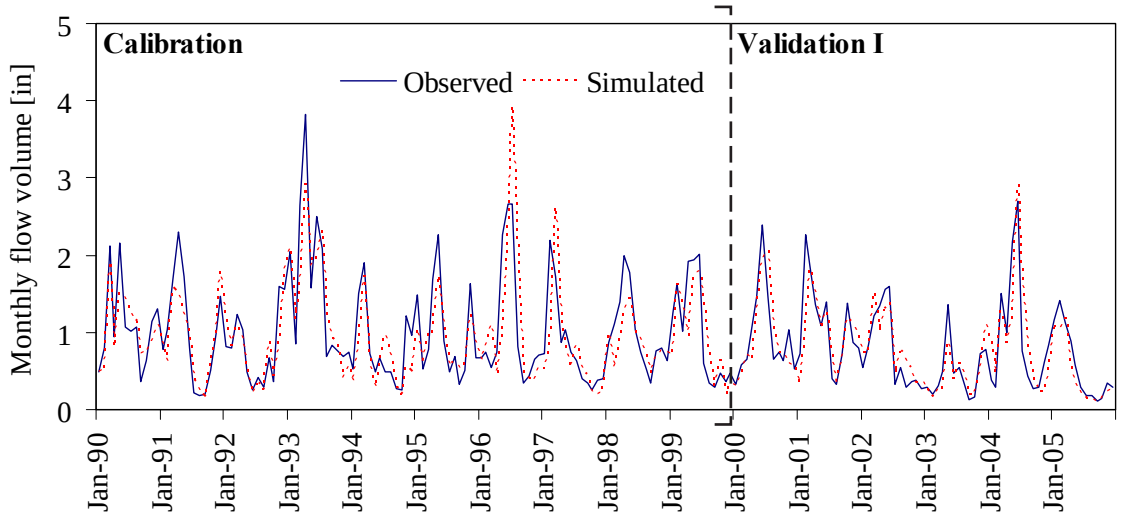

Figure 4.16c. Monthly flows for *USGS_05552500* at Dayton under CS-II

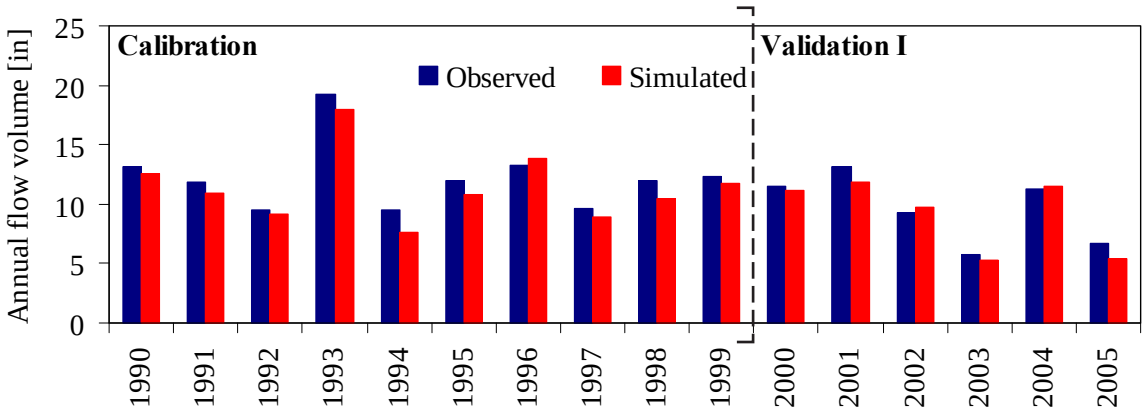

Figure 4.16d. Annual flows for *USGS_05552500* at Dayton under CS-II

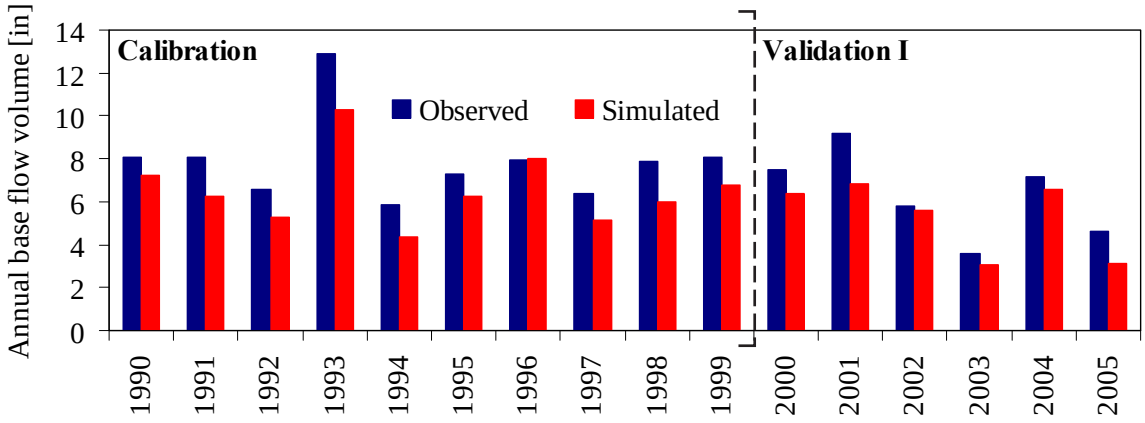

Figure 4.16e. Annual base flows for *USGS_05552500* at Dayton under CS-II

Model Evaluations in the Long-term Drought and Baseline Periods

For long-term validation of the hydrologic simulation model developed, the model was evaluated for a 30-year drought period from 1931 to 1960. Two of the three calibration gauging stations, namely, *USGS_05550000* at Algonquin and *USGS_05552500* at Dayton, have complete flow records for this period. The *USGS_055454750* near New Munster has shorter records of flow data that date back to1940. Model evaluation was also performed for a period from 1971 to 2000, which is considered as the baseline period for simulating the response in various climate scenarios. As indicated previously, the hydrologic model calibrated using the first calibration scenario was used to simulate the drought period, whereas calibrated parameters under the second scenario were used during model evaluation in the baseline period. Model evaluation results are presented using the performance statistics and graphical comparison of observed and simulated flows.

Streamflow Simulations for USGS_055454750 near New Munster

Table 4.12 lists the performance evaluation statistics obtained for flow simulations at *USGS_055454750* near New Munster during the drought and baseline periods. The *NSE* values obtained for daily, monthly, and annual flows during the drought period were 0.70, 0.76, and 0.86, respectively. The average percent deviation of simulated flows, which is given as *PBIAS*, is only 5 percent, and the worst *RSR* value obtained was 0.55. During the baseline period, *NSE* values of 0.64, 0.70, and 0.76 were obtained for daily, monthly, and annual simulations, respectively. The *PBIAS* and the worst *RSR* value for this period were 0.4 percent and 0.60, respectively. According to the evaluation guidelines, good simulation results have been obtained in both drought and baseline periods. In comparison, the model performed better in simulating average flow trends in the drought period as shown in the associated *NSE* values.

Table 4.12. Performance Statistics for Long-Term Simulations at *USGS_055454750*

Performance statistic	*Drought period (1940-1960)*	*Baseline period (1971-2000)*
PBIAS (%)	5.0	0.4
Daily		
RSR (-)	0.55	0.60
NSE (-)	0.70	0.64
Monthly		
RSR (-)	0.49	0.54
NSE (-)	0.76	0.70
Annual		
RSR (-)	0.38	0.49
NSE (-)	0.86	0.76

Graphical comparisons of observed and simulated daily hydrographs are presented in Figure 4.17a for the drought period and in Figure 4.17b for the baseline period. Daily flow duration curves for drought and baseline periods are illustrated in Figures 4.17c and 4.17d. The daily hydrographs and flow duration curves indicate good agreements in general flow trends between simulated and observed values. In the drought period, flows with more than 40 percent of exceedence were slightly overestimated. For both periods, simulated monthly and annual flow volumes are compared with their observed counterparts in Figures 4.17e, 4.17f, 4.17g, and 4.17h. The monthly and annual flows are well simulated in both periods. In addition, observed and simulated annual base flow volumes are plotted in Figure 4.17i for the drought period and in Figure 4.17j for the baseline period. The *NSE* values obtained for base flow simulations were 0.69 in the drought period and 0.43 in the baseline period. The average deviations of simulated annual base flows were 8.2 percent and 15 percent for drought and baseline periods, respectively. The *NSE* values and average deviations obtained indicate that base flow simulations are better in the drought period.

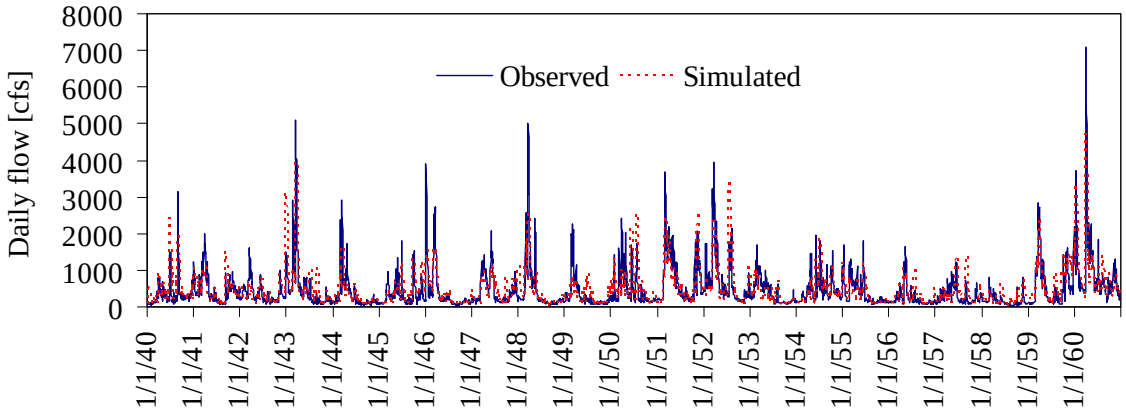

Figure 4.17a. Daily flows for *USGS_055454750* during the drought period

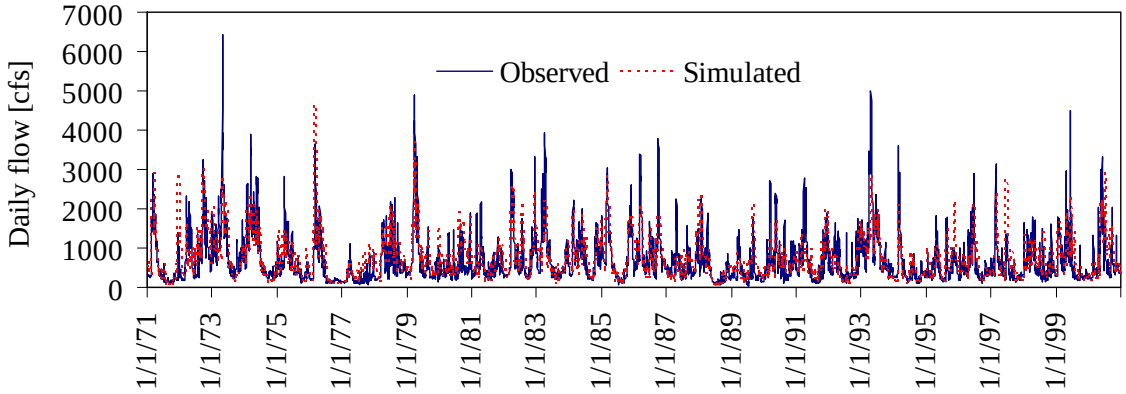

Figure 4.17b. Daily flows for *USGS_055454750* during the baseline period

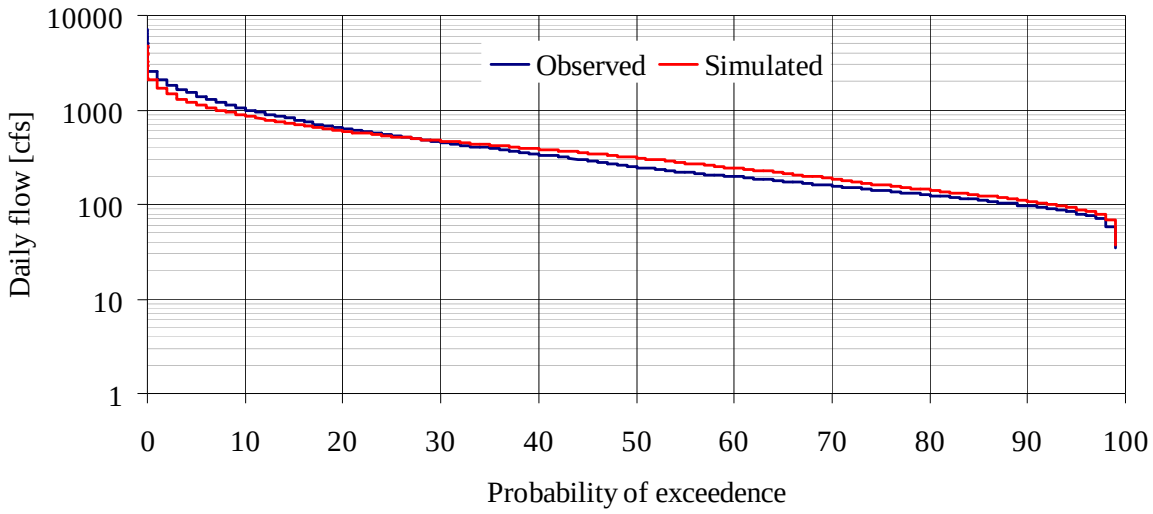

Figure 4.17c. Flow duration curves for *USGS_055454750* during the drought period

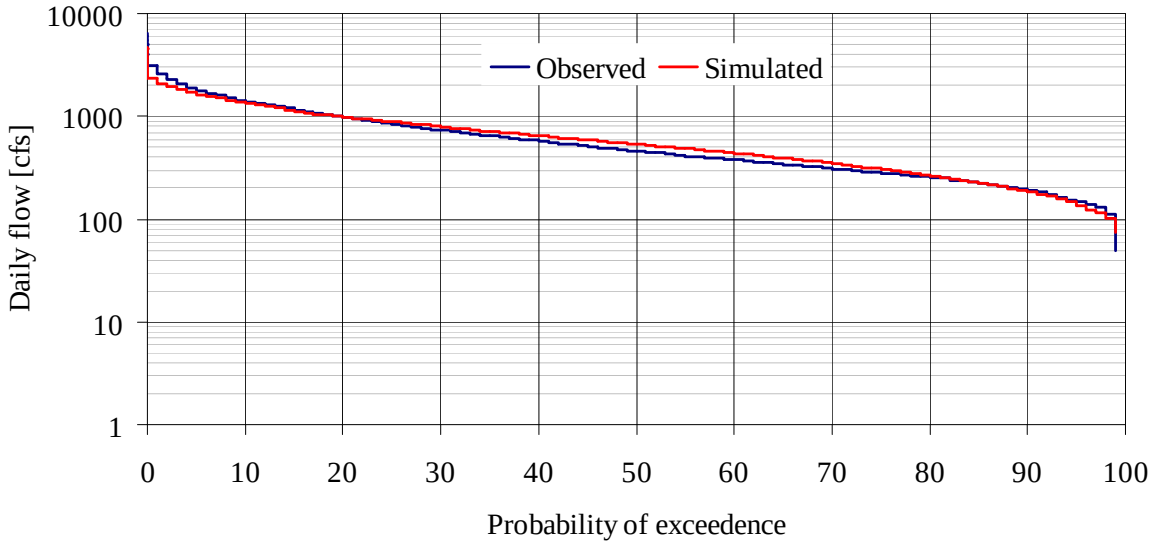

Figure 4.17d. Flow duration curves for *USGS_055454750* during the baseline period

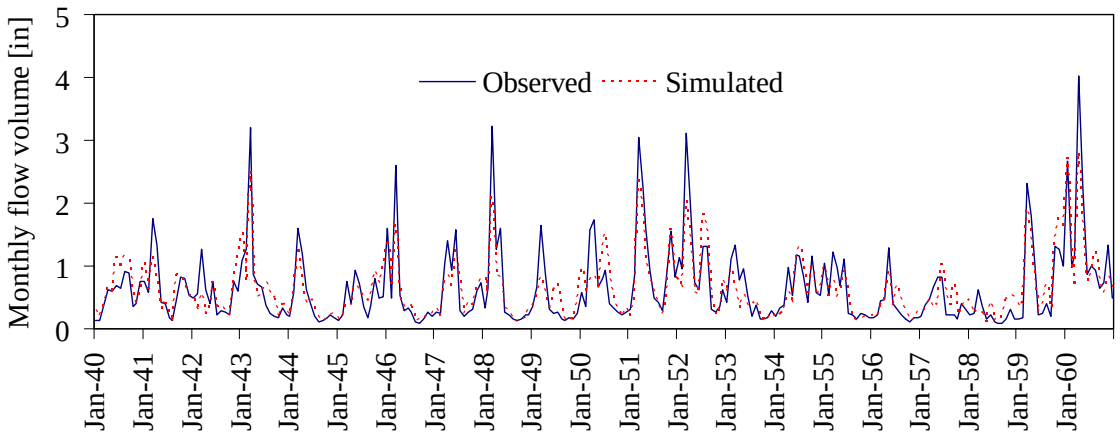

Figure 4.17e. Monthly flows for *USGS_055454750* during the drought period

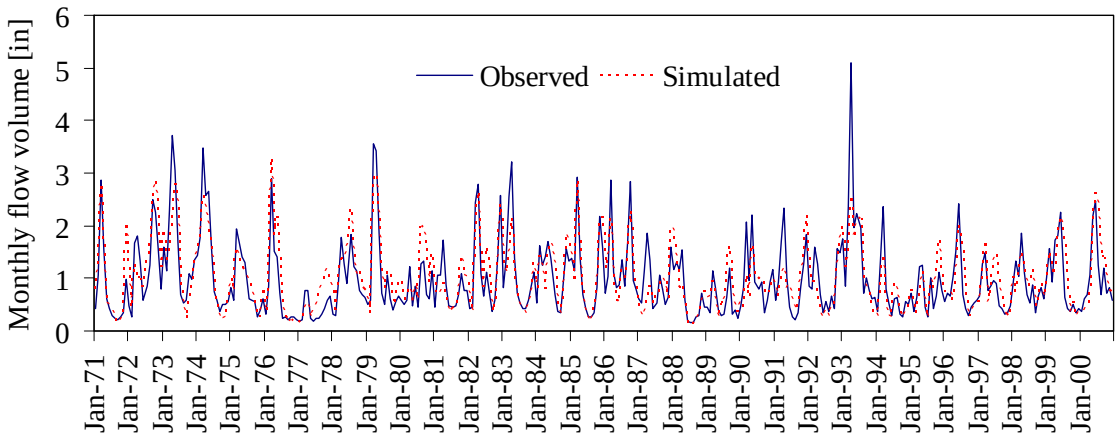

Figure 4.17f. Monthly flows for *USGS_055454750* during the baseline period

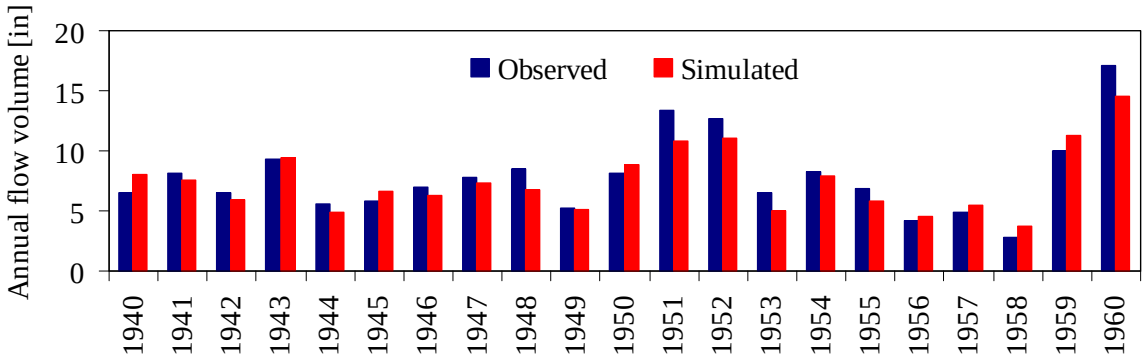

Figure 4.17g. Annual flows for USGS_055454750 during the drought period

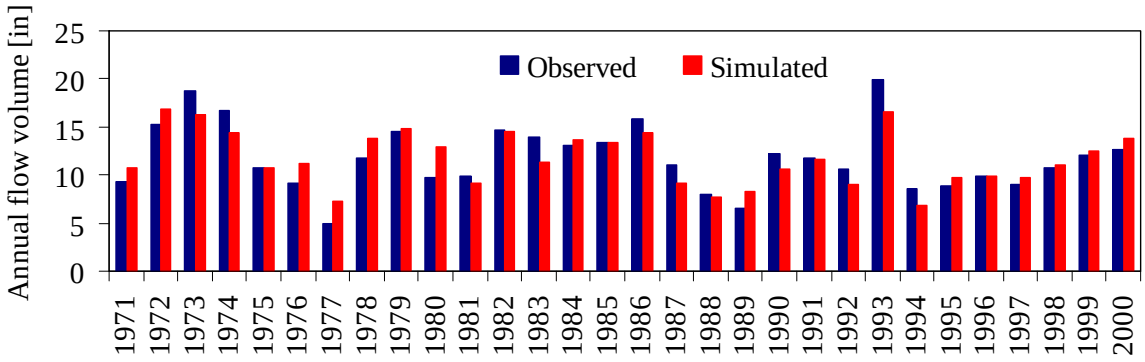

Figure 4.17h. Annual flows for *USGS_055454750* during the baseline period

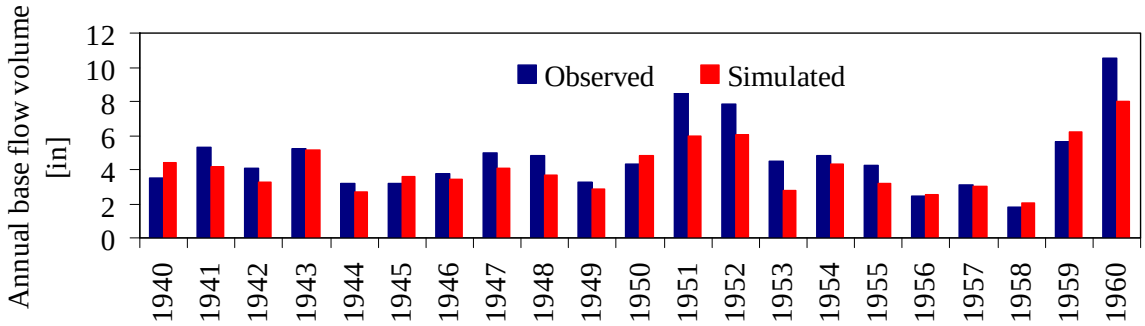

Figure 4.17i. Annual base flows for *USGS_055454750* during the drought period

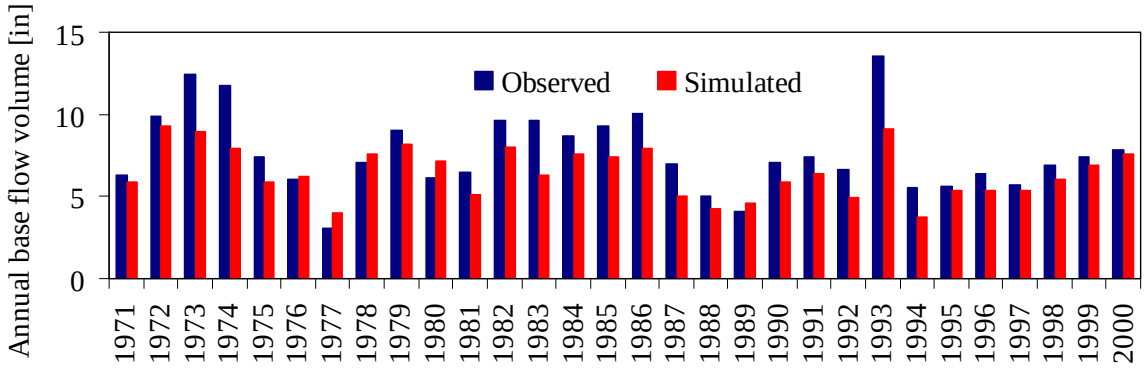

Figure 4.17j. Annual base flows for *USGS_055454750* during the baseline period

Streamflow Simulations for USGS_05550000 at Algonquin

For *USGS_05550000* at Algonquin, the performance evaluation statistics obtained for flow simulations during the drought and baseline periods are presented in Table 4.13. During the drought period, *NSE* values of 0.61, 0.70, and 0.81were obtained for daily, monthly, and annual flow simulations, respectively. An absolute *PBIAS* of 0.4 percent was obtained and the worst *RSR* value was 0.63 for simulations in this period. During the baseline period, the *NSE* values were 0.65, 0.72, and 0.79 for daily, monthly, and annual flow simulations, respectively. The absolute *PBIAS* and the worst *RSR* value for all simulations in this period were 5 percent and 0.59, respectively. In both the drought and baseline periods, the performance evaluation statistics indicate that the hydrologic model was able to simulate flows well for *USGS_05550000* at Algonquin. Comparable model performance was exhibited for simulations in both the drought and baseline periods.

In addition to the performance evaluation statistics, graphical comparisons of observed and simulated hydrographs and duration curves are made. Figures 4.18a and 4.18b show daily hydrographs for the drought and baseline periods, respectively. The corresponding flow duration curves are presented in Figure 4.18c for the drought period and in Figure 4.18d for the baseline period. Generally, good agreement was achieved between observed and simulated daily hydrographs, and the flow duration curves show the model's ability to simulate ranges of flows. In both the drought and baseline periods, the model tends to slightly overestimate flows as it was also shown in values of the corresponding *PBIAS*. Simulated monthly and annual flow volumes in both periods are compared with their observed counterparts as presented in Figures 4.18e, 4.18f, 4.18g, and 4.18h. Although the monthly and annual flow trends were well simulated in both periods, they exhibit overestimation of flows in the early 1930s and late 1970s. In addition, observed and simulated annual base flow volumes are plotted in Figure 4.18i for the drought period and in Figure 4.18j for the baseline period. The *NSE* values obtained for base flow simulations were 0.75 in the drought period and 0.72 in the baseline period. The average deviations of the base flow simulations were 2.9 percent in the drought period and 9.1 percent in the baseline period. The graphical comparisons and the performance statistics show better base flow simulations in the drought period than in the baseline period.

Table 4.13 Performance Statistics for Long-Term Simulations at *USGS_05550000*

Performance statistic	*Drought period (1931-1960)*	*Baseline period (1971-2000)*
PBIAS (%)	-0.4	-5.0
Daily		
RSR (-)	0.63	0.59
NSE (-)	0.61	0.65
Monthly		
RSR (-)	0.55	0.53
NSE (-)	0.70	0.72
Annual		
RSR (-)	0.44	0.46
NSE (-)	0.81	0.79

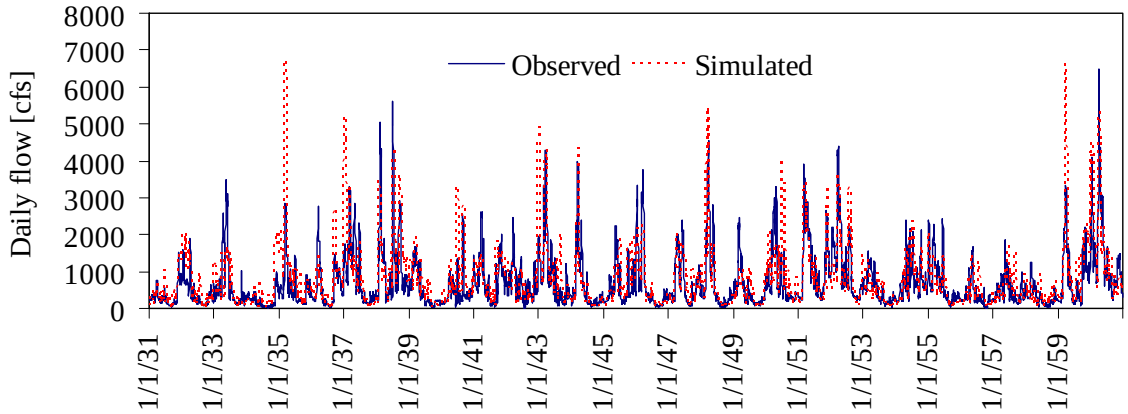

Figure 4.18a. Daily flows for *USGS_05550000* during the drought period

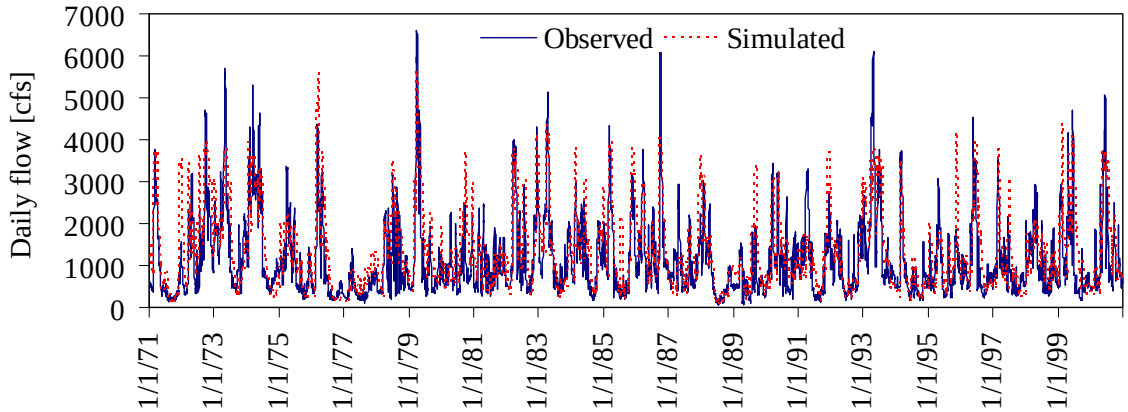

Figure 4.18b. Daily flows for *USGS_05550000* during the baseline period

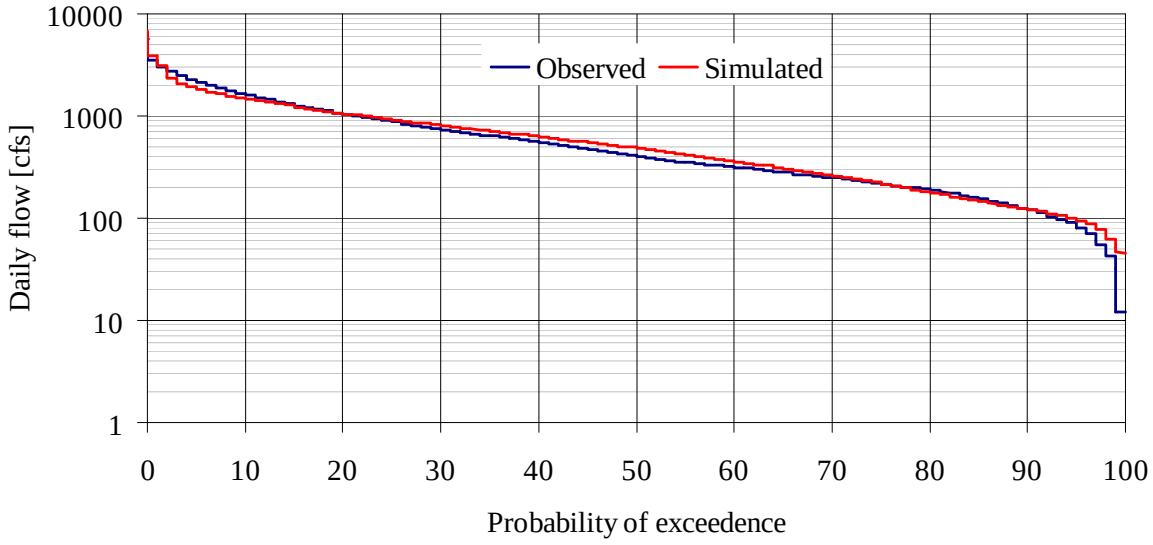

Figure 4.18c. Flow duration curves for *USGS_05550000* during the drought period

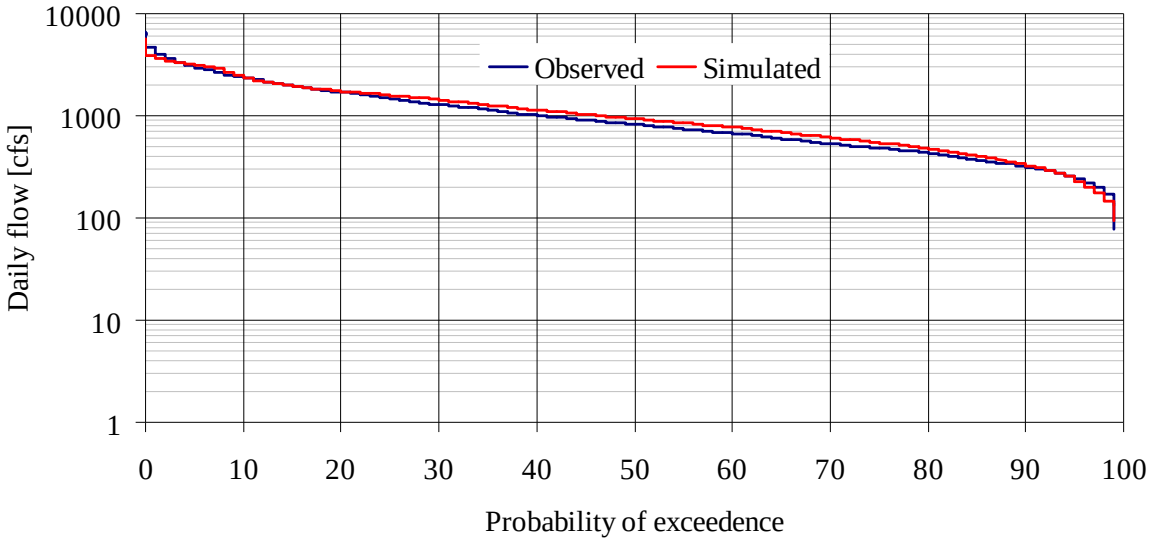

Figure 4.18d. Flow duration curves for *USGS_05550000* during the baseline period

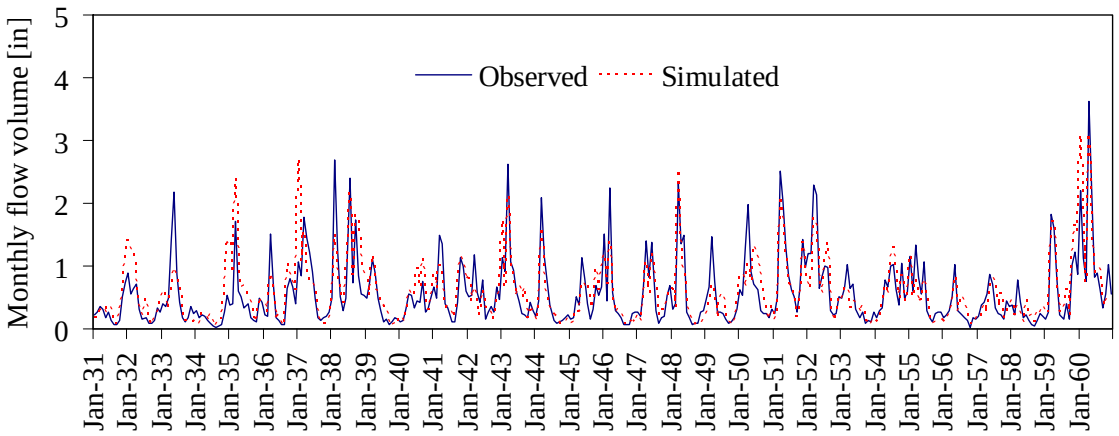

Figure 4.18e. Monthly flows for *USGS_05550000* during the drought period

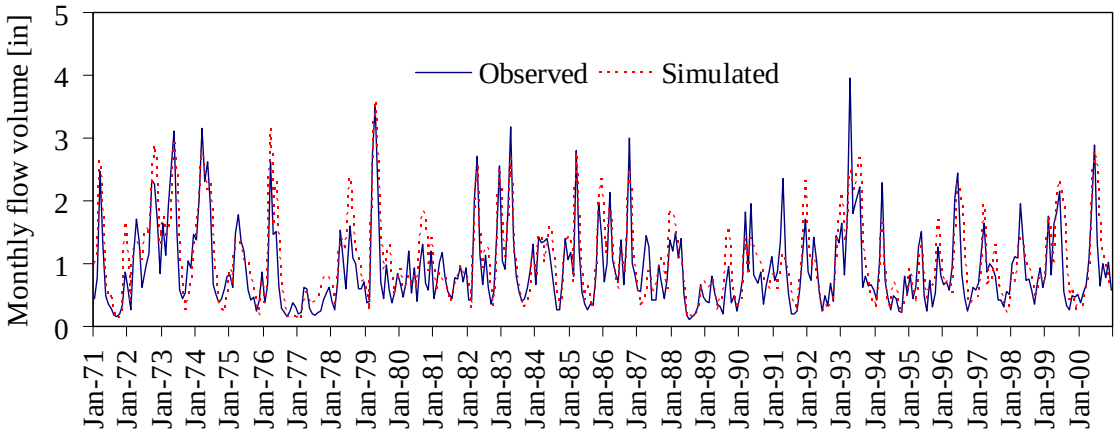

Figure 4.18f. Monthly flows for *USGS_05550000* during the baseline period

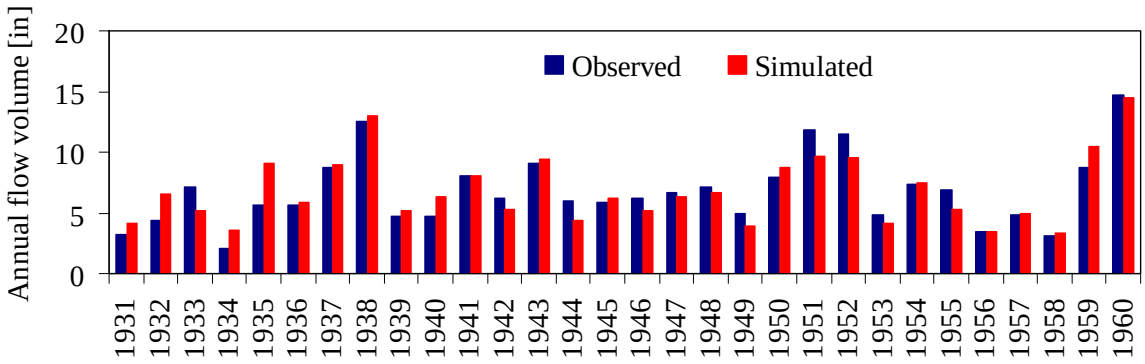

Figure 4.18g. Annual flows for *USGS_05550000* during the drought period

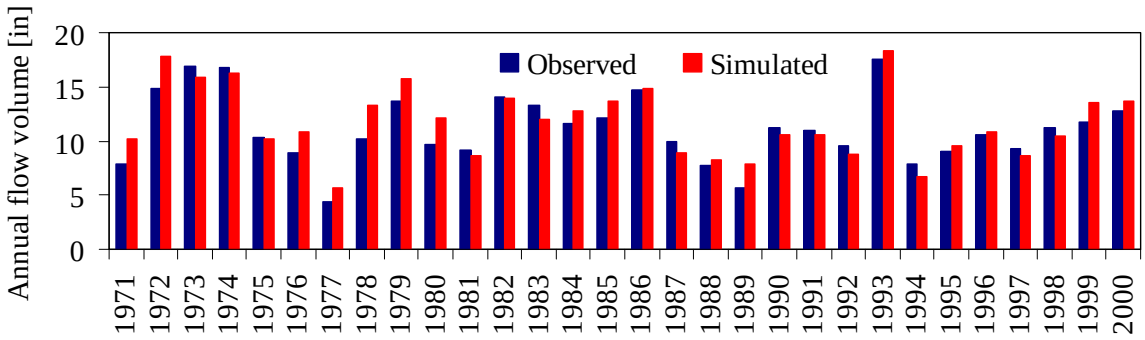

Figure 4.18h. Annual flows for *USGS_05550000* during the baseline period

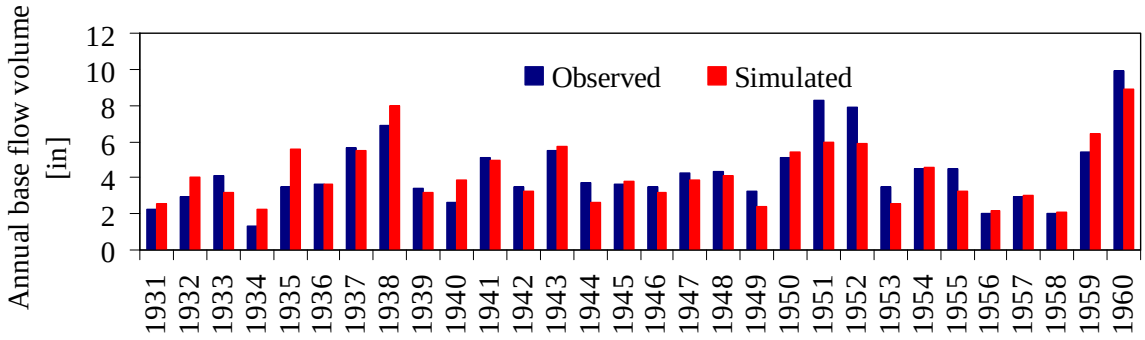

Figure 4.18i. Annual base flows for *USGS_05550000* during the drought period

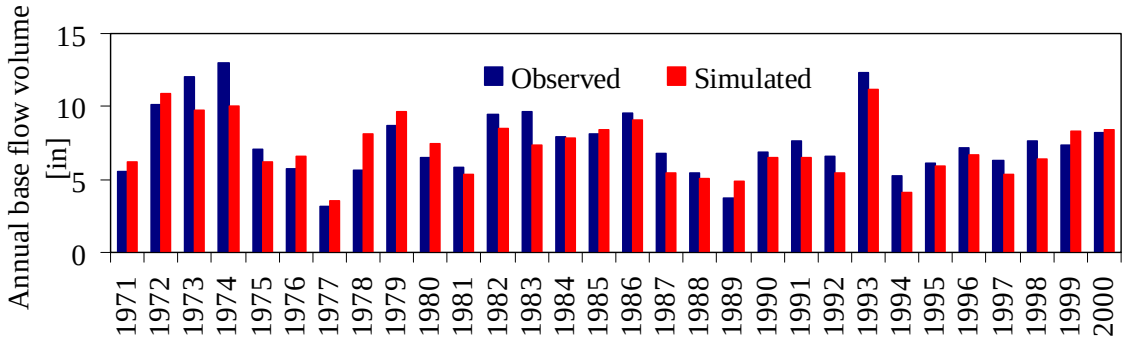

Figure 4.18j. Annual base flows for *USGS_05550000* during the baseline period

Streamflow Simulations for USGS_05552500 at Dayton

The *USGS_05552500* at Dayton is a flow gauging station close to the outlet of the Fox River watershed. The performance evaluation statistics obtained for simulations at this gauging station are presented in Table 4.14. The table shows values of *RSR*, *NSE*, and *PBIAS* for flow simulations in the drought and baseline periods. The *NSE* values obtained for daily, monthly, and annual flows were 0.50, 0.71, and 0.76, respectively, during the drought period. The *PBIAS* for this period was 2.4 percent and the worst *RSR* value of 0.71 was obtained for daily simulations. *NSE* values during the baseline period were 0.51, 0.73, and 0.88 for daily, monthly, and annual simulations, respectively. The associated *PBIAS* and worst *RSR* value were 2.8 percent and 0.70, respectively, for this period. Applying the evaluation guidelines for the monthly time-step, good monthly simulation results have been obtained in both drought and baseline periods and daily simulation were satisfactory. In both periods considered, the performance of the hydrologic model is comparable with slightly better simulations in the baseline period.

Observed and simulated daily hydrographs are compared in Figure 4.19a for the drought period and in Figure 4.19b for the baseline period. Daily flow duration curves for the drought and baseline periods are displayed in Figures 4.19c and 4.19d, respectively. The daily hydrographs and flow duration curves exhibit good agreements in general flow trends between simulated and observed values. In both periods, flows with less than 10 percent exceedence were underestimated as it is also indicated in the positive *PBIAS* values. Simulated monthly and annual flow simulations in the drought and baseline periods are compared with their observed counterparts in Figures 4.19e, 4.19f, 4.19g, and 4.19h. The monthly and annual flows are generally well simulated in both periods and the hydrologic model tends to underestimate flows during both periods. In addition, base flow simulations are compared with those computed from observed flows in Figure 4.19i for the drought period and in Figure 4.19j for the baseline period. The associated *NSE* values were 0.68 in the drought period and 0.60 in the baseline period. The average deviations of simulated base flows were 5.7 percent and 11.1 percent for drought and baseline periods, respectively. Both statistics show that base flow simulations in the drought period were better.

Table 4.14. Performance Statistics for Long-Term Simulations at *USGS_05552500*

Performance statistic	*Drought period (1931-1960)*	*Baseline period (1971-2000)*
PBIAS (%)	2.4	2.8
Daily		
RSR (-)	0.71	0.70
NSE (-)	0.50	0.51
Monthly		
RSR (-)	0.54	0.52
NSE (-)	0.71	0.73
Annual		
RSR (-)	0.47	0.35
NSE (-)	0.78	0.88

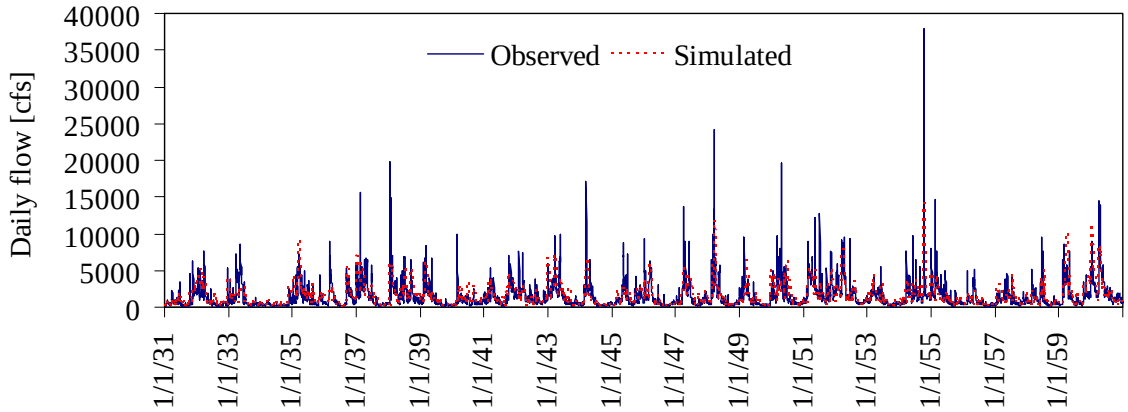

Figure 4.19a. Daily flows for *USGS_05552500* during the drought period

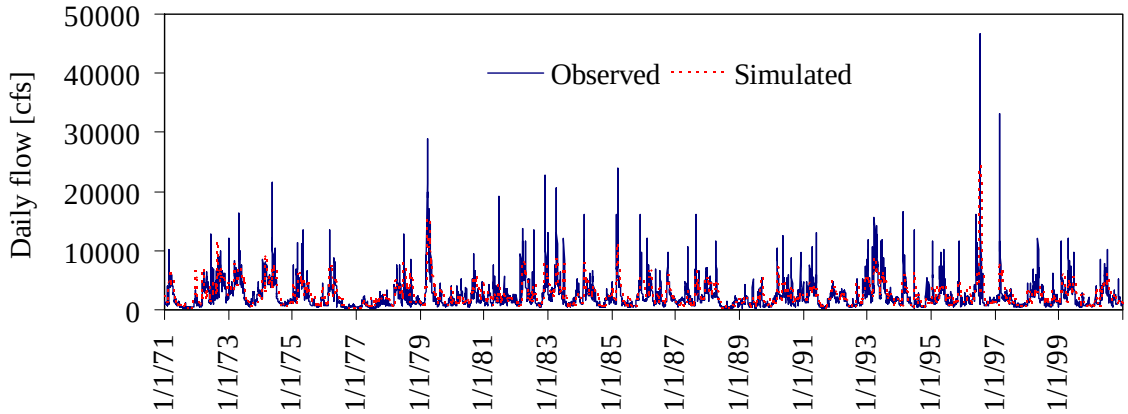

Figure 4.19b. Daily flows for *USGS_05552500* during the baseline period

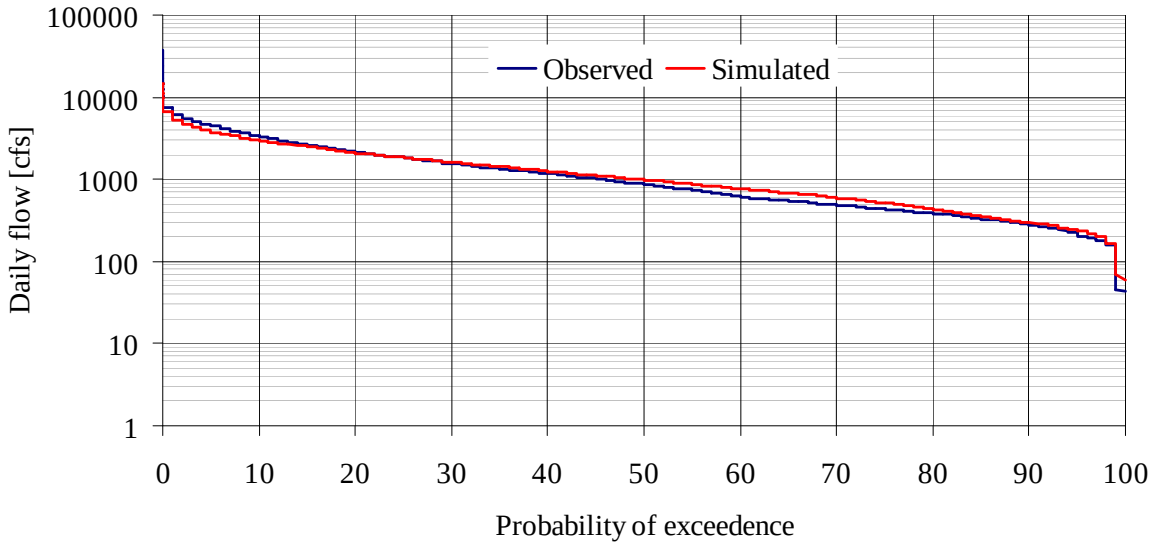

Figure 4.19c. Flow duration curves for *USGS_05552500* during the drought period

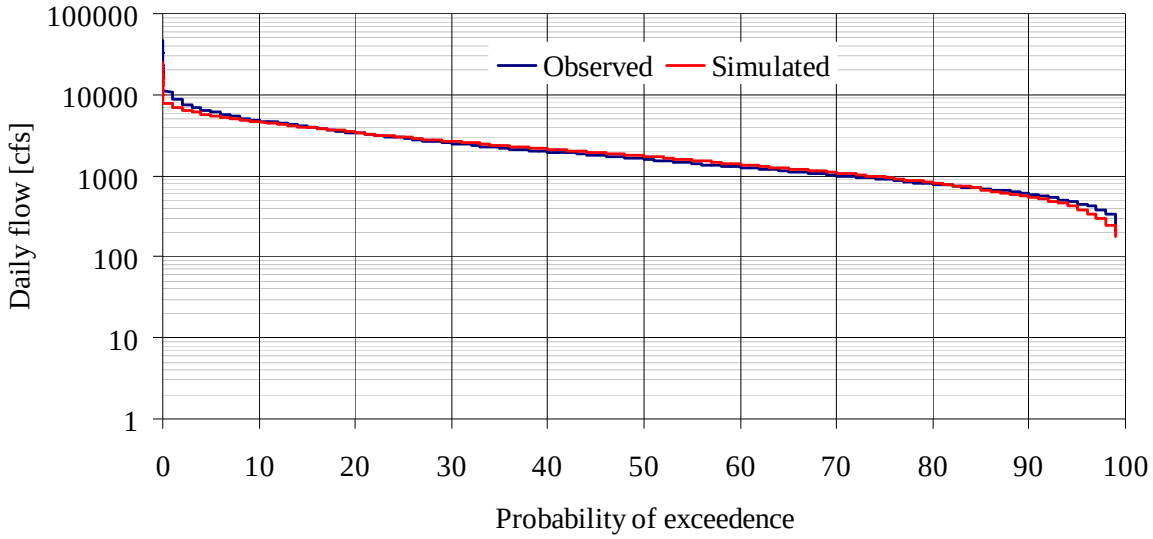

Figure 4.19d. Flow duration curves for *USGS_05552500* during the baseline period

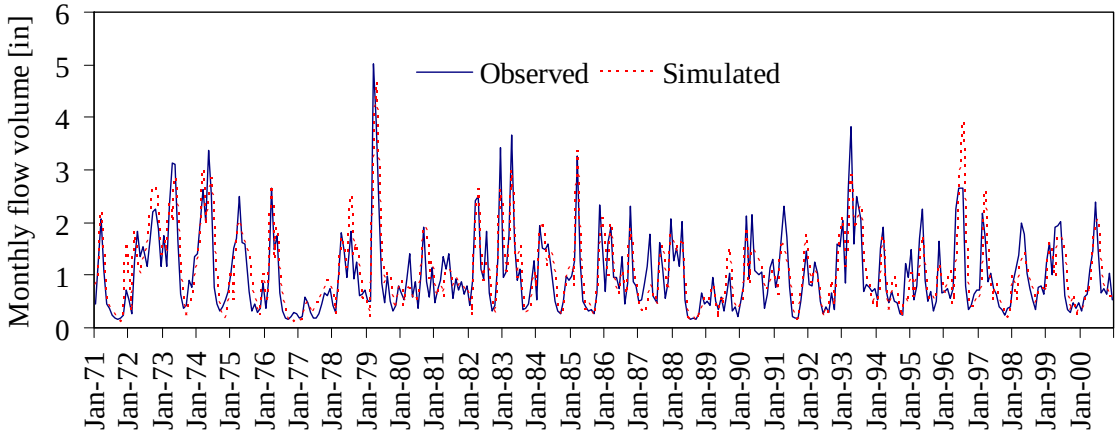

Figure 4.19e. Monthly flows for *USGS_05552500* during the drought period

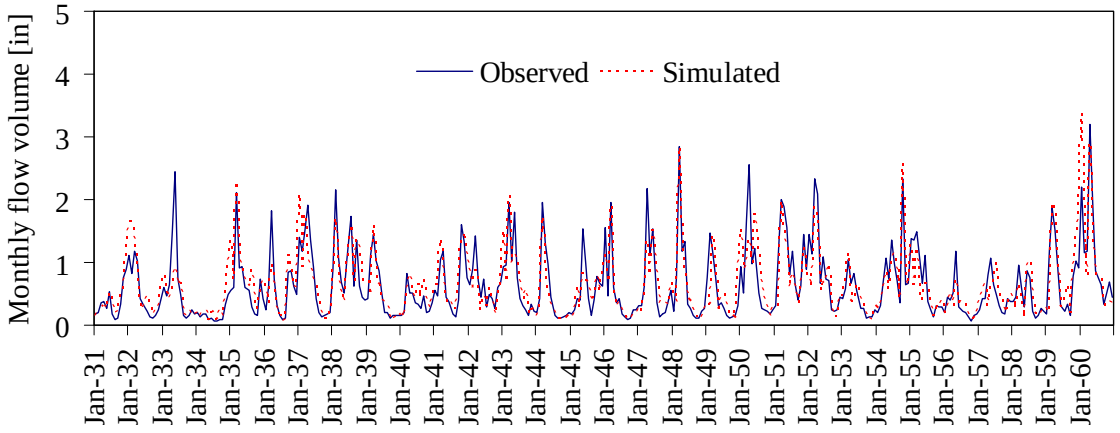

Figure 4.19f. Monthly flows for *USGS_05552500* during the baseline period

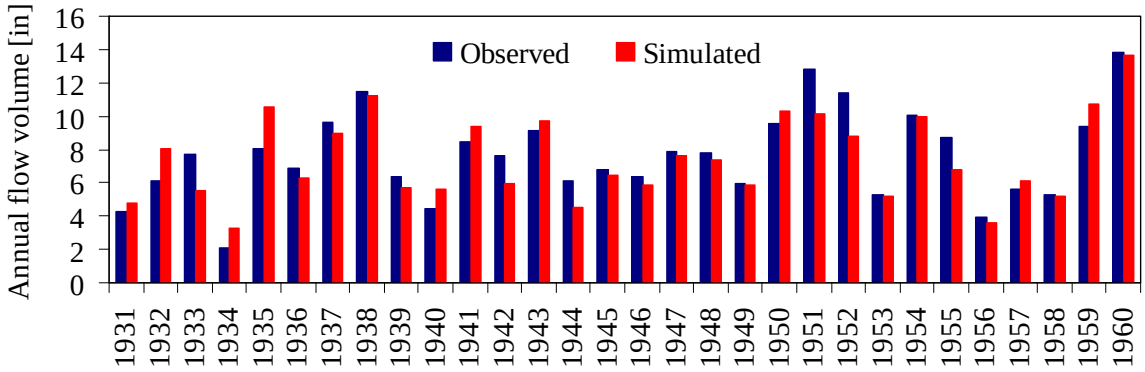

Figure 4.19g. Annual flows for *USGS_05552500* during the drought period

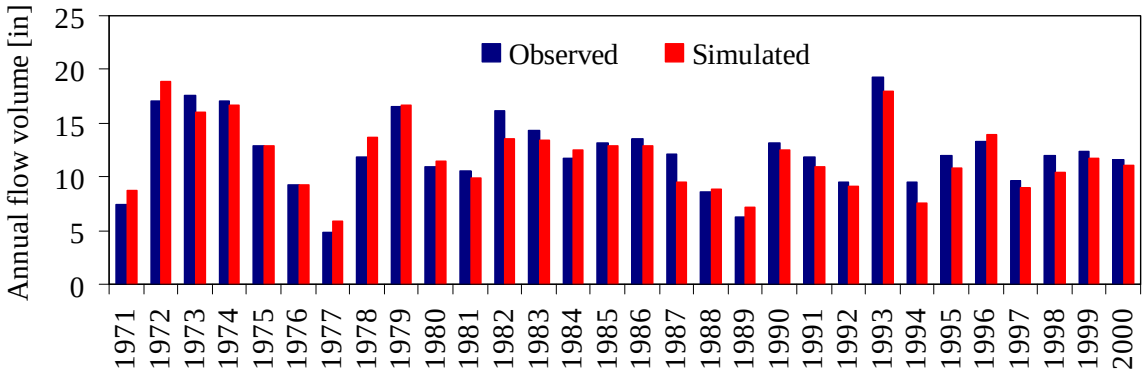

Figure 4.19h. Annual flows for *USGS_05552500* during the baseline period

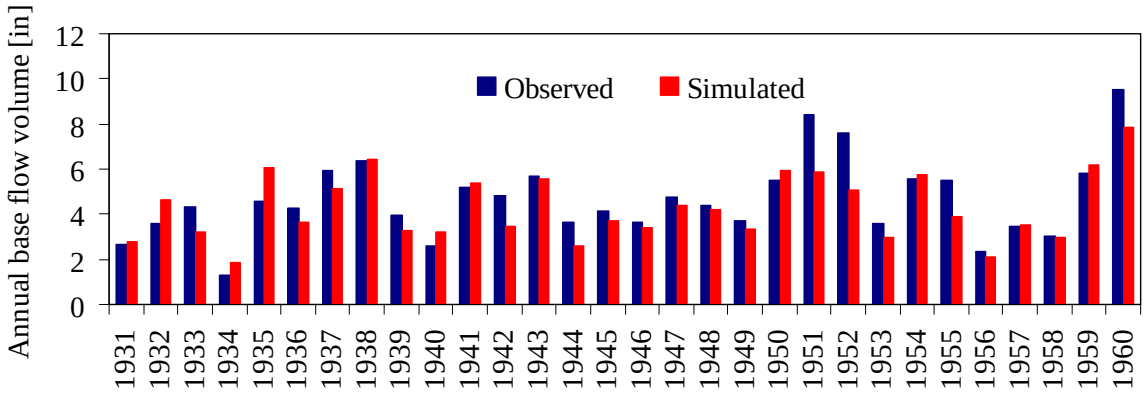

Figure 4.19i. Annual base flows for *USGS_05552500* during the drought period

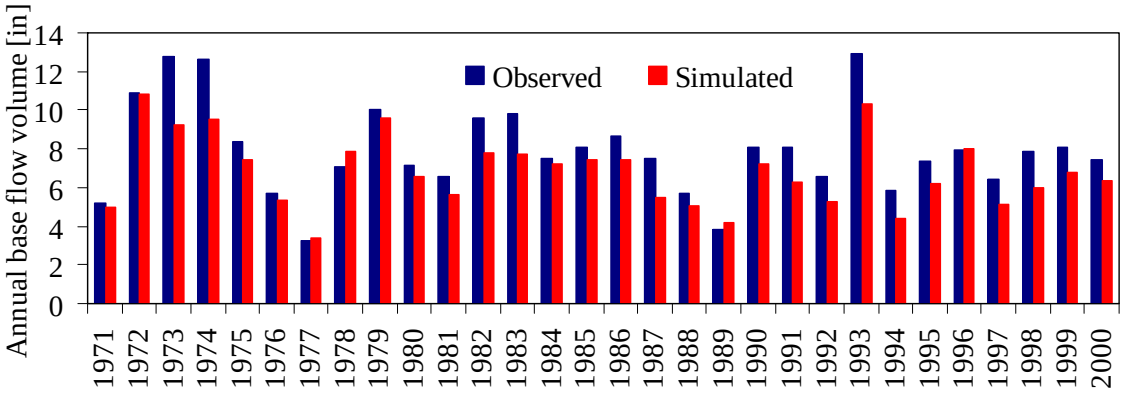

Figure 4.19j. Annual base flows for *USGS_05552500* during the baseline period

5. Summary

A suite of hydrologic models was developed for streamflow simulations in the Fox River watershed. The hydrologic models were developed for three subwatersheds designated as Subwatershed I, Subwatershed II, and Subwatershed III; a single model was also developed for the entire Fox River watershed. The development of subwatershed models serves two important purposes: (1) it ensures distributed parameter calibration, and (2) more observed data can be used during model parameter estimation. It must be noted that downstream subwatersheds require observed inflows at their upstream ends from a draining subwatershed located upstream. In addition, the partitioning helps to adequately sample values of parameter estimates between their acceptable ranges, and it also helps reduce computational demand during auto-calibration. These stand-alone subwatershed models can be used for streamflow simulations independent of one another. The FORTRAN version of the USDA's Soil and Water Assessment Tool (SWAT) and its ArcView interface (AVSWAT2000) were used in developing the hydrologic simulation models for the Fox River watershed. The AVSWAT2000 was mainly used to prepare input data for watershed simulation. These include defining stream networks, locating inlets and additional outlets such as effluent discharging points and flow gauging stations, delineating the watershed and its subbasins, identifying waterbodies such as reservoirs, identifying land uses and soil properties throughout the watershed, establishing hydrologic response units (HRUs) based on land uses and soils in a given subbasin, incorporating weather inputs, and setting up watershed simulation through a selection of various model processes. These processes generated several input files, which contain information about the watershed to be simulated and are used for the FORTRAN version of SWAT for watershed simulation.

For simulation of the Fox Chain of Lakes, a level pool reservoir routing procedure has been developed and incorporated into SWAT to account for the impact of the lakes on the streamflows downstream. The reservoir routing procedure was required in this particular application because SWAT simulates reservoirs using a simple water balance analysis that requires some sort of observed outflow data. Since the hydrologic model is developed for streamflow simulations under future climate scenarios, the use of observed reservoir outflow data can not be an option. An automatic calibration routine using evolutionary optimization techniques (i.e., genetic algorithm) was developed to search for optimal values of model parameters that result in a close match between observed and simulated streamflows. The three subwatershed models were calibrated using the auto-calibration tool. The parameter values have been manually adjusted further with the help of graphical comparisons between observed and simulated daily flow duration curves and monthly and annual flow volumes. The parameter estimates obtained during the calibration process were used in the hydrologic simulation model developed for the entire Fox River watershed.

In order to ensure the model's ability to simulate the response in streamflow to various climate conditions, the hydrologic model was calibrated under two scenarios representing drought and average conditions. A period from 1931 to 1969 was considered for the drought period calibration, validation, and long-term model evaluation, while a period from 1971 to 2005 was used in model calibration, validation, and long-term evaluation for average climate conditions. Note that the 30-year period from 1971 to 2000 is considered as the baseline period for simulation of various climate change scenarios, and it was used to evaluate model

performance under average conditions. In contrast, the 30-year period from 1931 to 1960 represents a dry period and is used to evaluate model performance under drought conditions. Comparison of parameter estimates obtained under the two calibration scenarios indicates significant variations in *GW_REVAP* and *CN2* values. The *GW_REVAP* is at least two times higher under drought conditions, which indicates a higher movement of water in the shallow aquifer to the overlying unsaturated soil zone in response to water deficiencies in drier periods. The *CN2* values are smaller than those obtained for average conditions, reflecting the condition of soil moisture under the drier calibration period. Estimates of the remaining calibrated parameters were identical under both calibration scenarios.

Calibration results were presented for streamflow simulations using performance evaluation statistics (i.e., *RSR*, *NSE*, and *PBIAS*) and graphical comparisons of hydrographs and flow duration curves. According to the evaluation guidelines adopted in this study, monthly streamflow simulations can be judged good if $RSR \leq 0.60$, $NSE > 0.65$, and absolute *PBIAS* is less than 15 percent. During model evaluations under both drought and baseline periods, the worst *RSR*, *NSE*, and *PBIAS* obtained at all three gauging stations were 0.55, 0.70, and 5 percent for monthly simulations, respectively. This clearly indicates the model's good performance at monthly time-step. Applying the same guidelines, daily simulations can be judged as satisfactory, although recommended statistics for monthly time-steps are more stringent than those that apply to daily simulations. Graphical comparisons of simulated hydrographs with their observed counterparts show good agreements, and daily flow duration curves display the model's ability to adequately simulate low, average, and high flow trends. Annual flow volumes were very well simulated during both periods with the minimum *NSE* values of 0.78 and a maximum average deviation of 5 percent. In addition, model results indicate that base flow simulations were better in the drought period when the base flow proportions were normally high.

In conclusion, the hydrologic simulation model developed in this study can be used to analyze the potential impacts of various climate change scenarios on flows and surface water availability. Such analyses provide valuable information for future water supply planning and management.

6. References

Allen, R.G. 1986. A penman for all seasons. *Journal of Irrigation and Drainage Engineering,* ASCE **112**(4):348-368.

Allen, R.G., M.E. Jensen, J.L. Wright, and R.D. Burman. 1989. Operational estimates of evapotranspiration. *Agronomy Journal* **81**:650-662.

Arnold, J.G., and P.M. Allen. 1999. Automated methods for estimating baseflow and groundwater recharge from streamflow records. *Journal of American Water Resources Association* **35**(2):411-424.

Arnold, J.G., P.M. Allen, and G. Bernhardt. 1993. A comprehensive surface-groundwater flow model. *Journal of Hydrology* **142**:47-69.

Arnold, J.G., J.R. Williams, R. Srinivasan, and K.W. King. 1999. *SWAT: Soil and Water Assessment Tool*. USDA, Agricultural Research Service, Temple, TX.

Bekele, E.G., and H.V. Knapp. 2008. Hydrologic modeling of the Fox River watershed: Model calibration and validation. Proceedings of the 2008 World Water and Environmental Resources Congress, May 12-16, ASCE, Honolulu, Hawaii.

Brakensiek, D.L. 1967. Kinematic flood routing. *Transactions of the ASAE* **10**(3):340-343.

Cunge, J.A. 1969. On the subject of a flood propagation method (Muskingum method). *Journal of Hydraulics Research* **7**(2):205-230.

Di Luzio, M., R. Srinivasan, J.G. Arnold, and S.L. Neitsch. 2002. ArcView Interface for SWAT2000- Users'Guide. Blackland Research Center, Texas Agricultural Experiment Station, Temple, TX.

Goldberg, D.E. 1989. *Genetic algorithms in search, optimization and machine learning*. Addison-Wesley Publishing Co., Reading, MA.

Green, W.H., and G.A. Ampt. 1911. Studies on soil physics, 1. The flow of air and water through soils. *Journal of Agricultural Sciences* **4**:11-24.

Gupta, H.V., S. Sorooshian, and P.O. Yapo. 1999. Status of automatic calibration for hydrologic models: Comparison with multilevel expert calibration. *Journal of Hydrologic Engineering,* ASCE **4**(2):135-143.

Hargreaves, G.L., G.H. Hargreaves, and J.P. Riley. 1985. Agricultural benefits for Senegal River basin. *Journal of Irrigation and Drainage Engineering* **111**(2):113-124.

Haupt, R.L., and S.E. Haupt. 1998. *Practical genetic algorithms*. John Wiley & Sons, New York.

Holland, J.H. 1975. *Adaptation in natural and artificial systems*. University of Michigan Press, Ann Arbor, MI.

Hooghoudt, S.B. 1940. Bijdrage tot de kennis van enige natuurkundige grootheden van de grond. *Versl. Landbouwkd. Onderz* **46**(14):515-707.

Knapp, H.V., and T.W. Ortel. 1992. *Effect of Stratton Dam Operation on Flood Control along the Fox River and Fox Chain of Lakes*. Illinois State Water Survey Contract Report 533, Champaign, IL.

McKay, M.D., W.J. Conover, and R.J. Beckman. 1979. A comparison of three methods for selecting values of input variables in the analysis of output from a computer code. *Technometrics* **21**:239-245.

Moriasi, D.N., J.G. Arnold, M.W. Van Liew, R.L. Binger, R.D. Harmel, and T.L. Veith. 2007. Model evaluation guidelines for systematic quantification of accuracy in watershed simulations. *Transactions of the ASABE* **50**(3):885-900.

Nash, J.E., and J.V. Sutcliffe. 1970. River flow forecasting through conceptual models: Part I – A discussion of principles. *Journal of Hydrology* **125**:277-291.

National Resources Conservation Service (NRCS). 1996. *National Soil Survey Handbook, Title 430-VI.*, U.S. Government Printing Office, Washington, D.C.

Neitsch, S.L., J.G. Arnold, J.R. Kiniry, and J.R. Williams. 2001. *Soil and Water Assessment Tool Theoretical Documentation Version 2000*. Grassland, Soil and Water Research Service, Temple, TX.

Overton, D.E. 1966. Muskingum flood routing of upland streamflow. *Journal of Hydrology* **4**:185-200.

Priestley, C.H.B., and R.J. Taylor. 1972. On the assessment of surface heat flux and evaporation using large-scale parameters. *Monthly Weather Review* **100**:81-92.

Sangrey, D.A., K. Harrop-Williams, and J.A. Klaiber. 1984. Predicting groundwater response to precipitation. *Journal of Geotechnical Engineering* **110**(7): 957-975.

Sargent, R.G. 1991. Simulation model verification and validation. *Proceedings of the 1991 Winter Simulation Conference*, December 8-11, Phoenix, Arizona.

Sloan, P.G., and I.D. Moore. 1984. Modeling subsurface stormflow on steeply sloping forested watersheds. *Water Resources Research* **20**(12):1815-1822.

Sloan, P.G., I.D. Moore, G.B. Coltharp, and J.D. Eigel. 1983. *Modeling Surface and Subsurface Stormflow on Steeply Sloping Forested Watersheds*. Water Resources Institute Report No. 142, University of Kentucky, Lexington.

Smedema, L.K., and D.W. Rycroft. 1983. *Land drainage – Planning and design of agricultural drainage systems*, Cornell University Press, Ithaca, NY.

Soil Conservation Service (SCS). 1972. Section 4: Hydrology. In *National Engineering Handbook*. Soil Conservation Service, Washington, D.C.

Soil Conservation Service (SCS). 1986. *Urban Hydrology for Small Watershed*. U.S. Department of Agriculture Technical Report 55, Washington D.C.

Williams, J.R. 1969. Flood routing with variable travel time or variable storage coefficients. *Transactions of the ASAE* **12**(1):100-103.

Williams, J.R. 1975. Sediment routing for agricultural watersheds. *Water Resources Bulletin* **11**(5):965-974.

Wu, K., and C. Johnston. 2007. Hydrologic response to climate variability in a Great Lakes watershed: A case study with the SWAT Model. *J. Hydrology* **337**(1-2):187-199.